Injectivity reduction in geothermal wells

Investigating the causes

T. J. van der Hulst

MSc Thesis
Petroleum Engineering & Geosciences

August 2019

TU Delft

Injectivity reduction in geothermal wells

Investigating the causes

by

T.J. van der Hulst

to obtain the degree of Master of Science
at the Delft University of Technology,
to be defended publicly on Thursday August 15, 2019 at 12:00.

Student number:	4394224	
Project duration:	December 1, 2018 – August 15, 2019	
Thesis committee:	Prof. Dr. D. F. Bruhn,	TU Delft, supervisor
	Dr. B. van Breukelen,	TU Delft
	Dr. P.J. Vardon,	TU Delft
	Dr. J. Eilers,	Shell
	Ir. A. Reerink,	Veegeo

This thesis is confidential and cannot be made public until August 15, 2019.

TU Delft

Abstract

This study investigated the three possible main causes of injectivity reduction in geothermal wells (suspended solids, scaling, biological activity). That has been done by obtaining water samples at three operating geothermal doublet locations in the Netherlands. This paper contains new geothermal data and the interpretation of them. At the moment, injectivity reduction is the biggest and least understood issue in geothermal projects in the Netherlands. Investigating this problem is valuable for current and future geothermal injectors and essential for the upscaling of geothermal energy in the Netherlands.

The three locations differ from each other in several aspects (reservoir, surface facilities, chemicals in use, injectivity reduction), which yields a good comparison. Water samples were taken at different moments in time, on different points in the geothermal systems and for different purposes: TSS, chemical composition and ATP concentrations. The data is obtained in the laboratory and used for scale analysis (using *Stream Analyzer* software from OLI Studio®) and microbial kill tests to determine the influences on growth. Scientific quality and data reliability are guaranteed by multiple pre-experiments (e.g. to verify sterility of sample bottles) and extra measurements (e.g. duplo samples, oxygen concentrations).

It has been found that TSS is reduced through the systems by filters (from 35-55 mg/L in production water to <8-16 mg/L in injection water). Also, scales can potentially form (calcite before- and barite after the heat exchanger). Furthermore, biological activity in the water is initially low, but can grow over time to high levels (>500.000 microbial equivalents).

Microbial growth is site-specific and correlatable to injectivity reduction. When there is microbial growth, corrosion inhibitor (CI) enhances this growth. Scale formation is possible, but has a limited likelyhood to cause significant injectivity problems. Furthermore, there is no reason for TSS to be problematic, but it can also not be excluded as possible source for injectivity reduction. Mitigation of these issues can be done by using more injection filters in a geothermal system (for further TSS reduction). Scaling inhibitor can be used preventive and a CI without nutrients (in the solvent) should be used, or a biocide should be injected simultaneously with the CI.

This report is interesting for geothermal operators, researchers and anybody else interested in geothermal operations in general or more specifically in injectivity reduction.

Acknowledgements

T. J. van der Hulst
Assen, August 2019

First of all I would like to thank my supervisors from TU Delft, Prof. David Bruhn and Dr. Boris van Breukelen, for their support during this MSc Thesis project. Without their scientific view and the freedom they entrusted to me, this project would not have been possible. I would also like to thank Dr. Phil Vardon (TU Delft), Dr. Joren Eilers (Shell) and Ir. Ayla Reerink (Veegeo) for their membership in my graduation committee.

This study has been performed as an internship in the Energy Transition Team of the Nederlandse Aardolie Maatschappij (NAM) in Assen. Being part of and contributing to this team was an honour for me and I would like to thank everybody for the pleasant cooperation. Especially I thank Martijn Kleverlaan and Eilard Hoogerduin-Strating for offering me the internship position and Marc Naus for setting up this project in cooperation with the stakeholders and supporting me as line-manager.

Many more people in NAM have contributed to this project. Special thanks goes to Joren Eilers, for his role as my supervisor in NAM. He has been very helpful and I am grateful for the time he invested in me and the unlimited amount of questions I was allowed to ask him Furthermore, I owe my appreciation to Jan Kweekel, for the guidence he offered me in his role as project lead of this study in the laboratory, to Roelof Evers, for the trust and freedom he gave me in the laboratory and the thinking along in his role of subject matter expert (SME) sampling in Shell and to Robert Horstman, for his co-operation in supplying necessities for the ATP measurements. Others that I would like to thank for their contributions are: Linda Garming, Rene Stoffers, Wiert Smit, Peter Draier, Twan Wittenberg, Jan Stuuring, Dinand Gerritsen, Bren Suichies, Bart van Assema, Thomas Lensvelt and Lars Zondag.

In addition, I want to thank the stakeholders in this project. Ayla Reerink (Veegeo), for her help in planning and supervision during all the samplings, her thinking along in order to get useful results and her time and availability. Also Barbara Cox (Hydreco) for offering me the reasearch topic, her expertise in the subject and interest in the progress.

Finally I would like to extend gratitude to my sister, parents and friends for their support during this MSc Thesis and my studies over the years.

Contents

1

Introduction

Geothermal energy is on the rise. An increase in the oil price in 1973 initiated the interest in this type of energy in the Netherlands (Gupta, 1980). This led to several evaluation projects and feasibility studies but did not result in actual exploitation of geothermal energy yet (Lokhorst and Wong, 2007). The first Dutch geothermal test well 'Asten-2' was drilled in 1987 but did not turn out to be successful (Hanegraaf, 2018, Lokhorst and Wong, 2007). After a period with less regard, geothermal energy received a new boost of interest in the past two decades due to its potential as a green energy source. The first successful geothermal doublet in the Netherlands started operating in Bleiswijk in 2007 (Hanegraaf, 2018). Currently 17 running doublets deliver a combined 3.7 petajoule (PJ) of heat per year, which is good for 0.12% of the Dutch energy consumption (CBS Statline, 2019, EBN, 2019). So at the moment geothermal still has a small contribution to the total energy demand. However, as a low carbon emission energy source it can play an important role in the Dutch energy transition. According to recent plans, geothermal energy can contribute 23% of the total heat demand in the Netherlands by 2050 (Platform Geothermie, 2018). The subsurface of the Netherlands has great potential for so called 'low-enthalpy' (<150°C) geothermal energy (Bender, 2012, Wiggers, 2009). Water temperatures of >62°C are present in practically all aquifers below 2000m depth (Bonté et al., 2012), as shown in figure 1.1. In terms of security of supply, geothermal energy is competitive to natural gas since it can always supply constant heat and therefore is suitable as a baseload energy source (DAGO, 2018).

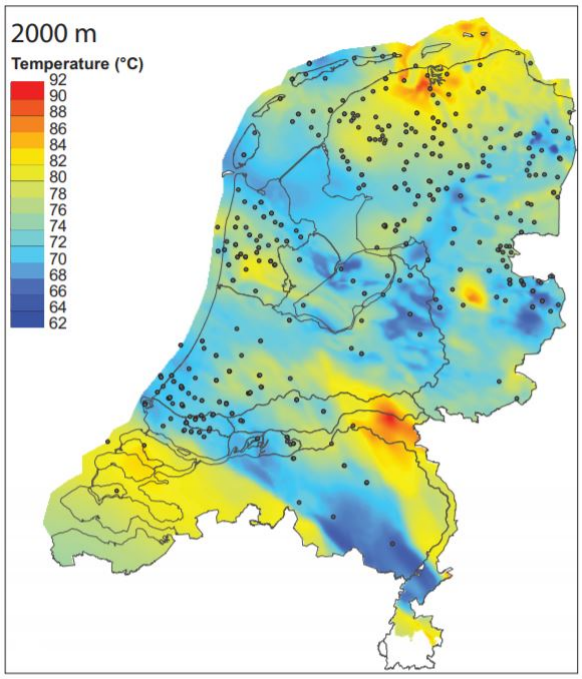

Figure 1.1: Temperature distribution in the Netherlands at 2000m depth below the surface, obtained from measurements in boreholes (Bonté et al., 2012)

In the period 2017-2019, more than 30 exploration license applications have been submitted to the Dutch Ministry of Economic Affairs, with a goal to drill for geothermal heat (NLOG, 2019). According to the current plans, the amount of geothermal doublets in the Netherlands is expected to grow exponentially to 175 in 2030 and 700 in 2050 (Platform Geothermie, 2018). This large upscaling will be accompanied with great employment opportunities in the sector, but it also sees challenges such as induced seismicity, public acceptance, or how to deal legally with the co-production of hydrocarbons (geothermal fluids contain gas in solution). The major operational challenges in geothermal installations are corrosion and injectivity reduction (Cox, 2018).

When developing a new geothermal doublet, first the wells are drilled. Then, generally there is a well test phase in which a set of planned data acquisition activities is excecuted. The acquired data is analysed to broaden the knowledge of the underground reservoir and determine production limits of the well (Schlumberger, 2019). After that, the doublet starts operating (production and injection at the same time). It is quite common that the injection pressure increases over time during the initial phase (first operating months) (Cox, 2018). In practice, the injectivity should stabilize at some point and the system reaches a steady state. This situation can then last for decades and provides a stable basis for long term production and injection. However, in practice this steady state point is not always established. The biggest and least understood issue in geothermal projects in the Netherlands at the moment is ongoing injectivity reduction (Cox, 2018). In some geothermal projects in the Netherlands, serious injectivity problems are encountered (Cox, 2018). In extreme cases, the injectivity can fall so heavily that it leads to shutdown of a doublet (Croese, 2018b). An example of an injection profile of a geothermal well with injectivity reduction is shown in figure 1.2. In this graph, several parameters are plotted over time (period of months). To enforce the same flow rate, more injection pressure is needed over time, so the injectivity decreases.

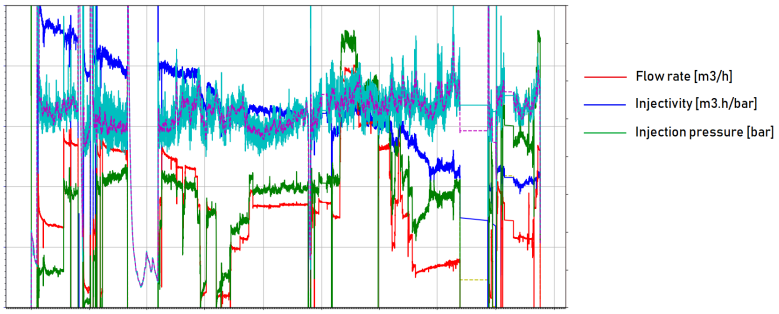

Figure 1.2: Injection profile of a geothermal injection well that encounters injectivity reduction, in the west of the Netherlands. Axes are hidden due to confidentiality. Injectivity (blue line) is decreasing over time (Reerink, 2018)

The exact cause of injectivity reduction in geothermal injection wells is not clear (Cox, 2018, Kas als Energiebron, 2015). It is known (also from oil & gas wells, where co-produced water is reinjected) that clogging can be caused by many different phenomena. Generally it takes place downhole in the injection well at the borehole/reservoir interface or in the near-wellbore region in the reservoir (Rousseau et al., 2008). Amongst all the different phenomena, literature distinguishes three possible main causes of clogging in wells (Kas als Energiebron, 2015, Martin, 2013, Yoo et al., 2013):

- Physical: suspended solids can accumulate and cause clogging
- Chemical: geochemical changes can cause precipitation of minerals
- Biological: growth of microbes, accumulation and slime formation can cause biofouling

Recent research suggests that biological activity can play an important role in causing injectivity reduction. Large amounts of active bacteria ($2.2*10^5$ cells/g) have been detected in the obstruction material from downhole in a clogged geothermal injection well (Croese, 2018a).

1.1. Objective

The goal of this study is to get a better understanding of the risk and main causes of injectivity reduction in geothermal wells. Different options to mitigate this risk and their effectiveness are also investigated. The aim is to get a complete overview of the main mechanisms causing injectivity reduction, with the hypothesis being that microbiology has the highest likelyhood of causing injectivity problems. The research question is formulated as follows:

What is the cause of injectivity reduction in geothermal injection wells?

This is not known yet, first of all because the problem is rather new in the Netherlands. Secondly, in many cases the injectivity can (temporarily) be recovered by chemical treatments using for example biocides or acids. As long as that works, there is limited urge to investigate the source of this problem due to the still marginal economic benefit, given the small operations/numbers of geothermal wells. It has been calculated that the shutdown of a single geothermal doublet can cost the operator ~€17.500 per day, excluding the costs of a well workover (Cox, 2019). This is limited when compared to an oil or gas well, but still significant. However, more knowledge about injectivity reduction can be valuable for future geothermal injectors and can contribute to the upscaling of geothermal energy in the Netherlands.

Sub-quesions

In order to answer the main research question, we look at the three possible main causes of clogging and the following sub-issues are investigated:

- **How many suspended solids are present in geothermal water? And how does that develop through the system? Do the filters work?**
  Suspended solids in a water stream can accumulate and cause clogging. The quantity of total suspended solids (TSS) can be measured by gravimetric analysis.
- **What are the scaling risks in these geothermal systems?**
  The scaling risk through a geothermal system can be modeled using the *Stream Analyzer* software from OLI Studio®. Herewith, the chemical composition of geothermal waters (obtained in the laboratory) can be linked with changing physical conditions through a geothermal system. By doing that, the thermodynamic scaling tendency is modeled for dominant scales. Based on that it can be estimated whether scaling is expected or not.
- **Is there biological activity in a geothermal system and what can cause growth of microbes? How can that be mitigated?**
  Extensive data on microbes in geothermal systems does not exist yet. This study is unique because not only bacteria but the total biological activity is measured, together with microbial growth potential and growth conditions (influences on that growth). By performing growth experiments with geothermal fluids which are sampled from surface facilities, the biological activity downhole in the injection well is simulated.

In order to find answers to these questions, geothermal fluids from three existing doublets in the Netherlands have been analysed. They produce from reservoirs in geological formations from Triassic and Cretaceous age. A complete water analysis has been performed on physical, chemical and microbiological content, to investigate the three possible main causes of injectivity reduction. In comparison to oil & gas wells, data from geothermal wells is limited. Obtaining this new information will be valuable for current and future injectivity issues in geothermal wells.

If there is biological activity, it is interesting to know whether the microbes were present naturally in the geothermal water, or whether they have been introduced from outside to the system. Also, if the biological activity is site specific, is it dependent on formation water composition? Or do factors related to the development of the geothermal doublet play a role? And can biological activity in combination with suspended solids and/or scaling exacerbate each others negative effects? The discussion in section 4.4 will cover these issues.

This research is an MSc Thesis project, performed in co-operation with the Energy Transition Team of NAM in Assen. Solving geothermal challenges is valuable for NAM/Shell since they are planning to start geothermal operations in the near future (Shell & Eneco, 2019). For this experimental study, NAM provides their production chemistry laboratory facilities. Since injectivity reduction is a current issue in the Dutch geothermal industry, two stakeholders that are facing this problem have been involved in this project; geothermal operator Hydreco Geomec B.V. and geothermal consultant Veegeo. They contributed by explaining and discussing operational issues and actively thinking along during this study in order to get useful results. Also they gave access to and offered guiding at three operating geothermal doublets, to acquire samples. Regarding those three locations, two of them report injectivity reduction and one does not experience any problems. They produce from two different geological reservoirs.

2

Literature Review

2.1. Geothermal Energy in the Netherlands

The annual primary energy consumption in the Netherlands is 3156 petajoule (PJ). Renewable energy covers 5.7% (181PJ) of that amount and again 2.0% (3.7 PJ) of that consists of geothermal heat (EBN, 2019). 3.7 PJ of heat is comparable to the average gas consumption of the Netherlands during one summer day (NAM, 2019). This indicates the still limited usage of geothermal heat nowadays in the Dutch energy sector. Currently 17 doublets are operating (figure 2.1), all used for providing heat to greenhouses (Platform Geothermie, 2018).

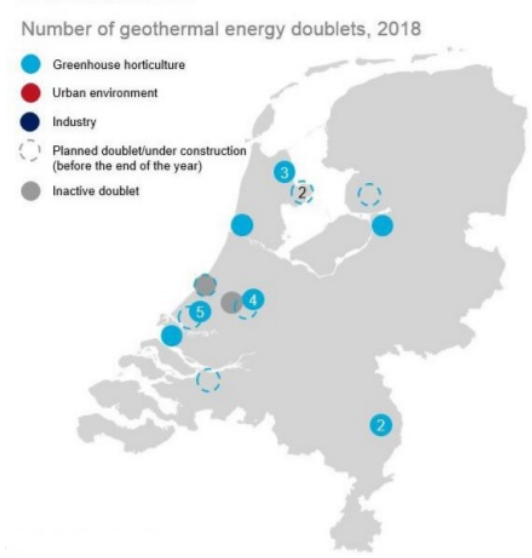

Figure 2.1: Active geothermal doublets in the Netherlands (Platform Geothermie, 2018)

In the Climate Agreement of Paris (2015), 195 countries have agreed to reduce the emissions of greenhouse gasses in order to counteract climate change and keep the maximum rise of the average temperature on Earth below 2°C, and preferably below 1.5°C (United Nations, 2015). Guidelines for the Netherlands are constructed in the Coalition Agreement for 2019-2021 and specified in the 'Klimaat- en Energieakkoord' of 2018 (Platform Geothermie, 2018). The Dutch goal is to reduce CO2 emissions relative to 1990 with 49% in 2030 and with 95% in 2050 (Ministry of EZK, 2018). In order to reach this, the Netherlands will make a transition from using fossil fuels, which is now >90% of our energy consumption (EBN, 2019), to more renewable sources of energy. One of the options with high potential for the Netherlands is geothermal energy. Geothermal energy is local, sustainable energy from the subsurface (DAGO, 2018). At some locations, geothermal energy is the cheapest sustainable energy alternative to natural gas. It has no or very little CO2 emissions and can deliver a constant heat supply (independent of season, weather type or time of the day). Therefore, geothermal energy has a high certainty, which means that (in contrast to wind and solar) it can be used as a baseload energy source (Platform Geothermie, 2018).

Geothermal energy uses heat from the deep subsurface (DAGO, 2018). The temperature in the ground increases with depth, on average about 30°C/km in the Netherlands (DAGO et al., 2018). The sources of this geothermal heat deep in the Earth are residual heat from planetary accretion (~20%) and for a larger part the radioactive decay processes that are active deep inside the Earth and induce heat (Turcotte and Schubert, 2002). Hot formation water, which is naturally present in the pores of reservoir rocks (mostly originally meteoric water) can be utilized for different purposes. There are three different types of applications of heat from the subsurface (DAGO, 2018, Platform Geothermie, 2018).

Types of geothermal applications

- Shallow geothermal: everything <500m depth. Mostly used for excess heat & cold storage (HCS), also referred to as Aquifer Thermal Energy Storage (ATES). This is the most common type in the Netherlands, with ~2500 ATES projects (Provoost et al., 2019). This type is often used for buildings, to fill the seasonal variations in demand for heat & cold in respectively the winter and summer.
- Deep geothermal: between 500-4000m depth, but often at 2-3km depth. It can be used for geothermal heat production in greenhouses (horticulture) or in urban heat-networks for residential heating. All geothermal heat produced in the Netherlands nowadays (3.7 PJ) is provided by this type of geothermal installations (CBS Statline, 2019).
- Ultra deep geothermal: >4000m depth. This type can be used in industry and for electricity production by steam turbines. It has not been developed yet in the Netherlands.

This study focusses on deep geothermal energy. Most injectivity issues are encountered here and this type will cover a large part of the expected growth in geothermal energy (Platform Geothermie, 2018). The research questions described in the introduction apply to this type of geothermal energy.

2.2. Geologic setting

Large parts of the Dutch subsurface have been proven to be suitable for so called 'low-enthalpy' (<150°C) geothermal energy (Bender, 2012, Wiggers, 2009). The main geological targets for geothermal energy exploitation in the Netherlands are: Main Buntsandstein (Triassic), Nieuwerkerk formation (Cretaceous), Rotliegend formation (Permian) and the Kolenkalk formation (Carboniferous). This section elaborates on the geological features of the geothermal region of interest for this study; the Western part of the Netherlands. The subsurface of this region belongs to the West Netherlands Basin (WNB). Extensive geological research has been done in this area in the search for hydrocarbon reserves (Wiggers, 2009). Seismic surveys have been performed and many wells have been drilled since the 1950's, primarily because of the presence of some oil fields (Rondeel et al., 1996). The WNB is SE-NW oriented (figure 2.2). To the southwest it is bounded by the London-Brabant Massif and to the north the Zandvoort Ridge and IJmuiden High separate the WNB from the Broad Fourteens Basin. The Roer Valley Graben is connected to the WNB in the southeast.

Sediments in the WNB basin date from Carboniferous (>300 Ma) till Tertiary (2.5-66 Ma) age (Bender, 2012). Figure 2.3 shows a SW-NE cross section of the Dutch onshore, the WNB is recognisable in the left part of this section. The deepest part of the WNB is located 4000m below surface.

Figure 2.4 zooms in on the WNB. It is clearly visible that the Altena and Schieland groups (respectively Late Jurassic and Early Cretaceous) cover the largest part of the WNB in terms of target depth/temperature for geothermal water exploitation, which is roughly between 1800-3000m. Only in the northeastern and most southwestern part of the basin, the Main Buntsandstein and other groups from Triassic age fall in this depth range.

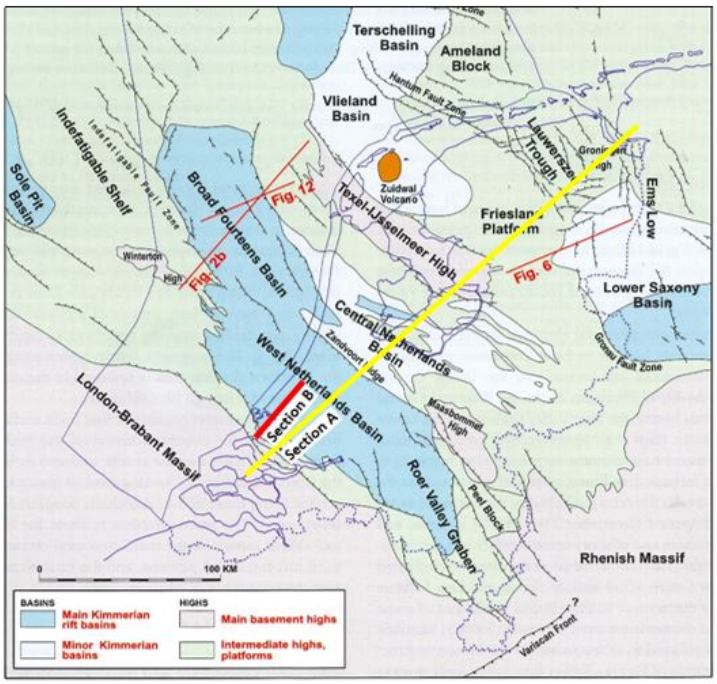

Figure 2.2: Structural elements map of the Netherlands during Late Kimmerian (modified after de Jager, 2007). The lines in yellow and red indicate the cross sections shown in respectively figure 2.3 and 2.4.

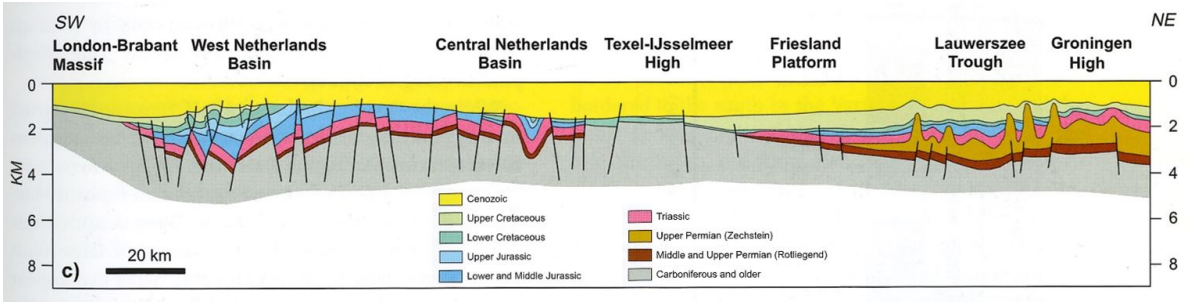

Figure 2.3: Cross-section of the Dutch onshore (de Jager, 2007)

The WNB has a complex geological history as it is located on top of an area with active tectonics. Literature distinguishes four crucial development stages from the Late Carboniferous till Tertiary (de Jager, 2007, van Balen et al., 2000, Ziegler, 1990). These stages are summarized in order to get an understanding of the geological development of the geothermal reservoirs in this study.

Late Carboniferous - Early Permian (305-265 Ma)
First, the area has been uplifted. This was caused by the Variscan orogeny, the collision of Laurasia and Gondwana (Ziegler, 1978). Erosion removed till 500m of sediments during that time. The uplift was less strong in the Southern part of the basin (see figure 2.4). Towards the end of the Carboniferous, the basin was filled with shale and coal deposits, which later formed the source rock for several hydrocarbon reservoirs in the WNB (van Balen et al., 2000).

Late Permian - Middle Jurassic (265-170 Ma)
From the Late Permian on, sedimentation resumed with deposition of fluvial and aeolian sandstones of the Rotliegend Group and later siltstones and carbonates of the Zechstein Group (Ziegler, 1990). Moving into the Triassic, sandstones and shales of the Main Buntsand-

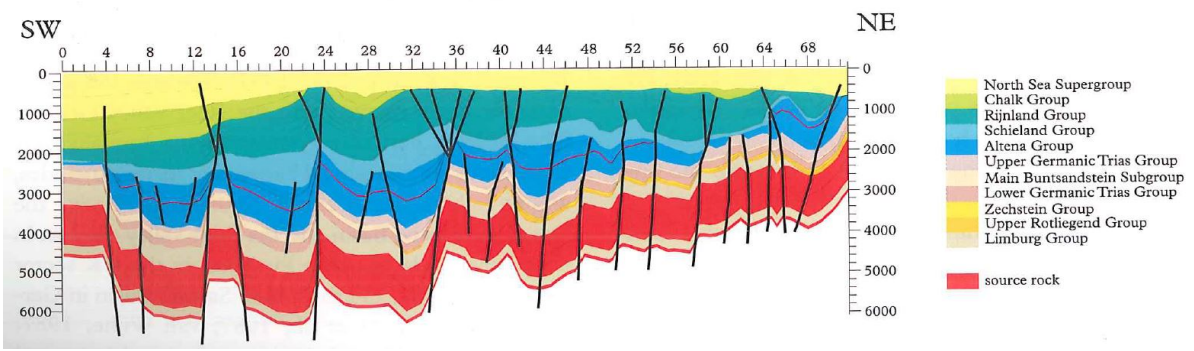

Figure 2.4: Modelled cross-section of different geological formations in the WNB (de Jager, 2007)

stein subgroup were deposited (Van Adrichem Boogaert and Kouwe, 1993-1997b). The WNB formed a tectonically quiet block (van Balen et al., 2000). After a short uplift period, the WNB was further developed by continuous thermal subsidence from the Middle Triassic till Middle Jurassic (250-170 Ma). This occurred during the Early Kimmerian extensional movement, driven by the break up of Pangaea (Gilding, 2010). During this tectonic phase, the WNB formed a large half-graben. Minor deformations during the Late Triassic formed the first sub-units in the basin (Bender, 2012).

Late Jurassic - Early Cretaceous (170-100 Ma)
A period of strong rifting occurred during this time (Late Kimmerian tectonic phase). The basin broke up in several sub units (Gilding, 2010). Syn-rift sedimentation created large thickness variations between different units. During this time, sandstone bodies in the Schieland Group and the Rijnland group (Early Cretaceous) were deposited. Tectonic activity abated rapidly towards the mid cretaceous (Ziegler, 1978).

Late Cretaceous - Quaternary (100-2.5 Ma)
From the Late Cretaceous onward (100 Ma), rifting slowed down and compressive movements related to the Alpine orogeny caused inversion of the WNB (Gras and Geluk, 1999). Many of the hydrocarbon-bearing structures formed during this phase (van Balen et al., 2000). The inversion ceased and the whole WNB was filled with new sediments again at the start of the Tertiary/Paleocene (66 Ma). New uplifting occurred during the Eocene-Oligocene period, which removed almost all Paleogene sediments again. Finally, subsidence accelerated again during the Neogene (from 23 Ma) resulting in a 600-1000m thick package of Tertiary shales and claystones (de Jager, 2007).

The developments as described above make the WNB nowadays a sedimentary basin with several hydrocarbon reserves and aquifers. Recently, the basin became important for geothermal purposes. Table 2.1 describes the target reservoirs for geothermal energy in the WNB, that are of interest for this study. Each of them will be introduced breefly.

Table 2.1: Main target reservoirs (of importance for this study) in the WNB, (van Balen et al., 2000, Wiggers, 2009)

Reservoir	Formation	Group	Geological age
Berkel sst	Vlieland sst	Rijnland	Early Cretaceous (Barremian)
Delft sst	Nieuwerkerk fm	Schieland	Early Cretaceous (Valaginian)
Buntsandstein	Lower Buntsandstein fm	Lower Germanic	Early Triassic (Skythian)

Buntsandstein
The Buntsandstein consists predominantly of reddish-brown sandstones from a mostly fluvial depositional environment. It also contains minor intercalations of silty claystones and conglomerates. The grain size of the sandstones has a limited distribution and varies from fine to medium grained (Van Adrichem Boogaert and Kouwe, 1993-1997b). The sandstone body of interest has a thickness of up to 290m.

Delft sst
One of the main target reservoirs for the extraction of geothermal water is the Delft sandstone member. Core analysis of this sandstone unit in the core lab of NAM in Assen (figure 2.5) provided the opportunity to see and touch the reservoir rocks. The cores show how complex and heterogeneous one of the purest sandstone members in the Dutch subsurface actually is. It consists of light grey, fine siltstone to coarse grained gravel. The Delft sandstone is interpreted as stacked channel sandstone deposits, from a lower coastal plain setting. It is not a homogeneous package of sand grains, as it contains several floodplain shales. Due to the syn-rift deposition of the sediments, the thickness of the body varies considerably between 30 and 100m. The Delft sandstone member is overlain by the Rodenrijs Claystone member (Wiggers, 2009).

Buntsandstein
The Berkel sandstone is 5 Ma younger than the Delft sandstone. It consists of very fine to medium grained sandstones and silty claystones, as well as some limestone beds. The body is 80 to 200m thick and the sediments were deposited in a shallow marine environment (Van Adrichem Boogaert and Kouwe, 1993-1997a).

Figure 2.5: Cores of the Delft sandstone member in the core lab of NAM in Assen (02-04-2019)

2.3. A Geothermal doublet

A geothermal doublet consists of two wells: a production well and an injection well. At the surface they may be very close to each other (just a few meters apart), while in the underground the spacing becomes larger (in general 1-2km) as the wells deviate towards different directions (figure 2.6). One well produces hot water from a water bearing formation deep in the Earth. This happens via an Electric Submersible Pump (ESP), located in the production well just below the bubble point pressure. At the surface, the produced water flows through several components of the geothermal system as will be described in section 2.4. The main goal is to exploit the heat. After that, injection pumps re-inject the heat depleted water through the second well into the reservoir where it was extracted from. This

maintains the reservoir pressure and the water is re-heated to almost its original temperature after several decades (Clevis, 2018).

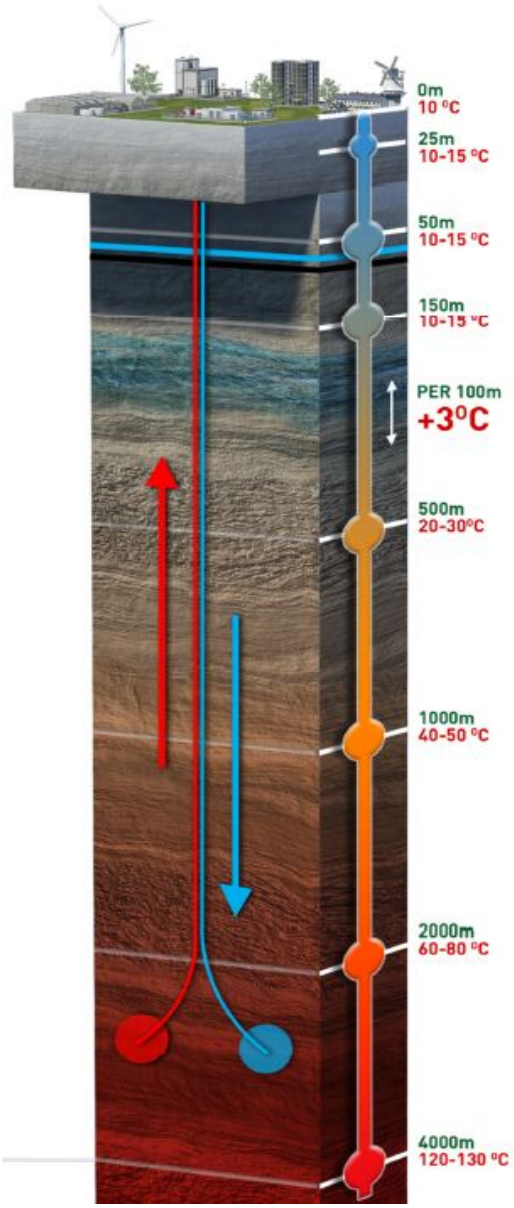

Figure 2.6: Schematic subsurface 3D view of a geothermal doublet (Platform Geothermie, 2018)

2.4. The geothermal system

Geothermal fluids are hot saline, slightly acid, brines containing a methane rich (80-95%) gas phase in solution (Kas als Energiebron, 2015). Once this fluid is produced through the production well, it arrives at the wellhead from where it enters the surface facilities. First a separator separates the geogas from the water. This gas can be transported to a boiler which supplies extra heat to the warm fresh water used in a secondary network supplying consumers with heat. There are also cases where the geogas is used to generate electricity. After the separator, production filters capture solids that are suspended in the formation water to protect the heat exchanger against damage and clogging. After the filter streets, heat exchangers transfer heat from the formation water to the fresh water network that goes to consumers (DAGO, 2018). After that, the formation water flows (possibly via injection

filters) to injection pumps which increase the pressure for re-injection. Figure 2.7 shows a simplified piping & instrumentation diagram (P&ID) of a standard geothermal system in the Netherlands.

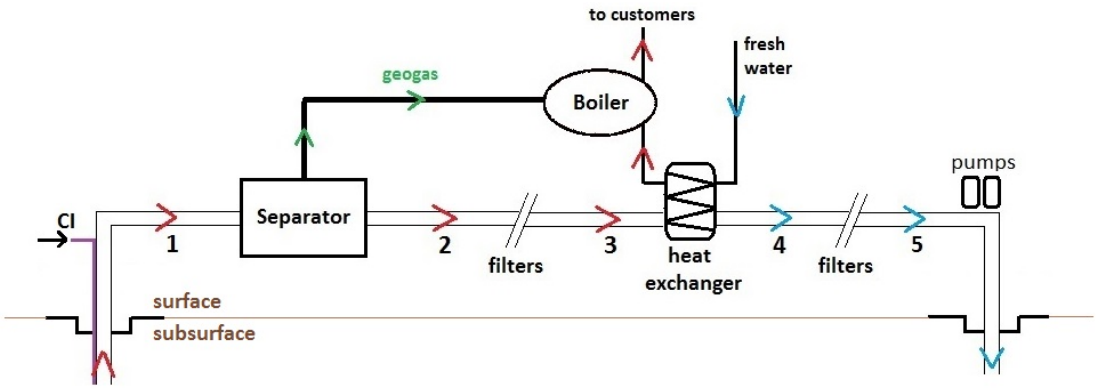

Figure 2.7: Schematic overview of the surface facilities in a geothermal system. The numbers indicate possible sample points

2.4.1. Sample point naming

The numbers (1 to 5) in the scheme in figure 2.7 indicate possible locations in the system where samples of the subsurface fluids can be taken. They are referred to throughout this report. So for example sample ”A2” indicates a sample that has been taken in between the separator and the production filters at location A. When another sample is named ”C5”, it means that it has been taken at the last point in the system before reinjection (after the injection filters) at location C. In other words, it is the geothermal injection water at location C.

2.5. Injectivity reduction

The principle behind a geothermal doublet is that it operates with two wells: a producer and an injector. Except for the well test phase, a geothermal system never produces without reinjection. The key factor for injecting of the cooled-off water is the injection pressure. This is legally limited by ’Staatstoezicht op de Mijnen’ (SodM) to mitigate induced seismicity. The maximum injection pressure is set according to equation 2.1 (SodM & TNO, 2013).

$$THP_{max} = Dt * (0.135 - G_w) \tag{2.1}$$

Where:
THP_{max} = maximum Tubing Head Pressure (THP) at the injection well [bar],
Dt = depth of the injection well from surface to the top of the reservoir [m, TVD],
G_w = hydraulic gradient of the local injection water as function of the salinity [bar/m]. Usually in the range of 0.103-0.108 bar/m.

For an average geothermal reservoir in the Netherlands (D_t = 2000m, G_w = 0.105 bar/m) the maximum THP at the injection well will be 60 bar. Injectivity [m3.h/bar] is the amount of water that is reinjected (debiet) into the reservoir per bar excess pressure. When by using the same excess pressure, less water is injected into the reservoir (lower injection rate), the injectivity is reduced. Sometimes, it can temporarily be recovered by just increasing the THP at the injection well. However, at some point the legal maximum THP is reached. Then the injection rate can not be increased anymore and therefore also the production rate is limited, because production can not exceed the injection. At that moment, the injecitivity problem limits the performance of the geothermal doublet, which is an unwanted situation. Apparently something is clogging the injection well, resulting in this injectivity reduction. In theory,

clogging can have several types of causes with different associated clogging processes. Three main types are concidered (Martin, 2013).

Main clogging types

- Physical: suspended solids can stack behind obstacles and accumulate
- Chemical: geochemical reactions can result in precipitation of minerals
- Microbiological: growing bacteria can accumulate and form biofilms and/or slimes

Given the fact that these types of clogging are most probable for causing problems, they will be investigated in this study. Sections 2.6, 2.7 and 2.8 give more important background information about these types of clogging.

2.6. Suspended solids

Produced formation water often contains insoluble solid particles that are co-produced from the geological formation. These particles can be small sand grains or other suspended matter (organic and inorganic) that is smaller than the sand screen downhole in the production well. All those particles together are referred to as total suspended solid (TSS). Suspended solid control in water injection systems is extremely important (Patton and Foster, 2007c). There is not a specific legal limit for TSS in injection water in The Netherlands. Often, this is agreed per individual injection permit. For reinjection of co-produced water during oil & gas extraction in the Netherlands, operators often need to indicate what kind of water they inject (for the injection licence). Often, maximum expected values for TSS of 30-100 mg/L are reported (NLOG, 2015).

Clogging of a reservoir can already occur at suspended solids concentrations of 1ppm (1 mg/L) and more (Reerink, 2019b). Filters in a geothermal system can take out suspended solids. Two main type of filters that are commonly used are cartridge filters (disposable) and bag filters, their mesh sizes vary between 1-10 μm.

2.7. Microbiology

Microbes (also referred to as microorganisms) are microscopic organisms that are too small to see with a naked eye, and often live under extreme conditions (Pelczar et al., 1986). There are different types of microbes (Whitby and Skovhus, 2009).

Types of microbes

- Bacteria: size 0.5-5 μm. More than 90% of all bacteria live below Earth's surface. Archaea are similar to bacteria, except for the fact that their DNA in the cell is protected by proteins while that's not the case for bacteria.
- Viruses: smallest microbes, size 20-40 nm. They are just a small package of proteins, DNA and lipids. Viruses can only replicate inside living cells of another (micro)organism
- Fungi: biggest microbes, size 2-10 μm. They grow the best in aerobic systems
- Algae: simple plants, which are able to photosynthesise
- Protozoa: simplest form of animal life. Aerobic, in water injection systems they can be found in open tanks

Algae, fungi and protozoa belong to the so called Eukaryotes. They consist of one ore more cells, with at least one nucleus per cell. Bacteria and Archaea are prokaryotes, organisms with just one cell and they do not have a cell nucleus (Whitby and Skovhus, 2009).

2.7.1. Bacteria

Bacteria are the type of microbes that are the main concern regarding micro-organisms within oil & gas production and water injection systems (Patton and Foster, 2007d, Sanders and Sturman, 2005). The reason that they can create a lot of trouble is that they can multiply very fast. Sometimes bacterial populations can be doubled within half an hour, under ideal conditions. Furthermore, bacteria can withstand a wide range of temperatures (-10 - 99°C), pH values (0 - 10.5), pressures (reservoir - atmosphere) and oxygen concentrations (0 - 100%) (Patton and Foster, 2007d). Also they can live in waters that vary from fresh till highly saline (brines). Stagnant conditions (or low flow velocities) are most preferred, together with the presence of enough organic matter/nutrients. Nutrients for bacteria are particularly short chain organic acids, also called volatile fatty acids (VFA's), and hydrogen from decomposed biomass. VFA's are fatty acids with less than six carbon atoms, they can occur naturally in formation water (Patton and Foster, 2007c). The most important external factors for bacteria to live somewhere are temperature and the presence/absence of oxygen. Bacteria can be classified in a number of ways, for example based on their appearance in a fluid stream, optimal temperature range for growth or oxygen requirements. These three characteristics are discussed next.

Appearance in the fluid stream

Bacteria can gather in colonies attached to surfaces ('sessile') or they can live suspended in the water ('planktonic'). Most of the bacteria are sessile. Since those are the ones that cause growth of population, they are the most interesting concerning injectivity issues in geothermal systems. A typical production/injection system contains 1.000-10.000 times as many bacteria attached to surfaces (pipes) than floating in the water (Watkins and Costerton, 1984). Most sessile bacteria (especially sulfate reducing bacteria) can produce exopolysaccarides. These are sticky extracellular polymetric substances (EPS) consisting of sugar residues (Braissant et al., 2007). These polymers are used as construction material and cause the mechenical properties of biofilms, aggregates in which microbes thrive (Flemming et al., 2000, Hsi et al., 1994). Microbes are protected inside such a biofilm and can easily grow and distribure through the system, which is shown in figure 2.8. Biofilms can reach a thickness of 1mm. Within the EPS layers, whole bacteria communities can arise (Sanders and Sturman, 2005). At a certain point a biofilm can disperse a part of its population, it continues as a planktonic colony, attaches to a surface somewhere else in the system and forms a new biofilm there.

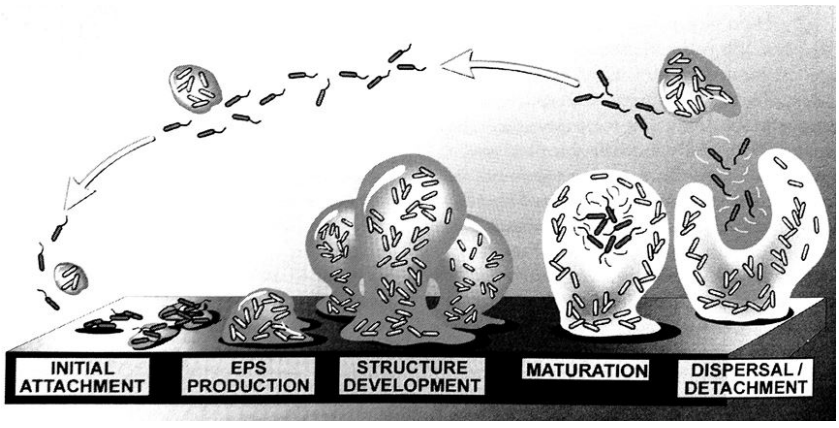

Figure 2.8: Formation and multiplication of a biofilm in different stages (Sanders and Sturman, 2005)

Optimal growth temperature

In general holds: the higher the temperature, the more and faster microbes grow. However, there is a limit. At temperatures >42°C, several proteins start to solidify so bacteria need an adapted metabolism to withstand this heat (Bioclear, 2019). Those bacteria are called thermophiles. Different types of bacteria have their own specific temperature ranges for op-

timal growth (figure 2.9). Thermophiles and hyperthermophiles are expected to grow well in production water (60-90°C), while mespohiles may grow well in injection water (20-40°C).

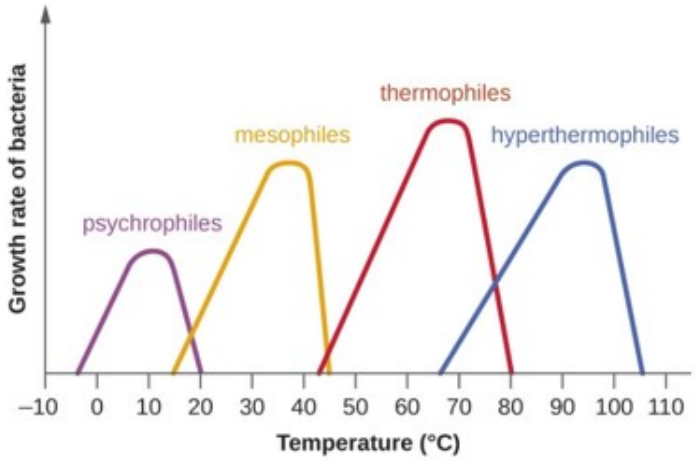

Figure 2.9: Bacterial growth rate as a function of temperature. The skewing of the growth curve reflects the rapid denaturation of proteins as the temperature rises past the optimum for growth of the microorganism (Lumen Microbiology, 2019)

Oxygen requirements

Aerobic bacteria need free oxygen to live and grow, while anaerobic bacteria can not live in the presence of oxygen. Facultative anaerobic bacteria can function in absence of and with small amounts of oxygen. When oxygen is present, their growth is enhanced (Eilers, 2019a). In theory, the conditions in a geothermal system are free of oxygen, which makes it a good living environment for anaerobic bacteria.

Bacteria are often naturally present in soil, formation water and (tap-)water. This can be different types, depending on the conditions (figure 2.9). A valid theory in microbiological studies is that also bacteria that are not adjusted to a certain environment, can still be present in that environment (for example: mesophiles in hot formation water). Those bacteria can be inactive for long times and waiting for ideal conditions under which they can become active and start growing (Williamson, 2009). However, other sources question why those bacteria would be naturally present at a place where they can not thrive. In that case, it is more likely that those bacteria are introduced from externally into a system, for example by well testing water that has temporarily been stored in surface basins (Patton and Foster, 2007b).

In a Dutch geothermal project that experienced huge injectivity problems, further investigation has been done on microbial presence (Croese, 2018b). A down-hole sample from obstruction material in the injection well has proven that slime on the casing wall contains large amounts of active microbes (>100000 active cells/gram sludge), including anaerobic Sulfate Reducing Bacteria (SRB's) (Croese, 2018b). The injection water in that system contained a lower amount of microbes ($2.0*10^3$ active cells/mL), comparable to what is found in Dutch tap water (van der Wielen and van der Kooij, 2010). Apparently this small amount of microbes is able to grow downhole. Biological activity in geothermal wells is unwanted because when microbes grow they can cause several problems such as plugging of equipment, well perforations or pores in the reservoir. Also they can cause microbial induced corrosion (MIC) (Patton and Foster, 2007d, Williamson, 2009) and H_2S production (under the influence of SRB's), usually called 'reservoir souring' (Croese, 2018b, Patton and Foster, 2007d, Vance and Thrasher, 2005).

2.7.2. Measuring biological activity

The microbial content of a water sample can be measured using different techniques. Untill a few years ago, culture tests were the standard method for measuring microbial activity in water samples over time. Via 'extinction-dilution' techniques or total plate counts, ranges of microbial growth could be obtained (Patton and Foster, 2007c). The disadvantage of these tests is that they require a lot of time. ATP analysis is a more recent method for determination of the microbial concentration in a water sample. Every active biomass contains the enzyme Adenosine Triphosphate (ATP) as energy carrier. Therefore, measuring the ATP content provides a direct concentration of active microorganisms in a sample (Lumen Microbiology, 2019). To convert an ATP concentration to an amount of microbial equivalents (ME's), the standard ATP content of an E-coli sized bacteria is used. So it is assumed that the average ME (also interpreted as 1 bacteria cell) contains 1 femtogram (fg) of ATP (1fg = 10^{-15}g) (Lee and Deininger, 2001, LuminUltra, 2016). ATP analysis has one very positive feature: it gives a quick indication.

Within any water sample, there can be two types of ATP (LuminUltra, 2016):

- Intra-cellular (or Cellular) ATP (cATP): ATP contained within living biological cells
- Extra-cellular (or Dissolved) ATP (dATP): ATP located outside of biological cells that have been released from dead or stressed organisms

The sum of these two types of ATP is referred to as Total ATP (tATP). The cATP content in a water sample provides a direct indication of total living biomass concentration. Figure 2.10 shows the (microbial) content of a typical water sample.

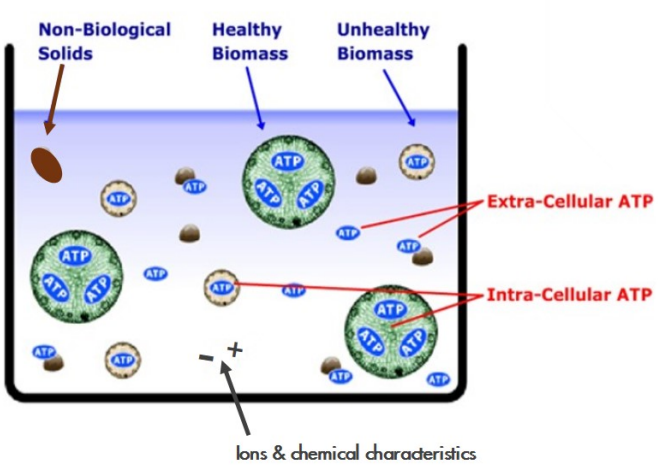

Figure 2.10: Content of a typical water sample; suspended solids, salts and microbes (modified after LuminUltra, 2016)

2.7.3. Microbiologically Induced Corrosion (MIC)

Corrosion is the wastage of a metal through contact with its environment (Schofield, 2003). When a metal is in contact with water, there is a tendency for metal atoms to oxidize to cations and go into solution. Next they can react with water and anions such as oxide or sulfide to a chemically-stable form, for example rust (Fe_2O_3*nH_2O).

A special type of corrosion is MIC, one of the reasons why microbial activity in a geothermal system is undesirable. Microbes can attach to a pipe and form a biofilm. MIC is caused by the activity of Sulfate Reducing Bacteria (SRB's) in a biofilm (Eilers, 2019a). Under and around such a biofilm, iron(0) can oxidize from metal pipes to iron(II), which can create corrosion pits. Next, the iron ions react with sulfide (S^{2-}) that is reduced from sulfate (SO_4^{2-}) occurring in the water, by SRB's in the biofilm. A black precipitation of Iron(II)sulfide is formed which

can cover the corroded areas (figure 2.11). Natural e concentration in the water is not the main driver of MIC, since sulfate can also be provided in other ways, for example by bacteria that convert bisulfite to sulfate. The sulfide can also react with hydrogen and toxic H_2S gas can be produced as a product of SRB activity. Hydrogen removal increases the corrosion reaction rate (Veldkamp et al., 2016). Once a metal pipe is corroded completely, severe leakages can arise resulting in injectivity reduction (when happening in the injection well) and uncontrolled spills.

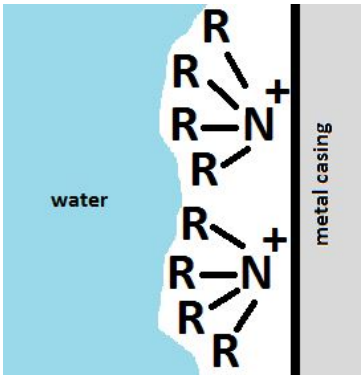

Figure 2.11: Schematic illustration of quaternary ammonium compounds working as corrosion inhibitor

2.7.4. Corrosion Inhibitor (CI)

Corrosion inhibitors (CI's) are chemical compounds that are added to fluid streams in order to prevent corrosion or lower the corrosion rate and thus extend the lifetime of pipelines and other metal equipment. They are often the most cost-effective way to prevent corrosion since they allow the use of cheaper metals in a corrosive environment (Schofield, 2003). CI is usually continuously injected into a geothermal system in low concentrations (2-20ppm), downhole in the production well via a capillary (small tube). This is different than in oil & gas systems, where higher CI concentrations (100-200 ppm) are common, since they contain molecules that can dissolve CI components into the water phase (Eilers, 2019a). The active substance in a corrosion inhibitor is often quaternary ammonium compounds. A quaternary ammonium compound is a molecule composed of an hydrophilic ammonium ion (head), attached to four hydrophobic organic groups (tails). The head of the compound is electrostatically adsorpted onto the metallic surface of the casing wall and the organic tails repulse the water (figure 2.12). In this way, water can not touch the steel so corrosion can not occur (Badawi et al., 2010). The active components in a corrosion inhibitor are dissolved in larger amounts of solvents, such as methanol, glycol and organic acids (Eilers, 2019a). Those chemicals can serve as nutrients for microbes, which can result in the side effect of enhancing biological activity and microbial growth. On the other hand, quarternary ammonium compounds itself can also have a biocidal effect (subsection 2.7.5).

Corrosion inhibitor is injected via a small tube downhole in the production well, just above the reservoir. From that point on, geothermal production water mixes with corrosion inhibitor and distributes it through the system. Therefore, formation water that reaches the surface system always contains some corrosion inhibitor restants (about 2ppm).

2.7.5. Biocide (BIO)

A biocide is a chemical that kills all forms of life in a system. It is mostly used as fighter against living microbes when microbial related problems occur. Although in a water system typically is tried to just kill bacterial populations, actually the term "bactericide" fits better. However, the word "biocide" is commonly used, hence also in this report. Often it is injected into a system at the surface in shock-form (100-1000 pmm) for a short amount of time (24-48

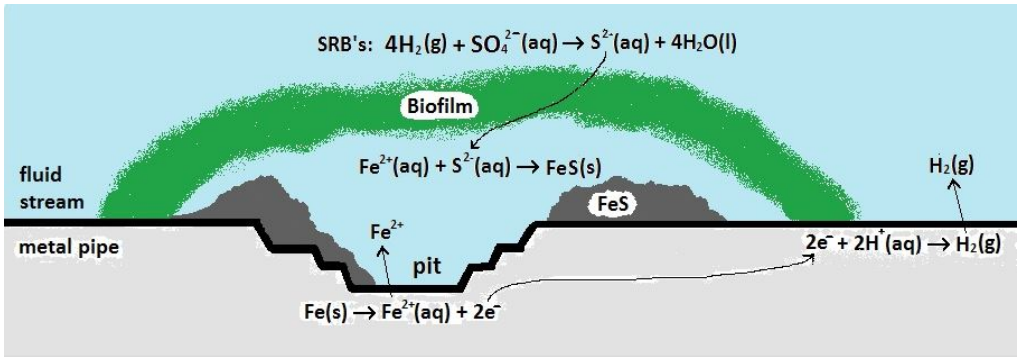

Figure 2.12: Sketch of microbiologically induced corrosion (MIC) process and related chemical reactions

hours). Also it can be combined with a bio-dispersant, which works more preventive. Active substances are often glutaraldehyde, Tetrakis(hydroxymethyl)phosphonium sulfate (THPS) or quaternair ammonium compounds. The latter is used both as corrosion inhibitor and as biocide, as discussed in section 2.7.4. As cell membranes in microbes also consist of hydrophylic and hydrophobic elements, quarternary ammonium compounds can interact with these elements. Physical disruption of the cell membrane occurs from the penetration of the hydrophobic chains into the cell membrane. The damage depends on the size of the organic groups; there is an optimum for how bulky they need to be, to cause maximal disruption. As a result, the selective permeability in such cell membranes is damaged and in this way quarternary ammonium can kill microbes (Badawi et al., 2010).

Most of the microbiology related subjects covered in this section, can result in injectivity reduction and related increasing OPEX costs for geothermal operators (Croese, 2018b). Therefore, it is important to investigate the presence of microbes in a geothermal system, the dependence of microbial growth on system conditions and mitigations against the above-mentioned risks (Patton and Foster, 2007d). How this is done is explained in section 3.3.

2.8. Chemical composition & Scaling

Several literature papers and PVT reports are available about production waters from reservoirs in the West Netherlands Basin (WNB). Those sources can be used to get a broad idea of what kind of chemical compositions of the geothermal waters in this study should be expected. In general, the aquifers in the WNB contain slightly acid (pH = 5.0-7.0), salty formation waters that are high in chloride concentration (50.000-150.000 mg/L). Other common ions are sodium (25.000-60.000 mg/L), calcium (2.000-12.000 mg/L), magnesium (500-3000 mg/L), potassium (100-2000 mg/L), strontium (25-600 mg/L), bicarbonate (70-400 mg/L), iron (10-400 mg/L) and sulfate (0-500 mg/L) (Griffioen et al., 2016, Pirlea, 2016, van der Weiden, 1983).

2.8.1. Scaling

Geothermal water that flows through a geothermic system undergoes large variations in pressure and temperature, which can shift chemical equilibria. A mineral scale is the cristallisation and irreversible precipitation of water-insoluble salts, often adhered to surfaces of pipelines, valves, vessels, etc. If the following conditions are satisfied, solids can precipitate and may form scale (Patton and Foster, 2007b):

1. The water contains ions that can form compounds of limited solubility
2. A change in physical conditions or water composition (temperature, pressure and pH being the most important) lowers the solubility limit below the concentrations present in the water

Formation waters often contain dissolved salts from the rocks they originate from. For example calcium chloride ($CaCl_2$) and sodium sulfate ($NaSO_4$). These salts are highly soluble in water. The ions are in solution and can recombine to compounds of limited solubility (PetroSkills LLC., 2016). An example of such a compound is anhydrite (figure 2.13). The solubility limit of certain minerals can be exceeded, which in turn can cause precipitation of solid material. When this is deposited on surfaces, it is often referred to as (surface) scaling. In solution, it is called bulk precipitation. Whether the concentrations present in solution exceed the solubility limit or not, depends on many (external) factors that trigger scale formation. These factors can be classified into different groups (PetroSkills LLC., 2016).

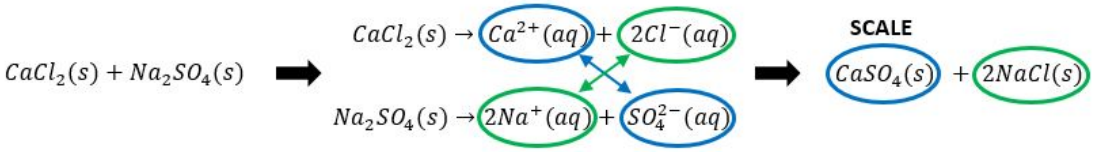

Figure 2.13: Recombination of ions in a solution and scale formation

Key factors for scaling occurance

- Physical factors: change in draw down pressure, temperature or pH, amount of dissolved solids (ionic composition), bubble point (gas evaporation causes turbulent flow)
- System factors: sudden pressure drops over system equipment (e.g. flow meter), disturbance of liquid flow at valves or restrictions, mixing of incompatible waters
- Rate factors: flow rate through system, scale adherence on surfaces of pipes, speed of crystal growth

2.8.2. Scaling risk quantification

Say a fictional solution contains a given amount of calcium sulfate ($CaSO_4$) and the measured concentrations of Ca^{2+} and SO_4^{2-} are respectively $C_{Ca^{2+}}$ and $C_{SO_4^{2-}}$. The activity coefficients (specific for individual species) of Ca^{2+} and SO_4^{2-} are known as respectively $y_{Ca^{2+}}$ and $y_{SO_4^{2-}}$. The scaling risk of $CaSO_4$ in this solution can be quantified as explained below (OLI systems inc., 2019, Patton and Foster, 2007a).

Scaling tendency

The risk of scale formation in a fluid is expressed as the scaling tendency (Ω). It is defined as the Ion Activity Product (IAP) divided by the solubility product constant (K_{sp}) (equation 2.2 (Harris, 2007)).

$$\Omega = IAP/K_{sp} \tag{2.2}$$

The solubility product constant is a conditional equilibrium expression of the solubility limit of a certain scale. It is a function of temperature and pressure (and pH), so it will change from place to place through a geothermal system. The constant is defined as the product of the activities of the aqueous species. The activity of those species is equal to the product of the concentration (in molality) and its corresponding activity coefficient. Expressions of the solubility product constant and activities for $CaSO_4$ scale is given in equations 2.3, 2.4 and 2.5 (OLI systems inc., 2019).

$$K_{sp} = (a_{Ca^{2+}})^1 (a_{SO_4^{2-}})^1 \tag{2.3}$$

$$a_{Ca^{2+}} = C_{Ca^{2+}} * y_{Ca^{2+}} \tag{2.4}$$

$$a_{SO_4^{2-}} = C_{SO_4^{2-}} * y_{SO_4^{2-}} \tag{2.5}$$

When a salt is in solution, it is often in a non-equilibrium state. This state is described by the IAP. The IAP has the same form as the equilibrium constant K_{sp}, but contains the actual activities of the solved species. The IAP for $CaSO_4$ scale is given in equation 2.6.

$$IAP = (a_{Ca^{2+}})^1_{actual}(a_{SO_4^{2-}})^1_{actual} \tag{2.6}$$

The values for scaling tendency are actually saturation ratios. They can be divided into three different groups, with the following meanings:

- $\Omega < 1$: indicates sub-saturation, solid formation is not expected
- $\Omega = 1$: indicates saturation. The solid is in equilibrium with water
- $\Omega > 1$: indicates supersaturation. Precipitation of the solid should occur

The above descriptions apply thermodynamically. Whether this time related actually happens, depends on the kinetic state. Geothermal water is just a couple of minutes (max. 10 minutes) in the surface part of the system, before it is reinjected again (Reerink, 2019a). This is most likely a too short time span to reach the thermodynamic saturation ratio. However, the thermodynamic state will in the end always be established, if time is infinite. For example when $\Omega < 1$, earlier precipitated solids present in a solution can theoretically be solved back into that solution. When this actually happens depends on the kynetic state of the solution. For example in a more acid solution this happens very fast (which explains the working mechanism of an acidification job), while in water this takes an eternity. So when $\Omega > 1$, the solution is thermodynamically supersaturated with $CaSO_4$. Precipitation can occur, but also may not occur (yet) in practice since solutions often remain supersaturated until enough energy is available (kynetic state) to crystallise solids from solution (Patton and Foster, 2007a).

Scales can narrow the flow diameter of pipes or obstruct parts of a geothermal system and are therefore a risk for geothermal operations. Examples of heavily scaled pipes are shown in figure 2.14.

Figure 2.14: Examples of carbonate scale (left) and sulfate scale (right) (Geothermal Museum Larderello, Italy)

Examples of common scales that form in aqueous environments are listed in table 2.2. Barite is an insoluble mineral, making it very likely that scaling will occur if Ba^{2+} and SO_4^{2-} ions are both present in water (Patton and Foster, 2007a). The relation between solubility limits and physical factors varies per scale type. Carbonate scales are more sensitive for pressure and pH, while sulfate scales are more dependent on temperature. Generally, scales have a lower solubility (which means an increasing probability of scaling) when pressure drops and when temperature and pH rise (PetroSkills LLC., 2016). However, for barite the risk of scaling increases when temperature decreases.

Table 2.2: Common scales and their solubility limits in H_2O at standard conditions

Mineral scale	Chemical formula	Solubility [mg/L]
Calcite	$CaCO_3$	12
Barite	$BaSO_4$	2.3
Siderite	$FeCO_3$	4.0

Gas stripping

At reservoir conditions, high pressure dissolves all the gas in the formation water. Once this water is produced, it reaches the bubble point and the gas phase starts to escape from the solution. When the surface is reached, the gas phase generally makes up >50% of the whole fluid. This 'geogas' mainly consists of methane (CH_4) and to a lesser extent of carbon dioxide (CO_2), nitrogen (N_2) and some other gasses. At the separator, this gas phase is extracted (stripped) from the fluid stream. The partial pressure of CO_2 reduces and the concentration of dissolved CO_2 decreases. As a result, H^+ is consumed to create more CO_2 as in reactions 2.7 and 2.8 (Patton and Foster, 2007a). This pH will increase (less H^+ present), which increases the concentration of bicarbonate (and carbonate) according to figure 2.15. The pH change also happens in sample bottles after sampling (therefore, pH is measured on-site). Note that H_2CO_3 in figure 2.15 indicates the portion of CO_2 as it decomposes to CO_2(aq) + H_2O(l) in an aqueous environment. So gas stripping increases the supersaturation of carbonates and the risk of carbonate scale formation (e.g. calcite) increases (Patton and Foster, 2007a).

$$CO_2(aq) + H_2O(l) \leftrightarrow H_2CO_3(s) \leftrightarrow H^+(aq) + HCO_3^-(aq) \tag{2.7}$$

$$HCO_3^- \leftrightarrow H^+ + CO_3^{2-} \tag{2.8}$$

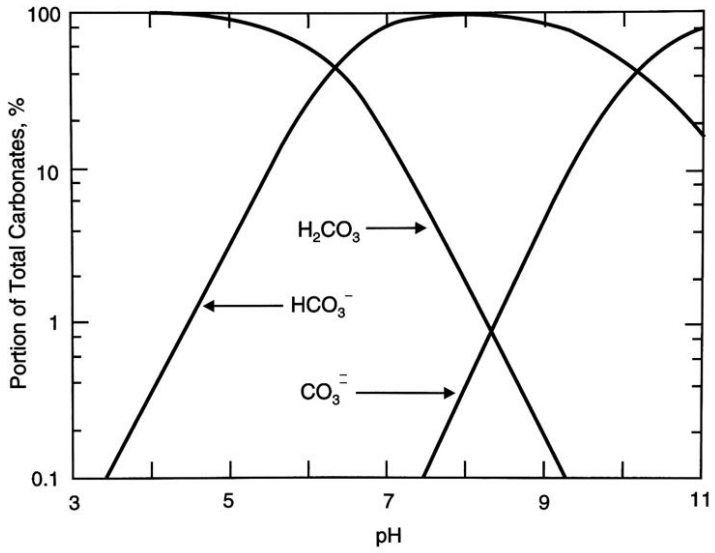

Figure 2.15: Portion of total carbonates dissolved in water versus pH (Patton and Foster, 2007a)

.

Scale control methods

Several options are available to mitigate scale formation in production & injeciton systems (Patton and Foster, 2007a). Examples of prevention methods are the removal of scaling ions (membrane filtration) or injection of scale inhibitors into the system. Removal methods can be chemical (dissolvers) or mechanical (pigging). Prevention of scale is often more economical than removal of scale (Eilers, 2019d).

2.8.3. NORM scales

Naturally Occurring Radioactive Minerals (NORM) are often found in production and injection systems. Radiation from NORM is classified as low specific active (LSA). This can be problematic for example when cleaning surface facilities (Eilers, 2019c). Scale can become radioactive when radioactive ions are co-precipitated during scale formation, for example thorium, radium, radon and lead. Those are decay products of Uranium and can be naturally present in geological formations (PetroSkills LLC., 2016). Radium emits alpha, beta and gamma radiation. Gamma radiation can penetrate into concrete/steel and poses a serious risk to health. Radium is in the same chemical group in the Periodic Table of Elements as Barium, Calcium and Strontium and therefore can easily co-precipitate when sulfate scales are formed (Patton and Foster, 2007a).

2.8.4. Iron precipitation

Dissolved iron occurs naturally in Dutch formation water in concentrations of up to 750 mg/L, depending strongly on geological formation type ((Veldkamp et al., 2016)). In the two geological formations this study focuses on, iron concentrations are usually not higher than 100 mg/L. Iron is found dissolved in formation water in its soluble form, Fe^{2+} (ferrous). Once it gets in contact with oxygen, it can be oxidized to an insoluble form, Fe^{3+} (ferric). Next, it can precipitate as Iron(III) hydroxide ($4Fe(OH)_3$) following the chemical reactions in equations 2.9, 2.10 and 2.11 (Huang and Zhang, 2018).

$$4Fe^{2+} + O_2 + 2H_2O \rightarrow 4Fe^{3+} + 4OH^- \tag{2.9}$$

$$4Fe^{3+} + 4OH^- + 8H_2O \rightarrow 4Fe(OH)_3 + 8H^+ \tag{2.10}$$

$$4Fe^{2+} + O_2 + 10H_2O \rightarrow 4Fe(OH)_3 + 8H^+ \tag{2.11}$$

In practice it is very difficult to keep a system completely oxygen free, also in the oil & gas industry (Eilers, 2019a). Small oxygen entries into a system will very quickly be taken away by steel. Iron precipitates often occur in the form of flakes which flow around in a fluid stream. They can cause clogging of screens in the injection well or pores in the aquifer matrix. Precipitation of iron oxides and iron hydroxides are one of the most frequent occurring forms of geochemical clogging, together with carbonate and sulfate scales (Martin, 2013, Veldkamp et al., 2016).

3

Methodology

In order to investigate the research questions stated in the objective (section 1.1), water samples have been taken from three different geothermal doublets, producing from geological formations from Cretaceous and Triassic age. In this report, these locations are not indicated by their real names due to confidentiality. Table 3.1 gives an overview of the sampling locations and their main characteristics. Sampling at these three locations happened at different moments in time, on different points in the geothermal systems and different samples were taken for different purposes. Table 3.2 contains an overview of all types of samples that have been taken during this study. For the naming of sample spots, consult section 2.4.1.

Table 3.1: Geothermal locations and their basic characteristics

Location	Geothermal Reservoir	Temperature		Reservoir Pressure	Production Rate	GWR*
		Prod.	Inj.			
A	Delft sst + Berkel sst	60°C	32°C	223 bar	320 m3/h	1.1-1.2
B	Delft sst	88°C	36°C	258 bar	298 m3/h	~1.1
C	Buntsandstein	83°C	35°C	215 bar	256 m3/h	1.1

**GWR = gas/water ratio at the separator*

Table 3.2: Overview on samples that have been taken during this study

	Location A	Location B	Location C
TSS	# samplings: 1 types samples: 2 A1 A4	# samplings: 1 types samples: 2 B1 B5	# samplings: 1 types samples: 2 C1 C5
comments	At all locations, a sample has been taken once from production water (before separator) and from injection water (before injection pumps)		
Chemical composition	# samplings: 1 types samples: 1 A1	# samplings: 1 types samples: 1 B1	# samplings: 1 types samples: 1 C1
comments	At all locations, just one sample has been taken from production water		
Microbiology	# samplings: 3 types samples: 4 A1 A2 A3 A4	# samplings: 1 types samples: 4 B1 B2 B4 B5	# samplings: 1 types samples: 4 C1 C2 C4 C5
comments	Samples have been taken 3 times: at original conditions, after a biocide shock and after acidification	Samples have been taken only at standard conditions, through the whole system	Samples have been taken 2 times: at original conditions and after a biocide shock

A complete list of all individual samples that have been taken, per location and per sample date can be found in Appendix A.1.

Samples for TSS analysis have been taken at the first and last point in the system, to compare the amount of suspended solids in production and injection water and to quantify the effect of the filters in the system. Samples for chemical analysis have been taken only at the first point in the system, because at this point in theory the most 'pure' composition of the formation water is found (closest to the reservoir, least external influences). For measuring the microbial activity, samples are taken at different points through the system. Sample moments were in line with certain treatment events at the locations. The type of treatment that is applied (and its result) is related to the nature of the injectivity problem has . For mitigation, it is interesting to know how those treatments (biocide shocks, acidification jobs) influence the microbial activity in a system. See table 3.3 for an overview of the strategic chosen sample moments at the different locations. It is also indicated for which analysis purpose (TSS, chemical composition or microbiology) samples have been taken at those dates.

Table 3.3: Overview of sample moments during this study

Location	Sample date	Purpose	System condition (events of interest)
A	29-01-2019	Microbiology	Natural conditions. The geothermal system has not been influenced by biodice shocks or other chemical injections recently
	04-02-2019	TSS, Chem. comp.* Microbiology	Three days after a biocide- & biodispersant shock (for 24h, 300-500ppm)
	27-03-2019	Microbiology	One month after acidification (for 24h, with acetic acid)
B	05-03-2019	TSS, Chem. comp.* Microbiology	Natural conditions. This system has never been treated with any chemicals
C	08-04-2019	TSS, Chem. comp.* Microbiology	Natural conditions. The geothermal system has not been influenced by biodice shocks or other chemical injections recently
	15-04-2019	Microbiology	Four days after a biocide shock (for 24h, 100ppm)

**Chem. comp. = chemical composition*

A complete set of data (physical, chemical and microbiological) is obtained from the geothermal water samples, using several analysis methods as described in this chapter. Most analyses are performed in the laboratory and some need to be determined on-site. All tests are performed using equipment from the production chemistry laboratory of NAM in Assen. This chapter describes how the samples are taken, which data are obtained from them and how that is done. The different method descriptions are divided into three themes, measurements related to: suspended solids (section 3.1), chemical composition (section 3.2) and microbiology (section 3.3).

3.1. Total Suspended Solids (TSS)

An easy, fast and accurate method to measure the total suspended solids (TSS) in a water sample is gravimetric determination. Suspended solids in a water sample are collected by filtration, then washed, dried and finally weighted (Harris, 2007).

Gravimetric determination

In the first step, a certain volume of a water sample is cast over a $5\mu m$ filter and another part over the$0.45\ \mu m$ filter (figure 3.1). The principle of this method is that solids larger than the mesh size stay behind on the filter. When all the water is through the filter, the solids on the

filter are washed with toluene and next the filter (including the solids) is dried for 45 minutes in an oven at 110°C. The weight of the collected solids (in milligrams) divided by the amount of water that passed through the filter (in liters) gives the concentration of suspended solids in mg/L (Harris, 2007, Patton and Foster, 2007c). Figure 3.2 shows dried membrane filters that are used for measuring TSS, with high and low amounts of collected solids.

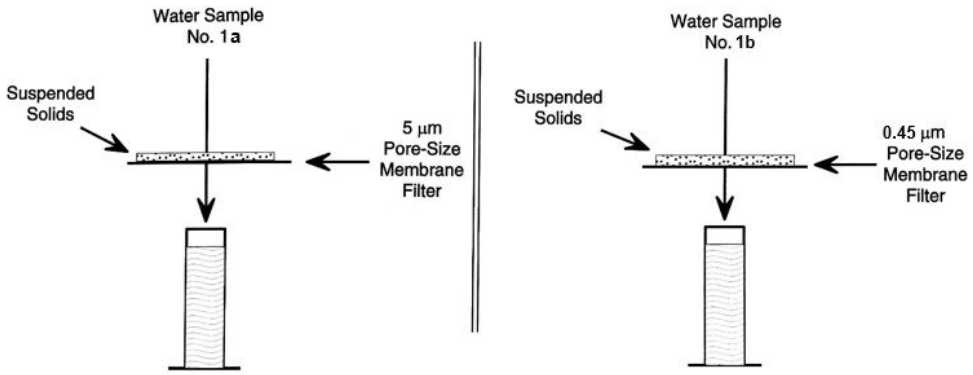

Figure 3.1: Schematic sketch of the setup for filtering suspended solids from a water sample

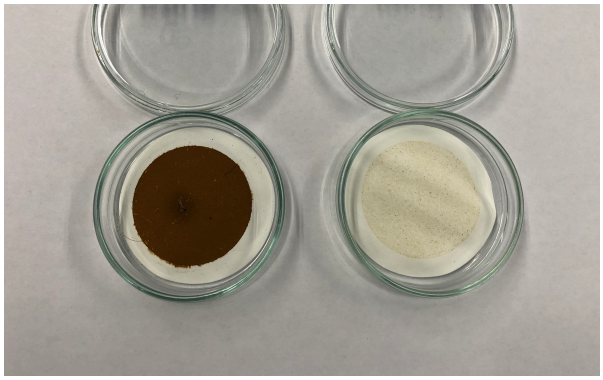

Figure 3.2: Two dried filters, indicating many (left) and little (right) suspended solids

The assumption is that all particles with a diameter smaller than the mesh size of the membrane filter will pass through the filter. Although this would definitely be the case for a sieve analysis for sizing dry particles, it does not have to be true for filtration of particles from a liquid sample. Particle bridging can occur when grains are wet, which can result in filtering particles smaller than the membrane mesh size. Therefore, filtration of particles from a liquid sample over a membrane filter should never be used to estimate the size of the suspended solids in the water. It should just be used to obtain an amount of total suspended solids in the water (Patton and Foster, 2007c).

3.1.1. Filters in a geothermal system

Almost all production systems (oil & gas and geothermal industry) have production filters, to protect surface equipment (e.g. heat-exchangers) against co-produced solids. Sometimes, injection filters are used as well, depending on several factors (reservoir characteristics, injectivity problems). The type (and suppliers) of filters and filter sizes differ per location (often between 1-10μm). Since filters can play a role in provoking or mitigating potential blockage problems, an overview of the filters used at the geothermal locations of this study is given in figure 3.4.

Table 3.4: Filters used at the geothermal locations

	Production filters		Injection filters	
Location	**Type**	**Mesh size**	**Type**	**Mesh size**
A	bag- and cartridge filters	10 & 2 μm	-	-
B	bag- and cartridge filters	10 & 2 μm	cartridge filters	1 μm
C	cartridge filters	5 μm	cartridge filters	1 μm

3.1.2. Analysing solid partiles

Solids can be chemically characterized using Energy Dispersive X-ray Fluorescence (EDXRF). This analytical technique relies on spectroscopy, the interaction between X-ray radiation and the sample's matter (Harris, 2007). The fundamental principle is that each chemical element has a unique atomic structure and corresponding peaks on its electromagnetic emission spectrum (Goldstein, 2003). The emission of those characteristic X-rays from a sample is stimulated by an induced beam of X-rays, focused into that sample. An EDXRF-scan is a qualitative measurement of elements starting from sodium (in high concentrations), organic matter is not detected.

3.2. Chemical composition & Scaling

To perform a scale analysis of the fluid streams through the geothermal systems, a complete chemical composition of these waters is required. This will be done by different analysis methods, which are described in this section. Some measurements need to be done on-site (pH), or within 24 hours after sampling (ATP, TSS). Others can be done in the weeks after sampling (density, ions, organic acids). Samples for chemical composition are taken at the first sample point in the system for all locations (point 1 in figure 2.7).

3.2.1. Temperature

On site temperatures through the geothermal system are always displayed on a control panel. Where needed, temperature is also measured (on-site) from the pH measurement device shown in section 3.2.6 or using a thermometer (in the laboratory).

3.2.2. Cations

The concentrations of several positively charged ions in the geothermal water, such as natrium (Na^+), potassium (K^+), calcium (Ca^{2+}), magnesium (Mg^+), strontium (Sr^{2+}) and barium (Ba^{2+}), are determined using a Microwave Plasma Atomic Emission Spectroscopy (MP-AES) device (figure 3.3). Nitrogen is used to heat up (~5000K) the microwave plasma, which is a good excitation source for atomic emission spectroscopy. First the sample is filtered, to make sure only dissolved cations are measured. Then it is diluted with nitric acid and next an aerosol (suspension of liquid droplets in a gas) is created from it by a nebulizer. The aerosol is introduced into the very hot microwave plasma and is dried, dissected and sprayed. The atoms excite and emit light with specific wavelengths, characteristic for every element when it falls back to a lower energy state. The emission is focussed on a monochromator which scans the wavelengths and sends a selected range towards a charge-coupled device (CCD). A CCD is an extremely sensitive detector that stores photo-generated charge in a two-dimensional array (Harris, 2007). So the electromagnetic radiation is transformed to an electric charge (for each ion/wavelength) and a cation concentration in the water sample can be calculated.

3.2.3. Anions

The concentration of anions in geothermal water can be determined by using ion chromatography (IC) combined with conductivity detection. This technique is only used for the anions bromide (Br^-) and phosphate (PO_4^{3-}) since more accurate methods are available for measuring sulfate (SO_4^{2-}) and chloride (Cl^-).

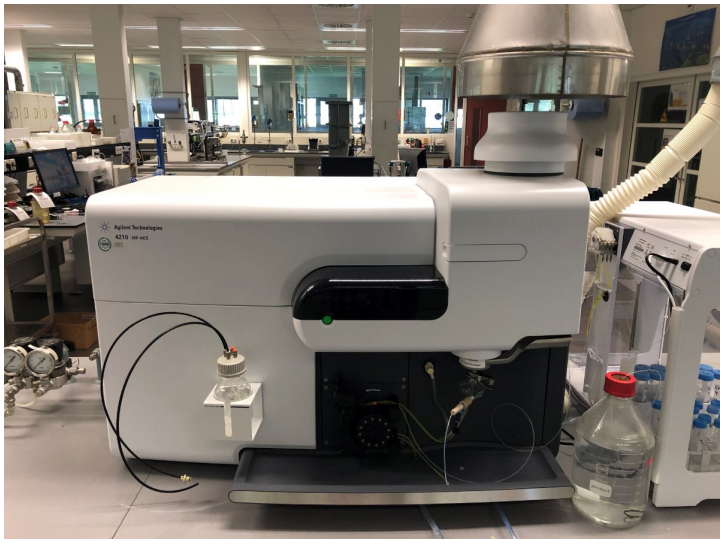

Figure 3.3: MP-AES device for measuring cations

First the sample is guided over an IC-column by an eluens fluid. Different target elements are separated over this column, after which the eluens is transformed to water using a suppressor through an anion-exchange membrane. The order of elution for the different elements is (with increasing retention time): chloride, bromide, sulfate and then phosphate (Harris, 2007). The conductivity of target elements is measured. Fluoride and organic acids eluate for chloride. A carbonate removal device (CRD) removes the carbonate present in eluens and samples, to prevent carbonate interference. Without a CRD, carbonate would eluate on the chromatogram in between bromide and sulfate. Identification and quantification of the anions is done by comparing the retention times and peak areas of the sample with known values of standard calibration solutions.

Figure 3.4: Ion Chromatograph for measuring anions

Sulfate measurements

The amount of sulfate in the geothermal water can be determined by turbidimetry. Turbidimetry is measuring the transmittance of light through the suspension of precipitate, during titration. A bariumchloride solution is titrated to the sample and barium will react

with sulfate to the insoluble bariumsulfate (barite) according to equation 3.1.

$$Ba^{2+}(aq) + SO_4^{2-}(aq) \rightarrow BaSO_4(s) \quad (3.1)$$

The turbidity caused by the precipitation is a measure for the sulfate concentration in the sample (Harris, 2007). The sample becomes progressively cloudier until an equivalence point is reached. At that point, the turbidity ceases to change because no more precipitate forms, since all sulfate in the sample is consumed to form barite. The sulfate concentration in the sample can then be calculated using a calibration standard. The detection limit of this method increases with the chloride concentration in the water. Chloride inhibits the formation of barite, so the measured concentration of sulfate will be lower than the actual concentration in the sample. This effect plays a role when the chloride concentration exceeds 5000 mg/L. The sample intake is reduced then, which increases the detection limit of the method.

Chloride measurments

To obtain a chloride concentration, the sample (diluted with nitric acid) is titrated with silver ions in the form of silvernitrate. This is called the Fajans titration (Harris, 2007). Silver reacts with chloride and forms a precipitation of silverchloride according to equation 3.2.

$$Cl^-(aq) + Ag^+(aq) \rightarrow AgCl(s) \quad (3.2)$$

During titration, the electric potential is measured with a voltmeter with a high entrance resistance. The concentration of silver ions and therefore the measured potential shows a notable spike at the equivalence point of this titration (when all chloride has reacted with silver). The amount of silver ions titrated at that point is known and is used to calculate the chloride concentration in the sample.

3.2.4. Alkalinity

Alkalinity is the capacity of water to uptake hydrogen ions. To a good approximation, alkalinity is determined by hydroxide (OH^-), carbonate (CO_3^{2-}) and bicarbonate (HCO_3^{2-}) (Harris, 2007), however also other ions present in water (e.g. iron, calcium, magnesium, phosphate and organic acids) can influence the reaction with hydrogen. The acid binding capacity of a fluid is determined using titration with the acid hydrogen chloride (HCl), to the end points of phenolphthalien (pH=8.2) and methylorange (pH=4.3). From the equivalents of acid required to lower the pH to these endpoints, the amounts of hydroxide, carbonate and bicarbonate are calculated.

The alkalinity titration is performed in the laboratory, as soon as possible (< 24 hours) after sampling. The longer is waited, the more carbonates could escape from the sample in the form of CO_2 (equation 2.7). Combining this with the fact that also other basic ions contribute to the alkalinity, can make the measurement of carbonate amounts by alkalinity unreliable (Kweekel, 2019a). Measured alkalinity values (and therefore reported carbonate values) are likely to differ from the actual carbonate content in the system water. To assess this difference, a separate method with higher accuracy for measuring the total carbonates is also used to obtain carbonate concentrations in the water (subsection 3.2.5).

3.2.5. (Fixing) total carbonates

The actual total amount of carbonates in geothermal water can be determined by first fixing all the carbonates in a sample and then measure it using gas detection tubes. During sampling on site, a certain volume of sampled water (~ 300mL) is added to a fixed volume (300mL) of a pink 0.02M buffer solution. The buffer solution (pH=8.5) preserves/fixes all CO_2, bicarbonate and carbonate present in the sample as bicarbonate and carbonate. This is because CO_2 can not exist (and not escape from the sample) at pH>8.2. At the laboratory, a sub-sample is taken from the preserved sample (figure 3.5) and put into a closed bottle. 6M HCl is injected into this bottle and the content is shaken well. All the preserved carbonates will react and escape from the solution as CO_2. This CO_2 is detected using Kitagawa CO_2 detector tubes, after which the amount of total carbonate is calculated (Kweekel, 2019b). Furthermore, the fractions of CO_2,

CO_3^{2-} and bicarbonate HCO_3^{2-} can be calculated using their molar masses and based on the pH that has been measured on-site (Kweekel, 2019a). The reported carbonate composition of geothermal water at the different locations will be a combination of alkalinity and total carbonate results. Both alkalinity and total carbonates have been measured at location A, to see the difference. At location B, alkalinity is used to measure the amount of carbonates (since preparation of the carbonate fixing sample was not possible here). At location C, only the total carbonate method is used. An overview is given in table 3.5.

Figure 3.5: Preserved sample for CO_2 fixation

Table 3.5: Performed carbonate measurements at the different locations

Location	Analysis method used		*Comments*
	Alkalinity	Total carbonates	
A	Yes	Yes	Both methods performed, to see difference in results
B	Yes	-	Carbonate content based on alkalinity results
C	-	Yes	Total carbonate amount from 'fixing carbonates'

Reporting the carbonate results

In the chemical results (chapter 4), concentrations of OH^-, CO_3^{2-} and HCO_3^{2-} are always based on alkalinity measurements. A 'total carbonates' concentration results always from the fixing carbonates method. Actual carbonate fractions are then calculated (using on-site pH) in the text. Values that are the closest to reality ('total carbonates' results, when available) are used for the scaling analysis.

3.2.6. pH

pH is measured on-site using a portable pH measurement device (figure 3.6). The main reason to measure pH on-site it to be ahead of CO_2 escaping from the sample (section 2.8.2).

Figure 3.6: Portable pH measuring device

Before usage, the device is calibrated with two buffer solutions (pH = 4.01 and pH = 7.01). Directly after sampling, the pH meter is directly inserted in the water to obtain a realistic pH. The water can still be very hot at that moment, however this will not cause the pH to be significantly different than at room temperature (pHT, 2008). The pH is written down once the display shows a (more or less) stable value. The temperature is also noted.

3.2.7. Volatile Fatty Acids (VFA's)

Volatile fatty acids are measured using a high performance liquid chromatograph (HPLC), combined with an UV-detector. Samples are prepared for measuring VFA's by filtering and dilution. The VFA's that are present in a sample are separated on a HPLC comumn with 0.0025M sulfuric acid as eluens. They absorp UV radiation (wavelength =204nm), which is measured. The different compounds are identificated in the following elution order: formic acid (CHOOH), acetic acid (CH_3COOH), propionic acid (C_2H_5COOH). Identification and quantification is done using a standard method for comparing the retention times and peak areas of the sample with comparable ones of a standard solution.

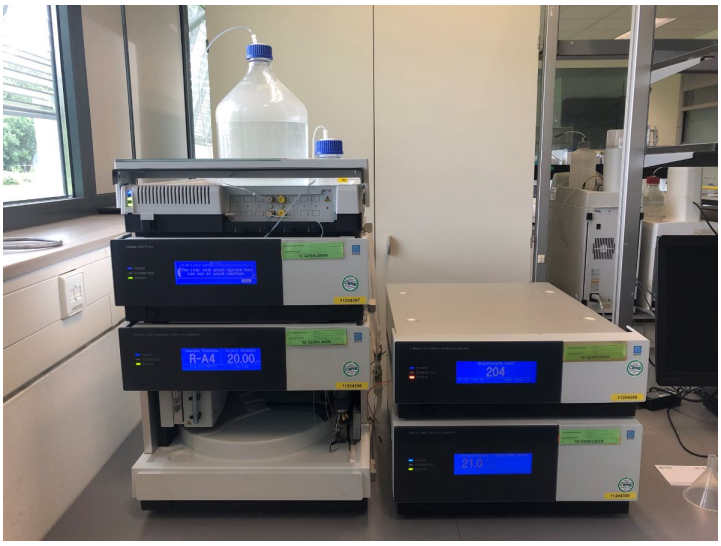

Figure 3.7: Measuring device for organic acids

3.2.8. Scaling analysis

Probability of scale formations in a geothermal system can be calculated on the basis of formation water composition and system conditions. This has been done for the three geothermal systems, using the *Stream Analyzer* software from OLI Studio®. The steps taken to perform a scale analysis are described in the workflow below. Additional screen-shots of this process can be found in Appendix A.8.

Scale modeling workflow

1. The chemical composition of the production water is obtained from the samples in the laboratory (tables 4.2, 4.7 and 4.10). This data is used as input to create a 'brine' in the model. In case the concentration of an ion resulted to be below a detection limit, a value just below that limit is used. By doing this, the 'worst case scenario' (highest ion concentrations) for scale formation is modeled. The created brine is reconciled, based on the measured pH. Reconciling means balancing the electro-neutrality of the sample: measured ion concentrations have small errors, but scaling calculations should be done based on an uncharged brine. The dominant ion (sodium) is used to balance the sample.

2. Gas data are entered to create a gas phase in the model. These data are extracted from recent PVT-analyses at the locations (table 3.6). In the model, gas composition

is normalized with Methane to 100 mole%. Then, the gas is reconciled to reservoir conditions (actually there is no gas phase present in the reservoir because of the high pressure, this is taken into account by the model itself).

3. Next, a 'saturate' is created in which the brine and the gas (step 1 & 2) are combined as fluid stream. Using the production flow rates and gas/water ratios displayed in table 3.1, the mixture is saturated first at reservoir conditions (solids are allowed to form). Minerals with pré-scaling tendencies of >1 in the reservoir (calcite and barite) are set manually to 1.0 because on a geological timescale, formation water always reaches a thermodynamic equilibrium with the reservoir rocks.

4. Finally, the geothermal system is modeled by adding several facilities. Every point in the system with unique physical conditions is included in this model; reservoir, ESP, separator, heat exchanger, booster pump and injection well. The 'saturate' created in step 3 is used as input. At the separator, the gas is excluded from the whole fluid ('saturate') and the brine continues its way through the system.

5. As a result, the model calculates the probability of scale formation at different points in the geothermal system. The *Stream Analyzer* software reports scaling risk as 'pre-scaling tendency' (Ω). This is defined as the scaling tendency before any solids are formed (all the species are suspended in solution), a non-equilibrium condition that can be viewed as the condition where time equals zero. Many industries, notably the up-stream oil & gas industry, use the pre-scaling tendency as an important indicator for scale management (OLI systems inc., 2019).

Table 3.6: Produced geogas compositions at the different locations (Pirlea, 2015, 2016, 2017)

Component	Amount [mole %]		
	Location A	Location B	Location C
Nitrogen	2.659	2.217	4.322
Carbon dioxide	0.459	8.547	3.412
Hydrogen sulfide	0.000	0.000	0.000
Methane	94.982	80.992	90.538
Ethane	1.044	0.969	1.298
Propane	0.088	0.191	0.155
Isobutane	0.054	0.094	0.028
n-Butane	0.154	0.089	0.056
Isopentane	0.089	1.432	0.024
n-Pentane	0.108	5.234	0.041

3.3. Microbial activity

In this section, all the methods related to the microbiological content of the samples are explained. First some measures are listed, that have been taken to guarantee (scientific) quality of the obtained data. For the microbiological part of the water content, some experiments have been performed in the laboratory prior to taking the real geothermal samples. The pre-experiments below contributed to better microbial sampling- and measurement-procedures for the real samples.

Pre-experiments

- **Sterile sample bottle test:** initially sterile sample bottles are required. This test has been done to check whether the sterilisation method for the sample bottles for ATP measurements is sufficient (Appendix A.2).
- **Temperature decline in sample bottles test:** temperature changes when transporting the samples are unwanted because this can possibly influence microbial growth. To predict the temperature fall of geothermal water in different sample bottles during transport to the laboratory in Assen, this test has been designed. Based on the result, a substantiated choice has been made on which sample bottles to use (Appendix A.3).

Also, during this study some procedures have been changed in order to improve research methods, or extra measurements were added in order to check the quality of procedures.

Additional quality improving measures

- **Duplo samples:** two identical samples can be taken to check the accuracy and reproducibility of the data. It is important that sampling procedure, transport and treatment in the laboratory is the same for all samples (section 3.3.6).
- **Oxygen free sampling:** introduced after the first two sampling moments. Since geothermal systems are in theory oxygen free, the samples should be so as well and only anaerobic or facultative anaerobic (section 2.7.1) microbial activity should be measured from them (section 3.3.8).
- **Oxygen measurement:** the oxygen content in some ”oxygen free” samples has been measured to check to which extent the desired result (sample to be free of oxygen) is achieved (Appendix A.4).
- **Demi water microbial growth experiment:** to compare the observed microbial growth in geothermal water samples with ’neutral’ demi-water. Is the observed growth caused by the microbial content and nutrients unique for that geothermal water, or can microbiology also grow under the same external conditions in demi-water? (Appendix A.5)
- **Thermos cans versus glass bottles:** since the type of used sample bottle has been changed during this study, it has been checked whether the material doesn’t influence the results initially (Appendix A.7).

3.3.1. Measuring microbial activity

The amount of cellular ATP in a water sample provides a direct indication of total living biomass concentration (section 2.7.2). Cells containing cATP are collected from a sample by filtration. Then the cATP concentration is quantified by measuring light produced through its reaction with naturally-occurring firefly enzyme luciferase (equation 3.3). This light is recorded using a device called a luminometer (figure 3.8).

$$ATP + O_2 + luciferin \xrightarrow{luciferase} AMP + PP_i + oxiluciferin + light \tag{3.3}$$

Figure 3.8: Luminometer device to measure ATP. A tube containing sample water and luciferase enzymes is placed into the blue cover

ATP monitoring procedure

Measuring the microbial activity in a sample via ATP monitoring is done in an fume cupboard. A couple of steps are taken in order to get an ATP concentration as a result. The procedure is described below.

ATP measurement procedure

1. After the sample bottle has been taken from an oven in which it was stored and is homogenized by shaking, a certain volume of geothermal water (preferably 20mL) is sucked up using a syringe
2. A membrane filter is screwed to that syringe and the water in the syringe is sprayed through the filter into a sink. Cells containing cATP are captured on the filter, while dATP passes through
3. 5mL of Lumiclean solution (loog) is sprayed over the filter, to remove any fat and/or oil remains from the sample
4. The syringe is sprayed 3 times with air, to dry the filter
5. 1mL of a solution, Ultralyse 7, is pipetted into the syringe and sprayed over the filter into a 9mL Ultralute tube. This solution breaks the cells on the filter and releases the cATP into the solution. This sample is collected for the ATP measurement
6. Luciferase enzymes are stored in the refrigerator to extend their stock life (~6 months). After defrosting the enzymes, the luminometer is calibrated. This is done by creating a reaction between 0.1mL of enzymes and 2 drouplets of an activation fluid that contains an overload of cATP. The amount of Relative Light Units (RLU's) from the luminometer is converted into an actual ATP concentration
7. Now the ATP content in the sample can me measured. After shaking, 0.1mL of the sample from step 5 is pipetted into a sterile plastic tube
8. 0.1mL of the luciferase enzyme is pipetted into the same plastic tube
9. The tube is swirled for about 3 seconds and placed into the luminometer. The reaction in equation 3.3 takes place now and light is emitted

10. The amount of light is measured and then the ATP concentration [pg/mL] is displayed on a connected computer monitor. This value is interpreted as described in table 3.7.

For most of the measurements, step 7-10 have been done three or four times. By doing that, multiple ATP concentrations were obtained for one sample (at one point in time). After detecting outliers using Dixon's Q test (95% confidence), an average ATP concentration was calculated as report value.

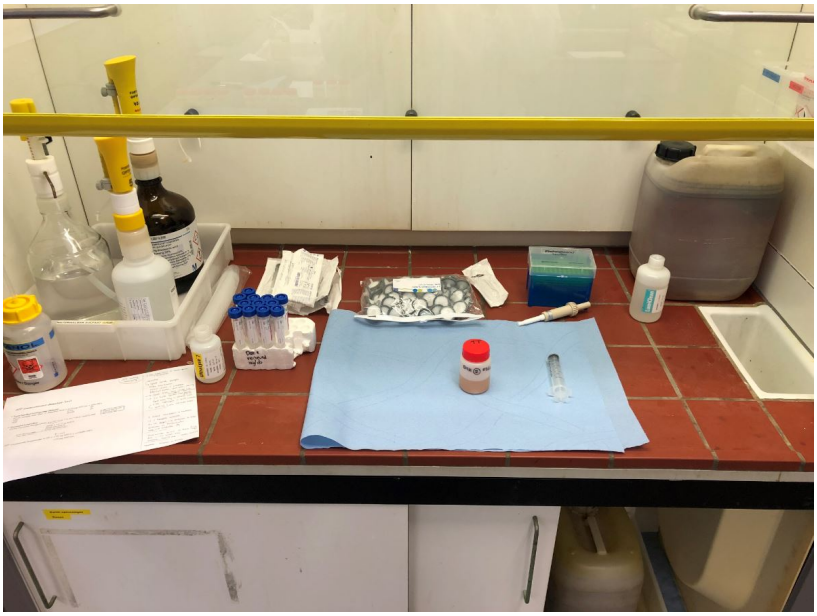

Figure 3.9: Setup and necessities for preparing a sample for ATP measurements (step 1-5 in procedure description); sterile syringes, filters, loog, Ultralute tubes

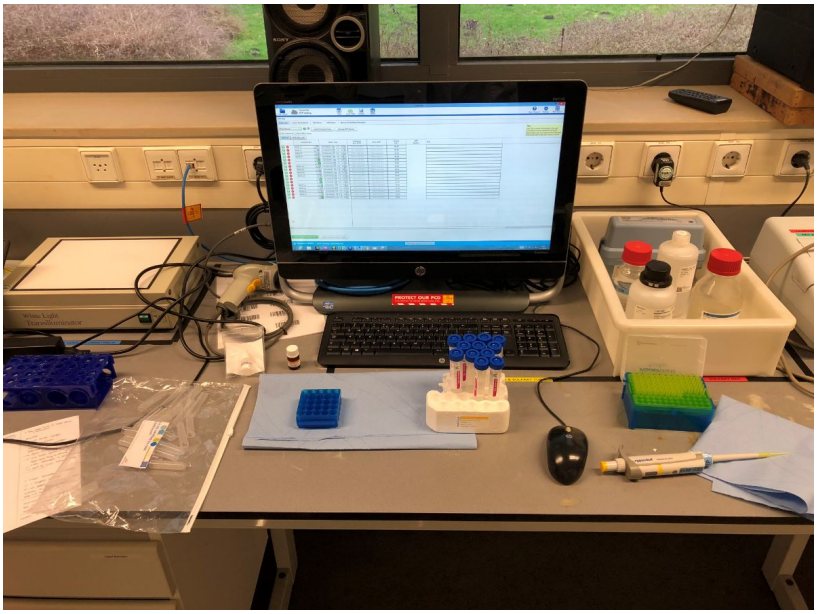

Figure 3.10: Setup and necessities for measuring ATP (step 6-10 in procedure description); enzymes, pipettes, sterile tubes, luminometer, computer

Interpretation of measured ATP concentrations

The measured ATP concentrations can be interpreted based on practical experience in the oil & gas industry. Table 3.7 shows the interpretation of different ATP concentrations based on microbial induced corrosion (MIC) risk assessments (ATP, 2016), literature and maufacturer guidelines (Eilers, 2019b, Patton and Foster, 2007d, van der Wielen and van der Kooij, 2010). MIC occurence depends on the presence of (sessile) bacterial colonies (section 2.7.3), like injectivity reduction does (colonies clog the well). Therefore, MIC risk assessments can be extrapolated also to injectivity problems in geothermal wells, caused by biological activity.

Table 3.7: Important boundaries and the interpretation of ATP concentrations

ATP concentration [pg/mL]	Microbial equivalents [cells/mL]	Interpretation in oil & gas industry
12	~1200	Maximum biological activity in Dutch tap-water by law
100	~100.000	Below this level, microbiologically induced corrosion (MIC) problems are not likely. Above this level, monitoring of the biological activity in the fluid is recommended. Preventative action can also be considered
1000	~1.000.000	Alarmingly high value of biological activity in process water. Serious problems related to microbes should be expected above this concentration

3.3.2. Measuring moments

Samples are always measured for their ATP content within 24 hours, to obtain the initial microbial activity. Just after that, sub-samples (aliquots) with additives are prepared if desired. Then, in the days following, the samples are always measured at least twice again (possibly more) to see the microbial growth evolution over time (and for aliquots: the effect of additives). So corrosion inhibitor or biocides are always added to a sub-sample 24 hours after sampling. That explains why those aliquots never have a '<24h' measurement. Figure 3.8 contains an overview of the actions and measurements that are performed after sampling. Also, table 3.8 gives an idea of how a possible data set from the samples in figure 3.11 will be reported.

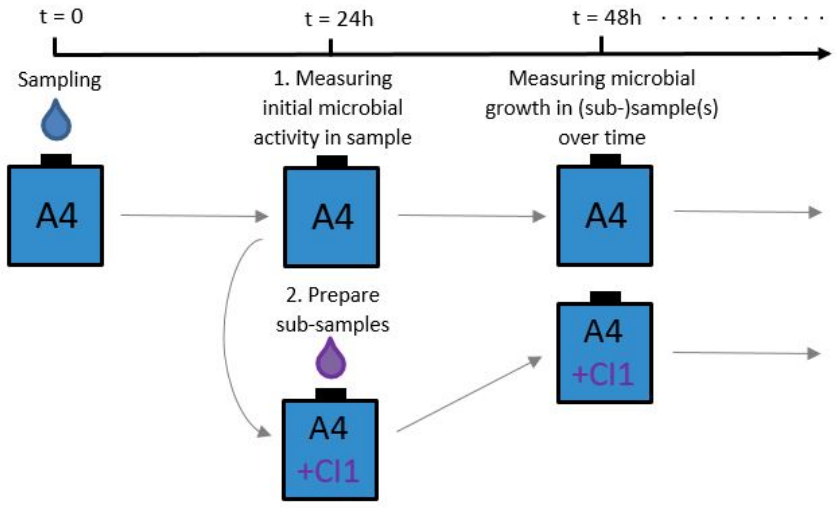

Figure 3.11: Time planning for measurements and actions on a sample after sampling

Table 3.8: Fictional ATP data for the example given in figure 3.11

	ATP content [pg/mL]			
(Sub-)sample	**< 24h**	**+48h**	**+....h**	**+....h**
A4	1.0	8.3	100.3	244.1
A4 + Cl1 [10ppm]		4.9	80.7	345.6

3.3.3. Sterile sample bottles

To guarantee reliable ATP measurements from the field samples, it is essential that all microbial activity in a sample originates only from the analysed water and not from other (external) sources of contamination (air, a dirty tap, or not-sterile bottles). Therefore, sterile sample bottles are of great importance. The following cleaning procedure is designed and tested to make sure sample bottles are free of any microbial activity before sampling. This sterilisation method is proven to be successful and produces sterile sample bottles (appendix A.2).

Sterilising sample bottles

1. Sample bottles are always standard cleaned in a dishwasher in the laboratory.
2. A clean sample bottle is sterilised using ethanol (96%). Two sprays of ethanol are put into the bottle, this volume is shaken around with a closed cap. After 10 seconds the bottle is emptied. This is done twice.
3. Next, the bottle is flushed with two sprays of acetone. After shaking vigorously, the bottle is emptied again. Because acetone has a lower density than ethanol, it will remove all the ethanol that might have stayed behind in the bottle. This is again done twice.
4. The bottle is dried with nitrogen coming from a pressure vessel. The nitrogen tube is sterilized every time before entering a sterile bottle.

3.3.4. Sample bottles

The conservation conditions of geothermal water after sampling should be ideally as close to the system conditions as possible. Every change in external conditions can possibly influence the microbial activity in the sample. As explained in section 2.7, temperature is the most critical factor together with oxygen content. So in order to keep samples at the same temperature, two types of sample bottles were available: thermos cans and coated glass bottles (figure 3.12).

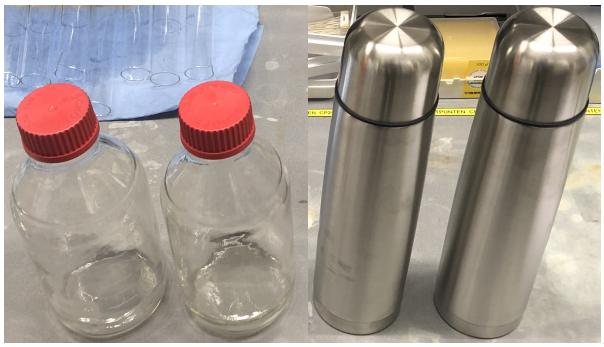

Figure 3.12: Different sample bottles: coated glass bottles (left) and thermos cans (right)

It has been shown by an experiment that thermos cans have a smaller temperature decline than glass bottles (Appendix A.3). Therefore, it has been (initially) decided to use thermos

cans to take samples. However, the type of sample bottles changed during the project, because of solid deposition on the sides of some thermos cans after the first time sampling at location A (29-01-2019). Since glass bottles gave comparable results on microbial activity (Appendix A.7) and are easier to clean, it has been decided to change to using glass bottles since then. So all samples taken at location B, location C and the last sampling moment at location A (27-03-2019) have been taken with coated glass bottles.

3.3.5. Sampling procedure

During the sampling moments on-site at the geothermal locations, local safety requirements were met and a set of personal protective equipment (PPE) was used.

PPE's used on-site

- protective clothing
- helmet
- safety shoes
- safety glasses
- gloves

In the geothermal systems, sample points can be different. An example of an easy accessible and operable sample point is given in figure 3.13. However, not all the desired sampling points did have the right equipment for sampling. Therefore, an adjustable tap was used (figure 3.14). This tap could be plugged into and disconnected again from the geothermal system. In order to reduce the risk of external contamination during sampling, a couple of guidelines were taken into account (listed below).

Figure 3.13: Example of a sample point at one of the geothermal locations of this study

Sampling guidelines

- The sample bottle may never touch the tap or any other parts of the geothermal system
- During sampling, the bottle cap is always held in one hand or laid upside down at a clean place above the ground
- Sterile gloves were used by the sample taker

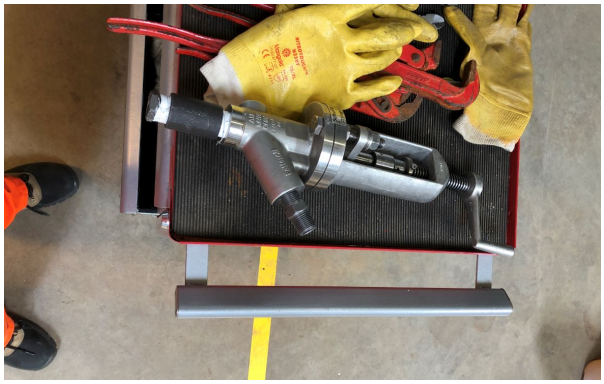

Figure 3.14: Adjustable tap used for sample points without a good tap facility

3.3.6. Duplo Samples

As one of the methods to check the quality of the acquired microbiological data, duplo samples are taken a couple of times throughout this study. A ”duplo” sample means that two sample bottles are filled at the same sample point at the same time and treated exactly in the same way. But the two bottles are considered as two different samples and measured separate from each other. By doing this it is possible to compare their data and check the reproducibility of the data (and whether the sampling and transport procedures and the treatments in the laboratory are done properly). The measurements of the duplo samples should be as close as possible in the ideal case, because you want your data to be reproducible. The following samples have been taken in duplo:

Duplo samples

- Location A (04-02-2019), sample ’A4’ and sub-sample ’A4 + CI1 [10ppm]’.
- Location C (08-04-2019), sample ’C5’ and sub-sample ’C5 + CI1 [40ppm]’.

3.3.7. Sample transport & conservation

After sampling, the samples are placed in insulating sample boxes and transported to Assen by car.

Figure 3.15: Sample box used to transport the sample bottles

Arrived at the laboratory, sample bottles are stored in an oven at their original temperature (figure 3.16).

Figure 3.16: Oven for storing samples at high temperatures in the laboratory

3.3.8. Oxygen free samples

In order to be sure that the anaerobic growth is measured, an ”oxygen free” sampling method has been designed. This sampling method was tested for the first time at the sampling at location B (05-03-2019) and is used in the sample moments that followed (table 3.11).

In this method, nitrogen is used to prevent any oxygen from intruding the sample. Every moment that the sample bottle is opened (when preparing the sterile bottle, during sampling, when preparing aliquots in the lab, when meauring ATP over time, etc.), nitrogen is bubbled through the water to avert any oxygen entering the sample bottle as shown in figure 3.17. On site, the nitrogen comes from a 500cc gas cylinder filled with 30 bar nitrogen and in the laboratory it comes from a vessel. The tube of the nitrogen outlet is always thoroughly sterilised before inserting it in the sample.

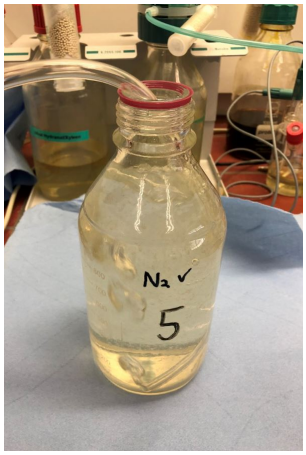

Figure 3.17: A sample is bubbled through with N_2 at the laboratory

Samples which are sampled ”oxygen free” and also have been treated afterwards to stay ”oxygen free”, have (N_2) in their name. It has been proven in extra oxygen measurements on different samples from location B that bubbling with nitrogen is successfully in terms of

really making the sample contain less oxygen. Those samples can be called ”oxygen free” and they represent anaerobic conditions (see appendix A.4).

3.3.9. Influence of Corrosion Inhibitors & Biocides

In most production & injection systems, chemicals are used to protect the equipment and mitigate operational issues. Examples of widely used chemicals are: scaling inhibitor, oxygen scavenger, acids, corrosion inhibitor and biodide. The last two are most frequently used in the geothermal systems of this study, so their working mechanisms is reviewed and their effect on the microbial activity in the geothermal water has been measured in so called ’kill tests’. The biocides and corrosion inhibitors that are used in the experiments for samples from a certain location, are always exactly the same as the chemicals that are injected in the geothermal system of that location in reality. Sometimes, the effects of chemicals from other locations have been tested as well to compare.

Kill tests

Certain concentrations of corrosion Inhibitor and Biocide are added to the geothermal water via intermediate solutions. For example, when an aliquot is prepared with 10ppm additive, first 1mL of that chemical is added to a 100mL flask with demi-water (using a syringe) to get a 10.000ppm intermediate solution. This flask is mixed and thereafter 0.1mL of the 10.000ppm intermediate solution is added to 100mL aliquot, resulting in a 10ppm concentration in the aliquot. This procedure is performed in a laboratory fume hood (figure 3.18).

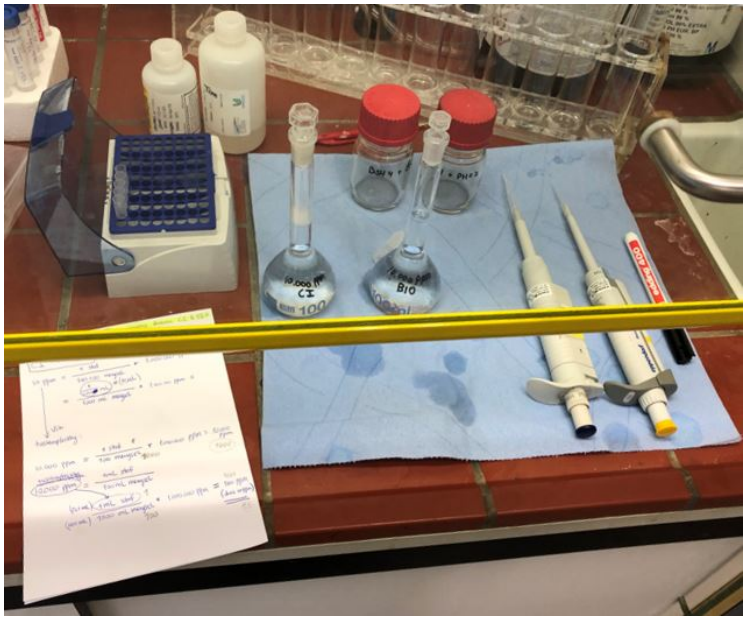

Figure 3.18: Equipment to add small concentrations of chemicals to geothermal water via intermediate solutions: flasks, syringe, plastic attachments, aliquot bottle, paper, marker

Corrosion inhibitor (CI)

Corrosion inhibitor is injected in a system to protect it against or slow down the corrosion forming process (section 3.3.9). Since corrosion inhibitor is injected downhole in the production well (section 2.4), geothermal water can distribute it through the whole system. Although most of it sticks to the casing wall of the production well, it should be noted that low CI concentrations (~2 ppm) are present in geothermal water in the surface system. So all samples contain this amount of corrosion inhibitor standard ((Reerink, 2019a)). In the kill test experiments, water samples get injected the type and amount of corrosion inhibitor that is also injected on-site at the location they come from. In addition, a 5 times higher dosage of corrosion inhibitor is tested in most of the tests.

Biocide (BIO)
Biocide is a widely used chemical for bacterial control in production & injection systems. A biocide kills all forms of life (section 2.7.5). In the kill tests, biocide is injected at the same concentration as on-site at the location. However, when dosing 100ppm biocide on-site, that is done continuously due to the large flow rate. When dosage stops, the concentration goes rapidly towards zero again, because new water removes it. However, in a sampling bottle just 1 injection of 100ppm is enough. The concentration will stay like that for a long time, because no supply of new water is present. It is important to keep this difference in mind.

An overview of the chemicals that are used in this study (and at which geothermal locations in reality) is shown in table 3.9. The first column contains the abbreviation (or "code") that is used for indication of the chemical substances through the rest of this report.

Table 3.9: Chemical products information

Code	Product Name	Type*	Main active substance	Used where
CI1	Corton CK990-G	CI	quaternair ammonium	locations A & C
CI2	CGW80007	CI	quaternair ammonium	location B
BIO1	Nalco 73500	BIO	glutaraldehyde	locations A & C
BIO2	Bactron UCA495-G	BIO	quarternair ammonium	-
BIO3	Bactron B1710	BIO	THPS	-

** Type of chemical: CI = corrosion inhibitor, BIO = biocide*

4

Results & Discussion

This chapter contains all the results of the different analyses and experiments that have been performed. Interpretations and discussions are also included. The results are divided into sections per geothermal doublet location. Within those sections, the data are divided into subsections containing different types of data (physical, chemical and microbiological). Note that when a result is reported as "<", the measured concentration is below the detection limit of the analysis method. To structure all the different data sets, a short summary is provided per location at the end of each section. A broader comparison between the different locations is given in section 4.4. That section also discusses issues that are not location-specific.

4.1. Location A

4.1.1. Total Suspended Solids (TSS)

Table 4.1 shows the suspended solid concentrations in the production water (sample A1) and injection water (sample A4) in the system of location A.

Table 4.1: TSS data location A (04-02-2019)

	Concentration	
Particle Diameter	**A1**	**A4**
> 5 μm	44 mg/L	< 8 mg/L
> 0.45 μm	48 mg/L	< 10 mg/L

Filtration with a smaller mesh size (0.45μm) logically results in a larger amount of suspended solids than filtering with a larger mesh size (5μm). However, no estimations about the size of the suspended solids can be made based on those numbers (section 3.1). It is clearly visible that TSS is removed through the system. Reported TSS concentrations for the injection water (<8 mg/L and <10 mg/L) are detection limits of the analysis method.

4.1.2. Chemical composition & Scale analysis

Chemical composition

The chemical composition of the production water at location A is presented in table 4.2. Concentrations of anions, cations, the alkalinity and pH are in the same order of magnitude as previously reported values for production water from reservoirs in the West Netherlands Basin (Griffioen et al., 2016, van der Weiden, 1983). Only the concentration of sulfate is quite low (<39 mg/L). At the same time, the detection limit is relatively high, due to the high chloride concentration in the water (section 3.2.3). Hardly any organic acids are measured (2.0 mg/L or less), which is normal for production water. Using the method described in section 3.2.5, a total carbonate concentration of 210 mg/L is measured. Using this value to calculate carbonate fractions (representative for the real situation) using the on-site measured pH, gives HCO_3 = 65mg/L and CO_2 = 107 mg/L. For bicarbonate, this amount is ~60% lower than the concentration found using alkalinity (160 mg/L). This difference is caused by other ions that also contribute to alkalinity, other than HCO_3 (section 3.2.4). This phenomena has obviously a larger impact than escaping CO_2 during and after sampling (section 2.8.2).

Table 4.2: Chemical composition Location A

Analysis Parameters	Result	Units
Sulphate (SO_4^{2-})	<39	mg/L
Bromide (Br^-)	35	mg/L
Phosphate (PO_4^{3-})	<5	mg/L
Chloride (Cl^-)	63000	mg/L
Total Iron ($Fe^{2+/3+}$)	35	mg/L
Sodium (Na^+)	32000	mg/L
Potassium (K^+)	250	mg/L
Calcium (Ca^{2+})	4300	mg/L
Magnesium (Mg^{2+})	850	mg/L
Strontium (Sr^{2+})	330	mg/L
Barium (Ba^{2+})	25	mg/L
Formic acid (CHOOH)	2.0	mg/L
Acetic acid (CH_3COOH)	< 2.0	mg/L
Propionic acid (C_2H_5COOH)	< 2.0	mg/L
Hydroxide (OH^-)	0.0	mg/L
Carbonate (CO_3^{2-})	0.0	mg/L
Bicarbonate (HCO_3^-)	160	mg/L
Total carbonate	210	mg/L
pH (@48.8°C)	6.0	-
Density	1.068	kg/L
Temperature	21.1	°C

Scale analysis

The chemical data in table 4.2 are used as input for scale modelling. The outcome of the scaling analysis for location A is shown in the graph of figure 4.1. Pre-scaling tendencies of dominant scales (calcium carbonate, barium sulfate and iron carbonate) are displayed through the different sections of the geothermal system. The main variables (pressure, temperature and pH) are plotted through the system as well.

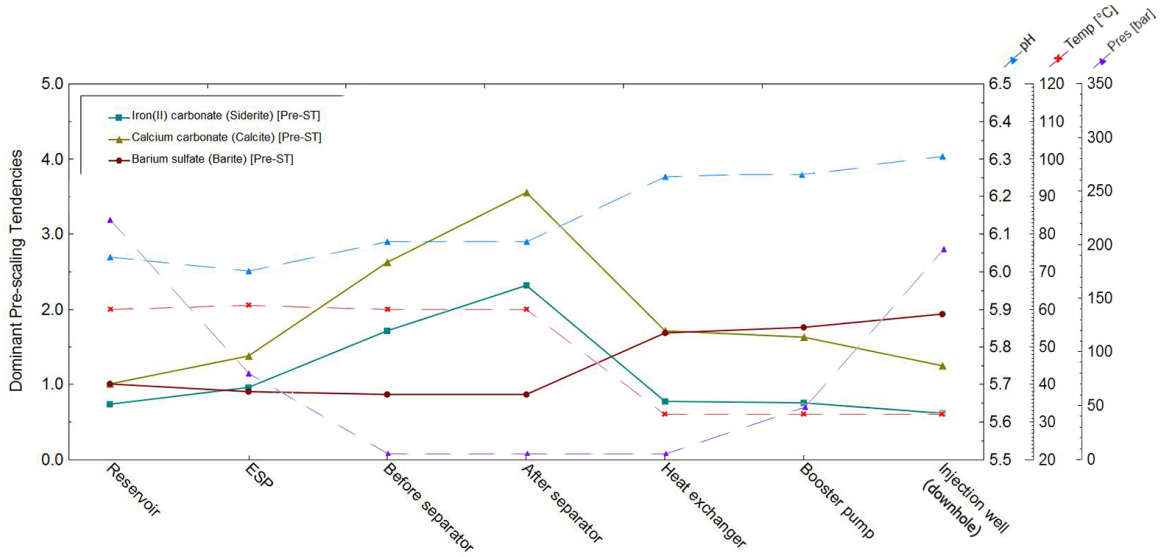

Figure 4.1: Scaling tendency (y-axis, left) and important physical/chamical variables (y-axis, right) through the different sections of the geothermal system (x-axis) at location A. Risk of carbonate scale formation increases towards peak risk just before the heat exchanger. After the heat exchanger, the risk of calcite scale decreases and the risk of barite scale increases. The highest scaling tendency for barite is found downhole in the injection well

At reservoir conditions, the formation water is saturated with barite and calcite (Ω=1), since it is in equilibrium with the reservoir rocks. When this water is produced and pressure decreases, the scaling tendencies for carbonate scales (calcite and siderite) increase while the risk on barite scaling stays equal. The peak scaling tendency for calcite (Ω ≈3.5) is found between the separator and the heat exchanger. The displayed tendencies apply thermodynamically. Whether scaling will actually occur is a matter of kinetics. Based on practical experience, a calcite scaling tendency of Ω ≈3.5 is interpreted as unlikely to cause significant productivity problems (Eilers, 2019d). After the heat exchanger, temperature decreases and pH increases which results in lower scaling tendencies for carbonate scales and a higher risk of barite scale. The peak risk for barite scale is found downhole in the injection well (Ω ≈2.0). It is not likely that barite scale will cause significant injectivity problems at these tendency values, based on practical experience (Eilers, 2019d). However, since NORM depositions are known to occur with barite scale, the obtained scaling tendency after the heat exchanger can cause NORM problems (Ω>1). The low specific activity (LSA) radiation can be problematic for example when cleaning surface facilities (section 2.8.3).

4.1.3. Microbial activity

The results of the ATP analysis are reported both in tables (raw data) and graphs (to visualize trends and comparisons between the different samples).

As described in the methodology (table 3.3), samples were taken at three different moments in time at this location. The results are reported and discussed in chronological order:
- 29-01-2019: original conditions
- 04-02-2019: three days after a biocide- and biodispersant-shock (24h, 300-500ppm)
- 27-03-2019: one month after acidification (24h, with acetic acid)

Interpretation of ATP concentrations

Horizontal dotted lines in all the graphs of the biological activity data, indicate important boundaries for biological activity (table 3.7 on page 35). Those boundaries are partially retrieved from MIC applications (ATP, 2016) and extrapolated to assess the risk of injectivity reduction by biological activity in geothermal wells. The green line (12 pg/mL) represents the maximum ATP concentration in Dutch tap-water by law. The yellow line (100 pg/mL) indicates a level below which no problems related to biological activity should be expected. Above this level, monitoring of the microbiology in a fluid stream is recommended. Alarmingly high values for biological activity (>1000 pg/mL) are reached above the red line.

Original conditions

After sampling, first the microbial activity is measured within 24 hours. Next, microbial growth in the geothermal injection water (sample A4) is measured over time. Aditionally, the effects of corrosion inhibitor (CI1) and biocide (BIO1) that are used at this location are analysed. Note that the reference sample (A4) already contains about 2ppm corrosion inhibitor (section 3.3.9). The results are displayed in table 4.3 and plotted in figure 4.2. Values are always given in picogram ATP per milliliter water, so multiplication with 1.000 gives the amount of microbial equivalents (ME) (section 2.7.2).

Table 4.3: ATP data Location A (29-01-2019)

	ATP content [pg/mL]*		
(Sub-)sample	**< 24h**	**+48h**	**+120h**
A4	8.5	419.8	540.1
A4 + CI1 [10ppm]		187.6	529.5
A4 + CI1 [50ppm]		1.3	877.5
A4 + BIO1 [100ppm]		1.1	0.6
A4 + BIO1 [500ppm]		0.8	0.3

**values x1.000 for microbial equivalents (ME)*

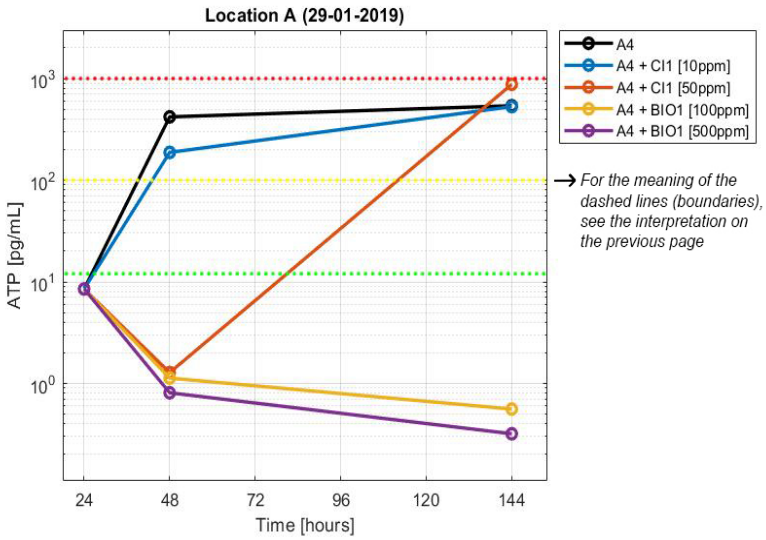

Figure 4.2: ATP concentration in geothermal water over time. For the dashed lines, Injection water sampled just before the reinjection well (A4) shows a rapid increase in biolobical activity. Aliquots with added corrosion inhibitor (A4 + CI1) show first a lower and in the end a similar or slightly higher biological activity compared to the reference sample (A4). Addition of biocide (A4 + BIO1) results in reduction of biological activity

The results show that initially (<24 hours after sampling) biological activity in the injection water is low (similar to Dutch tap water). Over time, the biological activity is increased rapidly to concentrations that would need monitoring if they were measured in a system (>100.000 ME/mL). The kill tests show that corrosion inhibitor has a time-dependent effect on this growth. Addition of 10ppm results first in a lower and in the end in a similar level of biological activity, compared to the reference sample. A concentration of 50ppm first reduces the biological activity (similar to the efficiency of a biocide), but in the end has a positive effect on the ATP concentration. In 6 days after sampling, the aliquot has reached an ATP concentration that is close to the level where microbiology is going to cause problems in a system. A possible explanation for this variable effect over time is that once the corrosion inhibitor is added to the water, first the biocidal side effect occurs (section 2.7.4), which kills a certain amount of the microbes that are present. After this effect has worked out, the corrosion inhibitor is nutrition for the microbes that were not killed initially and the biological activity can grow rapidly. Biocide decreases the biological activity in the injection water efficiently. Addition of a five times higher concentration than the 100ppm used on-site, results in (at the end) a two times lower bacterial activity. However, both concentrations result in values that are very low for process water (<10.000 ME's/mL).

After biocide shock

After the next sample moment, first the initial biological activity is measured again. Then, the microbial growth is analyzed over time in the injection water (sample A4), with extra aliquots created to test the effects of the corrosion inhibitor (CI1) and different kinds of biocides (BIO1, BIO2, BIO3 and BIOmix). This is performed in order to check the differences in effect between the biocides. 'BIOmix' is a self made mixture of the three biocides together in equal concentrations. The sample at the last point in the system before the injection well (A4) is taken in duplo, as well as the aliquot with added CI, to check the reproducibility of the data. Results are shown in table 4.4 and figure 4.3.

Initial microbial activity in the geothermal injection water (A4), measured within 24h after sampling, is about twice the Dutch tap-water norm now. This is three times as high as what was measured before the bio shock (figure 4.2). This can be the result of the fact that this measurement has been done ~3 hours later than after the first time sampling. Another explanation can be that one type of bactaria survived the bio-shock three days before. This type has no concurrence from others that were present before the shock. So they have free

Table 4.4: ATP data Location A (04-02-2019)

	ATP content [pg/mL]		
(Sub-)sample	**< 24h**	**+48h**	**+144h**
A4	25.5	414.6	566.3
A4 + CI1 [10ppm]		326.9	1015.6
A4 + BIO1 [100ppm]		1.5	1.5
A4 + BIO2 [100ppm]		2.8	1.5
A4 + BIO3 [100ppm]		2.4	1.0
A4 + BIOmix [100ppm]		3.5	1.9
A4 duplo	27.9	420.2	574.5
A4 duplo + CI1 [10ppm]		344.0	1010.7

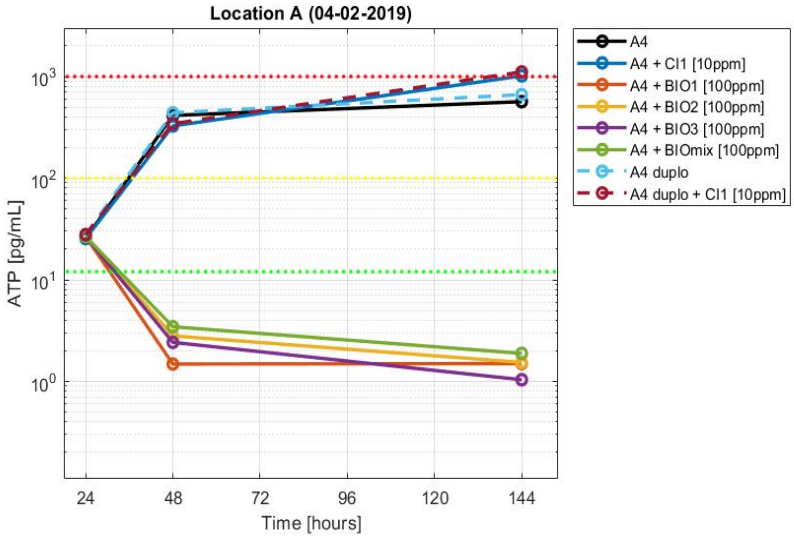

Figure 4.3: ATP concentration in geothermal water over time. Injection water sampled just before the reinjection well (A4) shows a rapid increase in biological activity. The aliquot with added corrosion inhibitor (A4 + CI1) shows first a lower, but in the end an almost doubled biological activity compared to the reference sample (A4). All aliquots with added biocide (A4 + BIO1/BIO2/BIO3/BIOmix) result in an efficient reduction of microbial activity. Duplo samples do not diverge more than 10%

reign and can grow faster. The same trend in microbial growth is visible as before the biocide shock. The effect of corrosion inhibitor is again time dependent: first it inhibits the biological activity, but in the end it enhances microbial growth. The same explanation can be given for this observation, as explained before the biocide shock. The different types of biocides all reduce microbial activity, with small mutual differences. BIO1 (the one that is used at this location) works a bit faster than the others. Duplo samples show the same trend and diverge not more than 10%. Note that this highest divergence holds for the lowest measured ATP concentration, so with the highest measuring error of the ATP measurment method itself. This confirms that the results are reproducible.

After acidification

The next sampling moment was performed after an acidification treatment in the system. After measuring the initial microbial activity, the growth over time is measured again for geothermal water sampled early in the system (after the separator, sample A2) and just before reinjection (sample A4). Different aliquots are created for the injection water to test different influences on microbial growth in this water: corrosion inhibitor (CI1), a low PH environment (pH=2) and biocide (BIO). Also, an extra production water sample from after the separator has been cooled down to injection water temperature (A2 @35°C), directly after the moment of sampling. The biological activity of this sample is measured over time to assess

the temperature dependence of the microbial growth. Furthermore, all those samples and sub-samples have an "oxygen free" variant (with 'N_2' in the name). Results are shown in table 4.5 and figure 4.4.

Table 4.5: ATP data Location A (27-03-2019)

	ATP content [pg/mL]		
(Sub-)sample	**< 24h**	**+48h**	**+120h**
A2	0.6	0.6	0.7
A2 (N_2)	1.2	0.5	0.3
A2 @35°C	0.4	0.5	1.7
A2 (N_2) @35°C	0.4	0.4	0.5
A4	1.8	1.1	0.5
A4 + CI1 [10ppm]		0.9	1.2
A4 + CI1 [50ppm]		1.7	0.8
A4 + pH=2		0.5	1.0
A4 + BIO1 [100ppm]		0.6	0.5
A4 (N_2)	1.9	1.4	0.4
A4 (N_2) + CI1 [10ppm]		0.5	0.5
A4 (N_2) + CI1 [50ppm]		0.6	0.9
A4 (N_2) + pH=2		0.3	0.3
A4 (N_2) + BIO1 [100ppm]		0.4	0.8

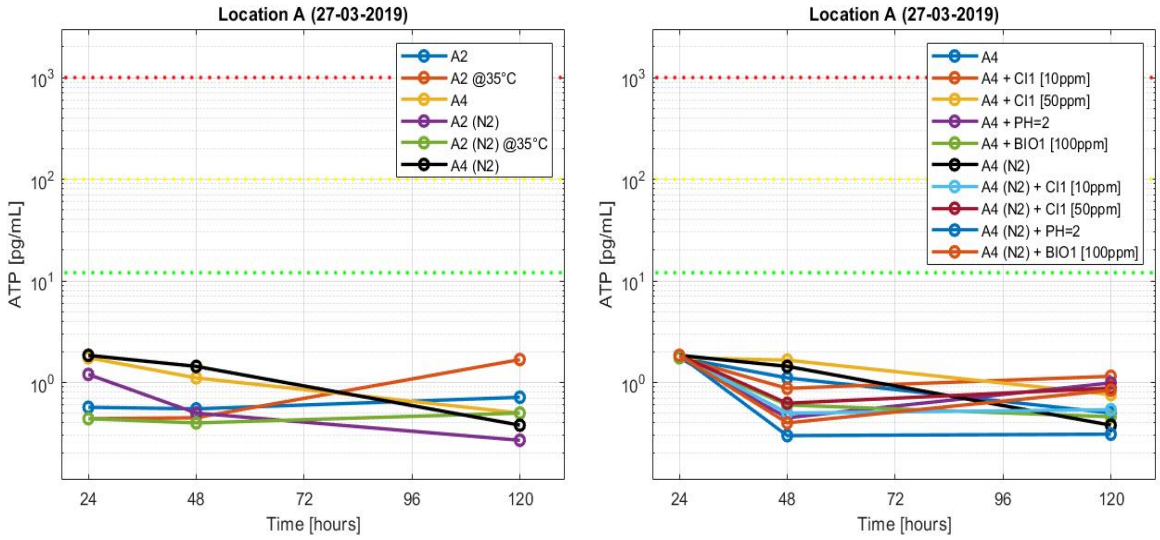

Figure 4.4: ATP concentration in geothermal water from different points in the system over time (left graph) and effects of different additives on injection water (right graph). Both production water (A2) and injection water (A4) samples, as well as production water at injection temperature (A2 @35°C) show initially very low bacterial activity and no microbial growth over time. Aliquots with added corrosion inhibitor (CI), biocide (BIO) and a low pH environment (pH=2) do not show any worth mentioning effects. Also oxygen free samples do not change anything in the observations

The results show a very low initial amount of microbial activity (<2.0 pg/mL through the whole system) and no microbial growth over time. Corrosion inhibitor, biocide, a low pH and the presence or absence of oxygen do not have any significant effects on the biological activity in the injection water.

It is striking that the biological activity in the geothermal water of this location seems to be gone after the acidification. Apparently microbes do not have the right living conditions in this water (anymore) to grow. It is difficult to imagine that this would be the result of the

acidification treatment, since a pH of 4.6 theoretically should not have any significant impact on biological activity. Logically a biocide shock should be more effective (since a biocide is designed to reduce biological activity) and that was measured to be not effective at all. An explanation for this unexpected observation (no biological activity anymore after acidification) has been sought in unusual process work, process interruptions, well interventions or not adequate dosage of the corrosion inhibitor on-site. However, none of these possible explanations appear plausible. A remaining explanation could be an inaccuracy in the sampling method during the first two sampling moments. For example the tap point and/or tap-tubes that have been used, could have been contaminated, which resulted in measuring microbial activity that is not really originating from the geothermal water. However, this is very unlikely because of all the measures that have been taken, such as tidy and sterile sampling (3.3.5) and verifying beforehand that the preparation and sample method is sterile (Appendix A.2).

Although the oxygen free samples did not show differences in the results for biological activity, samples will be taken "oxygen-free" as standard from now on. This has been decided to make sure the measured ATP is originating from anaerobic biological activity (injection well conditions).

4.1.4. Summary Location A

The most important results are summarized per different type of data.

TSS

- Normal amounts of suspended solids in production water (40-50 mg/L)
- Reduction through system by filters to below the detection limit (<10 mg/L for TSS >5μm)

Chemical composition & Scaling

- Geothermal water is low in sulfate (<39 mg/L), resulting in a reduced barite scaling tendency
- No volatile fatty acids are present in the water
- Other chemical properties of this water are normal
- Peak scaling risk in system is found just after the separator for carbonate scales ($\Omega \approx 3.5$) and to a lesser extent in the injection well (downhole) for barite scale ($\Omega \approx 2.0$). In practice, calcite is unlikely to create significant injection problems and barite scale can cause problems because of the possibility of NORM precipitation.

Microbiology

- Normal initial microbial activity (<30.000 microbial equivalents per mL)
- Microbial growth observed over time in injection water, at original conditions and after biocide shock
- CI1 has a time dependent effect on microbial growth. Finally it enhances microbial growth in injection water
- BIO1 reduces microbial activity
- Original situation and situation after bio-shock in this system do not differ much
- After system acidification, microbial activity is lower and there is no growth anymore. The reason for this has been sought in different causes, but stays unclear
- No differences between samples with and without oxygen found, because there was no microbial growth when testing this

4.2. Location B

4.2.1. Total Suspended Solids (TSS)

Table 4.6 shows the suspended solid concentrations in the production water (sample B1) and injection water (sample B5) in the system of location B.

Table 4.6: TSS data location B (05-03-2019)

	Concentration	
Particle Diameter	**B1**	**B5**
> 5 μm	37 mg/L	< 10 mg/L
> 0.45 μm	42 mg/L	11 mg/L

A larger amount of suspended solids is measured when filtering with a smaller mesh size (0.45 μm) than when filtration is done with a larger mesh size (5 μm). The results show that TSS is removed through the system. TSS is reduced to below the detection limit (<10 mg/L) for filtration with a 5 μm filter and to 11 mg/L for filtration with a 0.45 μm filter.

4.2.2. Chemical composition & Scale analysis

Chemical composition

The chemical data of the production water at location B is presented in table 4.7. Concentrations for anions, cations, alkalinity and pH are in the order of magnitude where they were expected. The density of this water (1.092 kg/L) is higher than the water at location A. This is relatable to the fact that most of the ions show higher concentrations, especially chloride. The detection limit for phosphate (<100 mg/L) is high. This has to do with the high chloride concentration in the water, which creates high and long continuing peak in the chromatogram. The peaks of the other ions in the chromatogram are hard to identify. To lower the peak of chloride, the sample needs to be diluted, which raises the detection limits. Lastly, some organic acids are present.

Table 4.7: Chemical data Location B

Analysis Parameters	Result	Units
Sulphate (SO_4^{2-})	210	mg/L
Bromide (Br^-)	200	mg/L
Phosphate (PO_4^{3-})	<100	mg/L
Chloride (Cl^-)	82000	mg/L
Total Iron ($Fe^{2+/3+}$)	65	mg/L
Sodium (Na^+)	43000	mg/L
Potassium (K^+)	330	mg/L
Calcium (Ca^{2+})	6000	mg/L
Magnesium (Mg^{2+})	790	mg/L
Strontium (Sr^{2+})	310	mg/L
Barium (Ba^{2+})	5.0	mg/L
Formic acid (CHOOH)	<2.0	mg/L
Acetic acid (CH_3COOH)	76	mg/L
Propionic acid (C_2H_5COOH)	6.9	mg/L
Hydroxide (OH^-)	0.0	mg/L
Carbonate (CO_3^{2-})	0.0	mg/L
Bicarbonate (HCO_3^-)	220	mg/L
pH (@60.1°C)	5.8	-
Density	1.092	kg/L
Temperature	21.4	°C

Scale analysis

The chemical data in table 4.7 are used as input for the scale modelling.The result of the scaling analysis for location B is shown in the graph of figure 4.5. Pre-scaling tendencies of dominant scales (calcium carbonate, barium sulfate and iron carbonate) are displayed through the different sections of the geothermal system. The main variables (pressure, temperature and pH) are plotted through the system as well.

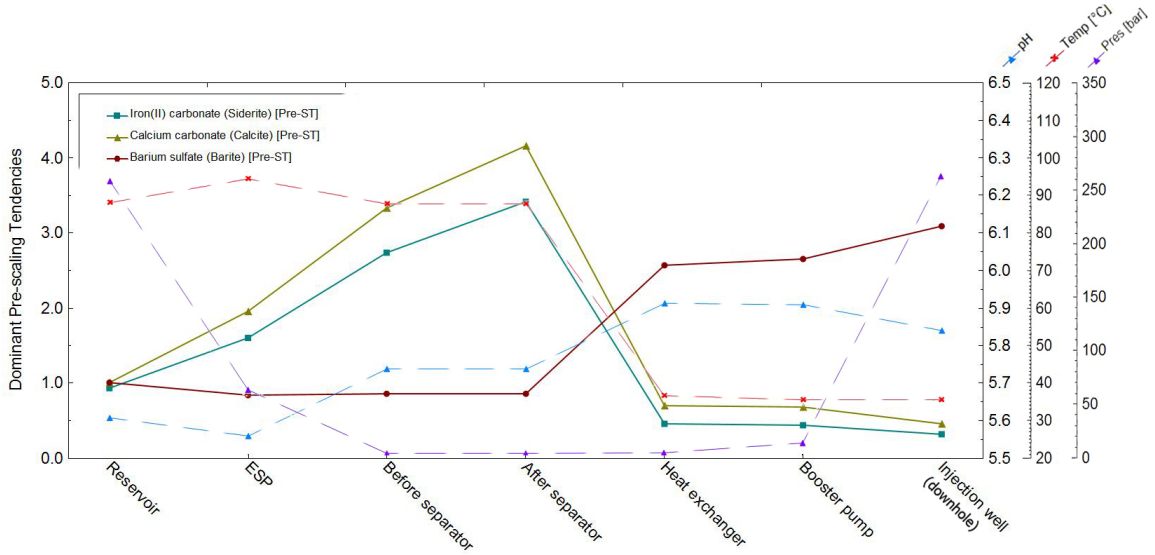

Figure 4.5: Scaling tendency (y-axis) through the geothermal system (x-axis) at location B. Risk of carbonate scale formation increases towards peak risk after the separator. After the heat exchanger, tendency of carbonate scales decreases significantly while the risk of barite scaling increases rapidly. The highest scaling tendency for barite is downhole in the injection well

At reservoir conditions, the formation water is saturated with barite and calcite (Ω=1), since it is in equilibrium with the reservoir rocks. Moving towards the surface facilities, the scaling tendencies for carbonate scales (calcite and siderite) increase while the risk on barite scaling stays equal. The scaling tendency increases till after the separator, where it reaches a value of Ω=4.1. Based on practical experience, this makes it kinetically just possible for calcite to actually form (Ω>4), and cause (significant) productivity problems (Eilers, 2019d). After the heat exchanger, temperature decreases and pH increases which results in significantly lower scaling tendencies for carbonate scales and an increase in scaling risk for barite. The peak risk for barite scaling is found downhole in the injection well (Ω ≈3.1). Barite scaling is kinetically unlikely to cause injectivity problems at these tendency values (Ω<5) (Eilers, 2019d). However, NORM depositions is likely to cause significant problems (Ω>1). So both scaling should be taken seriously at location B (section 2.8.3).

Precipitates in geothermal water of location B

Bulk precipitation was observed in the geothermal water from location B. Two types of solids were visible; reddish/brown fragments floating on the water surface and grey particles on the bottom of the sample bottles (figure 4.6). The phenomena arose ~30h after sampling and increased over time. The solids were observed in all oxygen free samples at this location but not in the samples with oxygen. Some solids were extracted from the fluid in sample B1 and analyzed under the microscope and using Energy Dispersive X-ray Fluorescence (EDXRF) (section 3.1.2). Results show that the major element in the particles is iron and minor elements are silicon and calcium. Based on the high iron content, these solids are most likely corrosion products (appendix A.6). The bottom and surface particles were similar in content, except for some minor trace elements (chloride and titanium). Individual particles are up to 200μm in diameter.

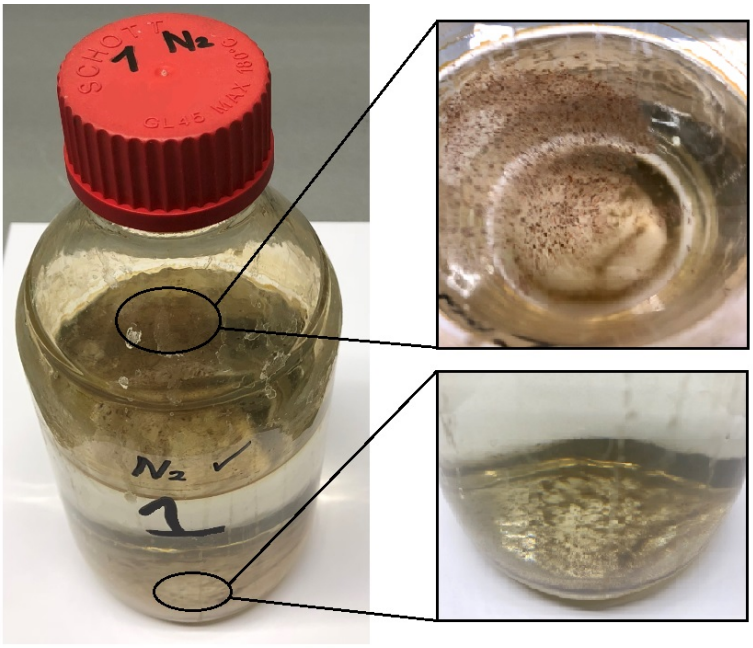

Figure 4.6: Solids formed in oxygen-free sample bottle "B1 (N_2)", 48 hours after sampling.

4.2.3. Microbial activity

Results of the ATP measurements at location B are reported again in tables and graphs. Horizontal dotted lines in the graphs indicate critical boundaries for bacterial activity, as explained in section 4.1.3). As described in the methodology (table 3.3), samples were taken at just one moment at location B: on 05-03-2019 (original conditions).

Original conditions

First the initial biological activity through the system is measured within 24 hours. Over time, the microbial growth is analysed in geothermal production water (sample B1) and injecion water (sample B5). The originally hot production water has also been tested at injection temperature (B1 @35°C). For injection water, the effects of addition of corrosion inhibitor (CI2), biocide (BIO1) and a low pH environment (pH=2) have been tested in aliquots. The ATP concentrations measured over time for location B are displayed in table 4.8 and figure 4.7. Although the effect of BIO1 has been tested on geothermal water from this system, it should be noted that in reality no biocide at all is injected in the geothermal system of location B.

Results are comparable with the last sampling moment at location A. The samples initially do not contain any worth mentioning amounts of biological activity (all <1 pg/mL) and over time no growth is measured in the injection water (B5), nor in the production water (B1). Also production water at injection temperature (B1 @35°C) shows very low bacterial activity (no growth) over time. Furhtermore, aliquots of the injection water with added corrosion inhibitor (CI2), biocide (BIO1) and a low pH environment (pH=2) do not show any significant effects on biological activity. Also oxygen free samples do not change anything in the observations.

Table 4.8: ATP data Location B (05-03-2019)

	ATP content [pg/mL]			
(Sub-)sample	**< 24h**	**+48h**	**+72h**	**+144h**
B1	0.3	0.3	1.6	0.4
B1 (N_2)	0.7	0.4	1.7	0.5
B1 @35°C	0.3	0.6	0.2	0.8
B1 (N_2) @35°C	0.2	0.8	0.6	0.7
B5	0.4	0.5	0.5	0.3
B5 + Cl2 [11ppm]		0.5	0.3	0.3
B5 + Cl2 [55ppm]		0.2	0.2	0.4
B5 + pH=2		0.5	0.4	0.2
B5 + BIO1 [100ppm]		0.3		0.2
B5 (N_2)	0.6	0.2	1.0	0.3
B5 (N_2) + Cl2 [11ppm]		0.2	0.3	0.3
B5 (N_2) + Cl2 [55ppm]		0.3	0.3	0.5
B5 (N_2) + pH=2		0.6	0.4	0.3
B5 (N_2) + BIO1 [100ppm]		0.3		0.5

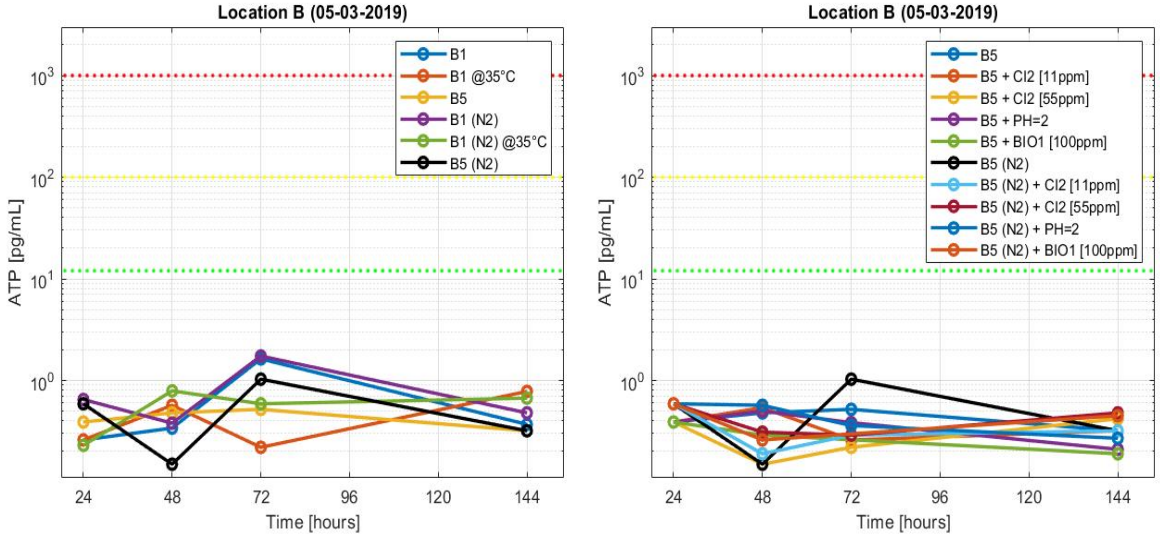

Figure 4.7: ATP concentration in geothermal water over time. At different points in the system (left graph) and effects of different influences on injection water (right graph). All samples and aliquots show very low bacterial activity (no growth) over time

4.2.4. Summary Location B

The most important results are summarized per different type of data.

TSS

- Normal amounts of suspended solids in production water (~40 mg/L)
- Reduction to below the detection limit (~10 mg/L) through system by filters Reduction through system by filters to below the detection limit (<10 mg/L) for TSS > 5μm in injection water. TSS > 0.45μm is not reduced to the detection limit (11 mg/L)

Chemical composition & Scaling

- Geothermal water has a high chloride concentration (82.000 mg/L) and a relative high density (1.092 kg/L)

- Some volatile fatty acids are measured
- Scaling tendencies in the geothermal system of location B are in general a bit higher than at location A, which is the result of higher ion concentrations in general at location B
- Peak scaling risks in system are found just before the separator (carbonate scales, $\Omega \approx 4.1$) and in the injection well (barite scale, $\Omega \approx 3.1$). These values for scaling tendency indicate that both scale types are likely to cause significant problems (calcite: productivity problems, and barite: NORM deposition problems)
- Bulk precipitation observed after sampling consists most likely of corrosion products or iron scales.

Microbiology

- Very low initial microbial activity (<1.000 microbial equivalents per mL)
- No microbial growth is observed over time in production water and injection water
- CI, BIO, acidic water (pH=2) and the absence/presence of oxygen do not change the observations (no growth)
- Results are similar to the last sampling moment at location A

4.3. Location C

4.3.1. Total Suspended Solids (TSS)

Table 4.6 shows the suspended solid concentrations in the production water (sample B1) and injection water (sample B5) in the system.

Table 4.9: TSS data location C (08-04-2019)

	Concentration	
Particle Diameter	**C1**	**C5**
> 5 μm	39 mg/L	<16 mg/L
> 0.45 μm	54 mg/L	<16 mg/L

The measured amount of TSS in the production water is significantly higher when filtration is done with a 0.45μm filter instead of with a 5μm filter (difference of 15mg/L). Although it seems logically to do, no estimations about the size of the suspended solids can be made based on these numbers, because bridging of small particles (even smaller than 0.45μm) could have occured (section 3.1). The results show that TSS is reduced through the system to below the detection limit (<16 mg/L) for both filter types. The detection limit is relatively high due to a small available water volume (0.3 L) for this analysis. On-site, an orange substance was observed on injection filters that were just replaced. The gunk contained iron, degraded corrosion inhibitor and some scaling products. Tool life of the filters varies from 13-100 days at this location, which is not bad (normal≈100 days).

4.3.2. Chemical composition & Scale analysis

Chemical composition

The water composition at location C is given in table 4.10. Concentrations for anions, cations and alkalinity are in the same order of magnitude as in comparable formation waters. Using the method described in section 3.2.5, a total carbonate concentration of 220 mg/L is measured. Calculating carbonate fractions using molar masses and the on-site measured pH, gives HCO_3 = 130mg/L and CO_2 = 68mg/L. The difference with location A is that a larger fraction of carbonates is now present as HCO_3 instead of CO_2. This matches with the slightly higher pH at location C, compared to the other locations (figure 2.15). The detection limit for phosphate (<100 mg/L) is high, due to the high chloride concentration (same as at location B). Organic acids have been measured in relatively high amounts (140 mg/l acetic acid).

Note on cations

Due to a broken cation measuring device in the laboratory, the cation concentrations have not been measured from sample C1. The displayed values (*) are obtained from an earlier analysis of the geothermal water from the production well at location C (Pirlea, 2015).

Table 4.10: Chemical data Location C

Analysis Parameters	Result	Units
Sulphate (SO_4^{2-})	310	mg/L
Bromide (Br^-)	210	mg/L
Phosphate (PO_4^{3-})	<100	mg/L
Chloride (Cl^-)	79000	mg/L
Total Iron ($Fe^{2+/3+}$)	15	mg/L
Sodium (Na^+)	42000*	mg/L
Potassium (K^+)	670*	mg/L
Calcium (Ca^{2+})	5800*	mg/L
Magnesium (Mg^{2+})	880*	mg/L
Strontium (Sr^{2+})	350*	mg/L
Barium (Ba^{2+})	4.1*	mg/L
Formic acid (CHOOH)	<2.0	mg/L
Acetic acid (CH3COOH)	140	mg/L
Propionic acid (C2H5COOH)	12	mg/L
Hydroxide (OH^-)	0.0	mg/L
Carbonate (CO_3^{2-})	0.0	mg/L
Bicarbonate (HCO_3^-)	130	mg/L
Total carbonate	220	mg/L
pH (@57.9°C)	6.5	-
Density	1.086	kg/L
Temperature	21.1	°C

** Data not extracted from sample C1, but from earlier analysis of production water from this well*

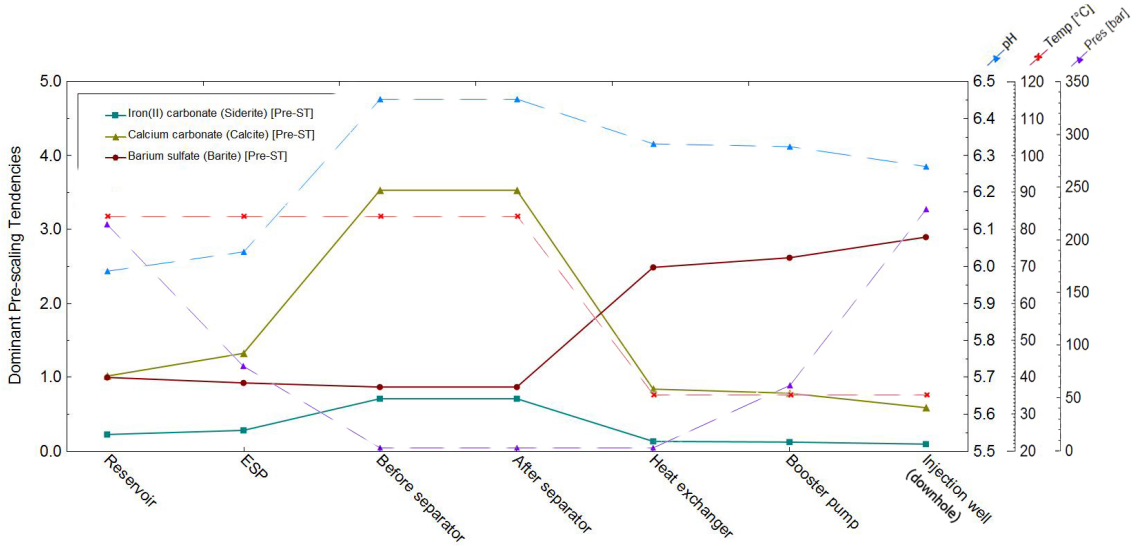

Figure 4.8: Scaling tendency (y-axis) through the geothermal system (x-axis) at location C. Risk of several carbonate scale formations is the highest between the ESP and the separator. Tendency for of calcite scales decreases a bit after the separator and drastically after the heat exchanger. The risk of Barite scaling decreases rapidly after the heat exchanger. Highest scaling tendency for Barite is in the injection well

Scaling analysis

The result of the scaling analysis through the system of location C is shown in figure 4.8. Pre-scaling tendencies of dominant scales (calcium carbonate, barium sulfate and iron carbonate) are displayed through the different sections of the geothermal system. The main variables (pressure, temperature and pH) are plotted through the system as well. In the system of location C, the scaling tendency for siderite is significantly lower (Ω<0.9 through the entire system) than at the other locations. This is a result of a relative low iron concentration at location C (15 mg/L). The highest scaling tendency before the heat exchanger is found for calcite around the separator ($\Omega \approx 3.5$). Kinetically, calcite precipitation can form. However with this scaling tendency (Ω<4.0) it wil be unlikely for calcite to cause significant productivity problems. After the heat exchanger, the risk of calcite scaling decreases and the risk of barite scaling increases. Barite has its scaling tendency peak downhole in the injection well ($\Omega \approx 3.0$). Barite scale formation is interpreted as unlikely to create injectivity problems (Ω<5), but likely to cause NORM deposition problems (Ω>1) (Eilers, 2019d).

4.3.3. Microbial activity

As described in the Methodology (table 3.3), samples were taken at two different moments in time at location C:

- 08-04-2019: original conditions
- 15-04-2019: four days after a biocide- and biodispersant-shock

Original conditions

This time, microbial growth in the water was measured initially and over time for all the different sample points in the system. Furthermore, the effect of corrosion inhibitor (CI1), biocide (BIO1) and a low pH environment (pH=2) has been measured over time. The sample of the injection water (C5) has been taken in duplo. From that duplo sample, an extra aliquot was made (C5 (N_2) duplo + CI1) in which the effect of CI1 has been tested. The results are displayed in table 4.11 and figure 4.9.

Initial biological activity is low (equal or lower than Dutch tap water) in the whole geothermal system of location C. Note that all the samples are taken according the ”oxygen-free” procedure this time, so those values are all about anaerobic biological activity. Over time, the biological activity in the injection water increases to values that need monitoring when measrured in a system (>100.000 ME’s/mL). The microbial growth occurs more slowly than was observed at location A: ATP concentrations > 100 pg/mL are measured now from 96 hours after sampling, while this already happened at 48 hours after sampling at location A. The initial biological activity is also lower, which can explain why more time is needed to grow. Although the biological activity in the duplo sample from the injection water (C5 duplo) deviates up to 50% (at +72h after sampling), the measured ATP values confirm the trend in the reference sample. In end-value, they differ ≈ 20%, which could indicate a faster nutrient limitation for the lower sample than for the higher sample. This matches with the trend that is visible (first the duplo sample gives lower ATP concentrations, and in the end higher ones), it is similar to the addition of different concentrations of corrosion inhibitor (figure A.11). Chemical injection is not always directly homogeneous over time, so a possible explanation is that the reference sample (C5) contained a bit less CI1 than the duplo sample (C5 duplo).

In other samples than the injection water, no increase in biological activity is observed. The fact that sample C4 doesn’t show any microbial growth over time (and C5 does), suggests that it is not just the temperature decrease in the geothermal system after the heat exchangers that creates the growth (because C4 is also on the ’cold’ side of the heat exchanger). Apparently there is something present in the geothermal water causing the increase in biological activity after the injection filters (C5) that is not there yet before those filters (C4).

Furthermore, corrosion inhibitor (CI1) enhances microbial growth in the injection water. In 96 hours after sampling, the aliquot with 40ppm CI1 has reached an ATP concentration

that exceeds the level where microbiology is expected to cause problems in a system. Biocide decreases the biological activity in the injection water efficiently to a very low level (<1.000 ME's/mL), as does acidification of the water to pH=2. The small peak in biological activity in the aliquot with pH=2 (at +96 hours) is probably an outlier, as the value decreases again in the next time step and lies outside of the trend.

Table 4.11: ATP data Location C (08-04-2019)

	ATP content [pg/mL]					
(Sub-)sample	**< 24h**	**+48h**	**+72h**	**+96h**	**+192h**	**+240h**
C1 (N_2)	0.7		0.3			0.3
C2 (N_2)	2.1		0.2			0.4
C4 (N_2)	0.5		0.2			0.3
C5 (N_2)	1.0	10.4	46.6	215.2	215.7	
C5 (N_2) + CI1 [8ppm]		8.0	92.5	517.1	806.5	
C5 (N_2) + CI1 [40ppm]		13.3	278.7	1796.3	1884.7	
C5 (N_2) + pH=2		0.3	0.2	3.51	1	
C5 (N_2) + BIO1 [100ppm]		0.6	0.2	0.2	1.2	
C5 (N_2) duplo	0.3	11.0	23.5	284.5	260.5	
C5 (N_2) duplo + CI1 [40ppm]		13.8	294.7	1763.8	1663.1	

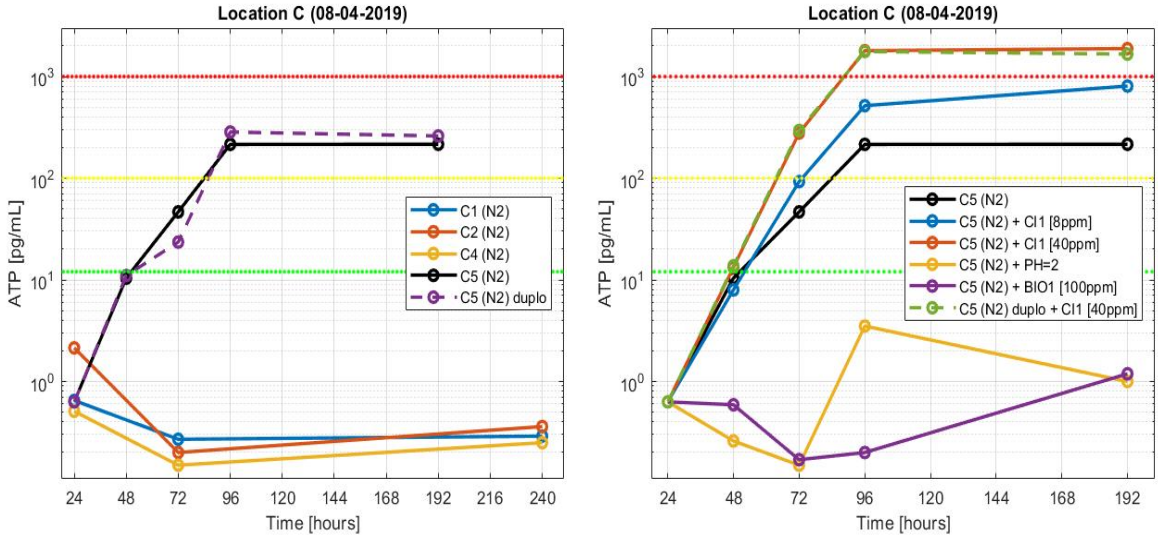

Figure 4.9: ATP concentration in geothermal water over time, at different points in the system (left graph) and the effect of different chemical additions (right graph). Geothermal water from before and after the separator (C1 and C2) and before the injection filters (C4) show low biological activity over time. Injection water sampled after the injection filters (C5) shows an increase in biological activity over time. Addition of corrosion inhibitor (CI1) enhances this growth, while biocide (BIO1) and a low pH environment (pH=2) keep the biological activity low. Duplo samples show similar trends

After biocide shock

First the microbial activity through the system is measured again within 24 hours. Next, the microbial growth over time in geothermal injection water from sample points before (C4) and after (C5) the injection filters have been measured. The latter has also been taken under aerobic (with oxygen) conditions. The effect of corrosion inhibitor (CI1) and biocide (BIO1) on the injection water is tested as well. Results are shown in table 4.12 and figure 4.10.

Table 4.12: ATP data Location C (15-04-2019)

	ATP content [pg/mL]			
(Sub-)sample	**< 24h**	**+72h**	**+192h**	**+240h**
C4 (N_2)	0.3		0.7	0.5
C5	0.2	0.3	38.8	117.3
C5 (N_2)	0.2	0.4	94.4	146.9
C5 (N_2) + CI1 [8ppm]		1.2	255.8	500.3
C5 (N_2) + CI1 [40ppm]		1.1	1679.9	1790.2
C5 (N_2) + BIO1 [100ppm]		0.6	0.2	0.7

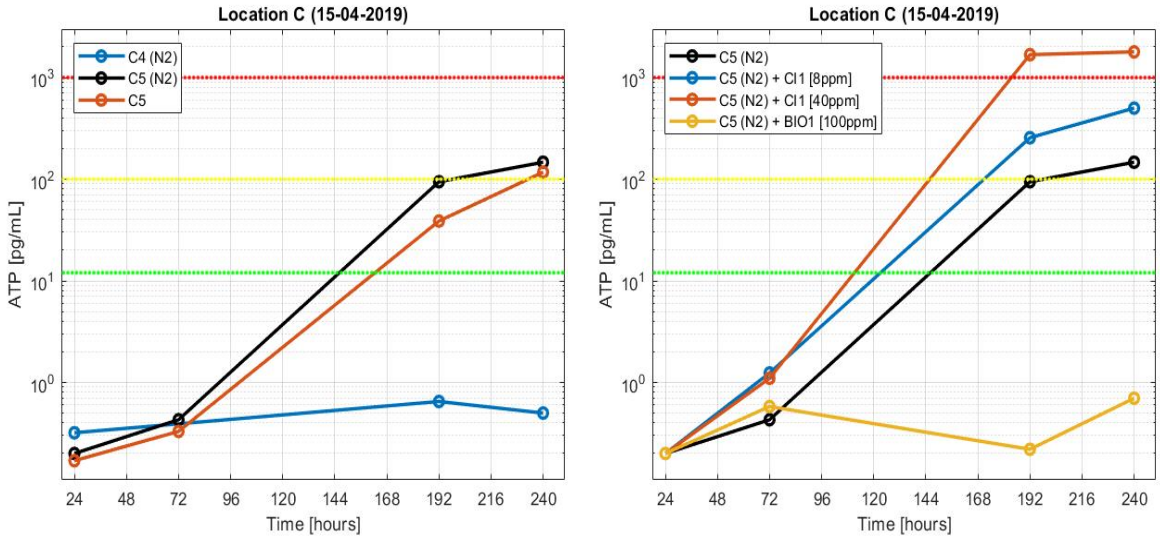

Figure 4.10: ATP concentration in geothermal water over time. Microbial growth at different points in the system (left graph) and the effect of different chemical additives (right graph) on that growth. Injection water sampled after the injeciton filters (C5) shows an increase in biological activity over time, while no growth is visible in injection water sampled before the injection filters (C4). Corrosion inhibitor enhances microbial growth to a severe level. Biocide keeps the biological activity low

Initial biological activity of the injection water (before and after the heat exchanger) is very low (<500 ME's/mL). Over time, microbial growth is observed in the water sampled after the heat exchanger (C5), while the water sampled before the injection filters (C4) does not show any increase in biological activity again. The microbial growth starts relatively slowly now compared to the growth in this water before the biocide shock. At 240 hours after sampling, ATP concentrations are reached that are a bit lower, but quite similar to what was measured before the biocide shock. The biological activity in the oxygen-free injection water sample (C5 (N_2)) is a bit higher, but quite comparable to the sample with oxygen access. This indicates that the biological activity that is measured may come from facultative anaerobic bacteria. They can function in absence of and in presence of oxygen (section 2.7.1). However, this may also not be the case, since those type of bacteria should actually show extra growth when oxygen is present. Addition of CI shows the same effects as have been observed before the biocide shock, the biological activity reaches a severe level (> $1*10^6$ ME's/mL). Addition of biocide (100ppm) keeps the biological activity on the initial, very low level.

4.3.4. Summary Location C

The most important results are summarized per different type of data.

TSS

- Normal amounts of TSS in production water (35-55 mg/L), significant differences between measurements with different filter sizes

- Reduction through the system by filters, to below the detection limit (<16 mg/L for both filter sizes)

Chemical composition & Scaling

- Geothermal water has a quite high TDS and density (1.086 kg/L)
- Volatile fatty acids are present in the water (140 mg/L acetic acid, 12 mg/L propionic acid)
- pH is slightly higher than at other locations (pH=6.5). Other chemical properties of this water are normal
- Peak scaling risk in system is found around the separator for carbonate scales ($\Omega \approx 3.5$) and for barite scale downhole in the injection well ($\Omega \approx 3.0$). In practice, calcite and barite are unlikely to cause flow problems at those scaling tendencies. For barite scale, NORM deposition is likely to cause significant problems. This forms a risk for barite

Microbiology

- Low initial biological activity through the geothermal system (< 2.000 ME/mL). After the bioshock even lower (< 400 ME/mL)
- Increase of biological activity observed over time in injection water sampled after the injection filters. This microbial growth starts quite late (about 48 hours later than growth at location A)
- CI enhances microbial growth in injection water (at peak growth: 3.5 times more biological activity with 8ppm CI1, 12 times more biological activity with 40 ppm CI1)
- BIO1 prevents microbial growth (biological activity stays at initial concentration)
- Very small differences in microbial growth between samples with and without oxygen. Possibly facultative anaerobic bacteria present
- No increase in biological activity over time observed in geothermal water sampled before the injection filters
- Natural situation and situation after bio-shock in this system do not differ a lot, growth of biological activity over time is a bit less (~ 25%) after the bio-shock
- Duplo samples deviate a maximum of 50%. This difference is possibly caused by inhomogeneous distribution of corrosion inhibitor through the system water. However, duplo's show similar microbial growth trends

4.4. Comparison between the locations

This chapter discussed issues that are applicable to all locations, gives interpretations on the results and makes a comparison between the locations.

4.4.1. Total Suspended Solids (TSS)

The TSS values are in general at levels where they should be expected for Dutch production water (section 2.6). For all the locations, TSS values in the geothermal water are lower before reinjection than just after production. This can be explained by the fact that production filters (all locations) and injection filters (location B and C) are present between those sample points. In figure 4.11, the TSS data of the three locations are plotted together in one graph.

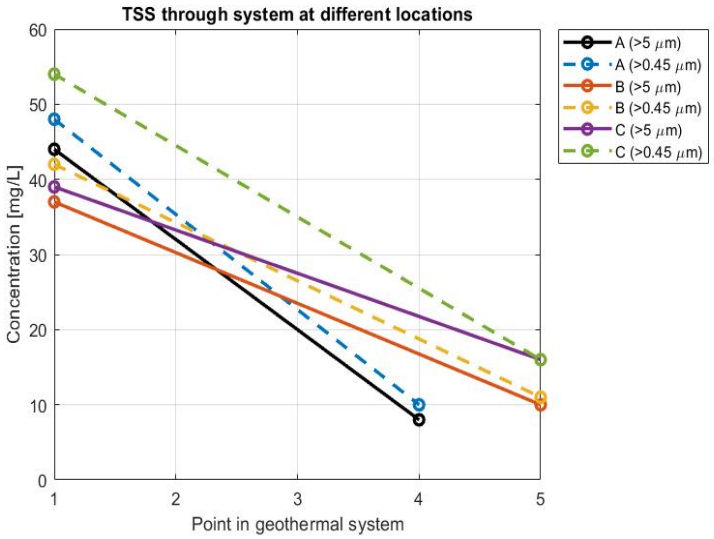

Figure 4.11: TSS quantities through different geothermal systems. TSS values decrease at all locations from before the separator (1) to after the heat exchangers (4) or after the injection filters (5)

It is clearly observable that concentrations of suspended solids in the water samples decrease through the geothermal systems at all the locations. Filters in the system reduce the amounts of suspended solids with at least 59% (mostly below the detection limits). So based on this data it is safe to say that filters in the systems are working well. However, based on these results, TSS related injectivity issues in geothermal wells should not be underestimated. The detection limits that have been measured (8-16 mg/L) are sufficient for water injection activities of NAM (section 2.6). However, in geothermal projects water is not a by-product such as in oil & gas operations. Therefore, larger amounts of water are injected, which increases the total amount of suspended solids that is injected (equation 4.1).

$$TotSI = Vw * TSS \tag{4.1}$$

Where:
TotSI = total amount of solids injected [mg],
Vw = volume of water that is injected in a certain amount of time [L],
TSS = concentration of total suspended solids in the injection water [mg/L].

So low concentrations of TSS can be more problematic in geothermal injection wells (compared to water reinjection in oil & gas systems) since large amounts of water are injected (up to 400.000 L/h). On the other hand, this large water flow can help again to 'flush' clogged solids away. Although the quantities of TSS found in the injection waters in this project (< 8-16 mg/L) are comfortable based on experience in the oil & gas industry, they should preferably be lower for geothermal injection wells (<1 mg/L) (section 2.6). The likelyhood of TSS being the main problem for injectivity reduction is small, but it can not be excluded either.

Detection limits

- The TSS concentrations of the injection waters are, except for the 0.45μm filter result at location B, always detection limits of the gravimetric determination method. Although there is statistically no proof, it is very likely that actual TSS concentrations are lower than these detection limits. Based on practical experience and an improved way of preparing control samples in the laboratory, it is quite safe to interpret these detection limit values as twice as low (Kweekel, 2019a).
- Detection limits vary between the locations. This is because different volumes of water were used for filtration, depending on how much was available after sampling (Appendix A.1). The larger volume of water is used, the lower the detection limit will be. Location A has the lowest TSS amount (detection limit) measured in the injection water, but it was the only location without injection filters. This may be purely caused by the fact that a larger volume of water was available for TSS measurement here than for the other locations.
- Quantities of TSS are known at the first and last point in the system. For location B, it is known that the production filters cause the TSS difference between those points. For location A and C, two types of filters (production & injection) are located between those point so it is not known which filters captured the most suspended solids. Furthermore, different filter types and sizes (from different suppliers) are used at different locations (table 3.4 on page 26). These factors can influence the effectiveness of the filters.

External factors influencing TSS measurements

As this study investigates injectivity problems in geothermal systems, the analysis results should ideally reflect what really happens in the geothermal systems. In theory, degassing (and to a lesser extent cooling down) of samples may have led to mineral precipitation and therefore higher measured TSS values than in reality in the system. Visible precipitation in the samples has been observed one time: in the oxygen-free samples from location B (section 4.2). This phenomenon started after ~30 hours, which is after the time limit for TSS measurement (<24 hours after sampling). Therefore, those formed solids did most likely not influence the TSS results. The procedure of sampling is modeled in *Stream Analyzer* to check the precipitation that can form due to sampling (Appendix A.10). The result confirms the assumption that changes after sampling did most likely not influence the TSS results.

4.4.2. Chemical compositions & Scale analysis

Chemical compositions

To see the link between the chemical composition of the waters and the scaling tendencies at the locations, the chemical data are compared in a Stiff diagram (Stiff, 1951) in figure 4.12.

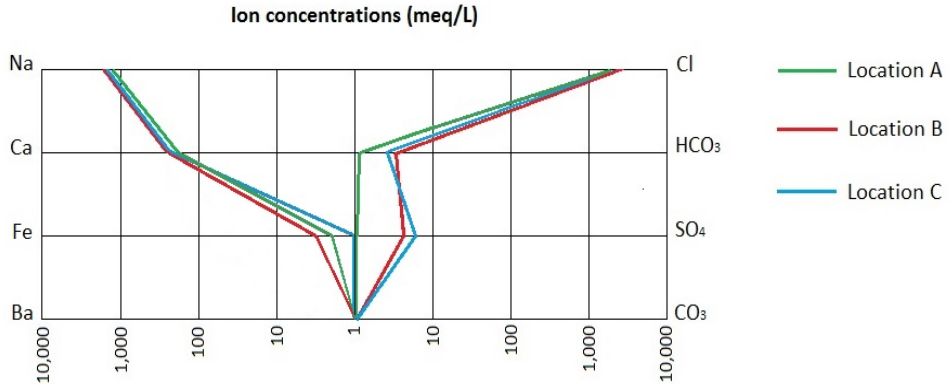

Figure 4.12: Main chemical composition of the different geothermal waters displayed in a Stiff diagram. Green = Location A, Red = Location B, Blue = Location C. The lines are mostly close together, so chemical compositions are similar. Only concentrations of sulphate, iron and bicarbonate show more variation between the locations

Original ion concentrations in mg/L as presented in tables 4.2, 4.7 and 4.10 are converted to milliequivalents per liter by dividing them through the ions equivalent weight (which is the atomic weight over the ion charge). Concentrations in meq/L are plotted in the Stiff diagram. The Stiff method is the most universally used fluid composition representation method in the oil & gas industry (Patton and Foster, 2007c). Concentrations of the main cations and anions are plotted on a logarithmic axis, to easily see similarities and/or differences between the different locations (figure 4.12). Most noticable differences between the locations are found in the concentrations of iron and sulphate. This correlates to the scaling tendencies for siderite and barite. For example, water at location C has a low iron content (15 mg/L so 0.75 meq/L), resulting in a lower scaling tendency for siderite compared to other locations.

Nitrate/ nitrite
Concentrations of nitrate and nitrite (NO_3^-/ NO_2^-) have been measured in sample 1 at all locations. However, they are not included in the result tables (to save space) since only values of 0 mg/L were found.

Scale analysis
At all locations, the highest scaling tendency before the heat exchanger (hot side) was observed for calcite and the highest scaling tendency after the heat exchanger (cold side) was observed for barite. This matches with the temperature dependency of barite precipitation and the pressure & pH dependency of calcite precipitation (section 2.8.1). At all locations, the separator (or just after it) is found to be the peak risk point in the system for calcite scale and the injection well (downhole) has the highest scaling risk for barite scale. The scaling tendency for siderite is the highest at location B, where the geothermal water also has the highest total iron content. Barite scaling tendency is the lowest at location A, where the lowest sulfate concentration is observed. Overall, scaling tendencies in the geothermal systems are not alarmingly high (never >5). However, sometimes they are at levels that tell us that light scaling can possibly occur. This observation fits with the latest update from several geothermal systems in the Netherlands, that small amounts of carbonate scales have been observed before the heat exchangers (Eilers, 2019b).

General note on scales
The three scale types shown in the graphs (calcite, barite and siderite) are not the only ones that can possibly form, but just the most dominant ones. Appendix A.9 shows an example of the scale analysis for location A, including all minor scales. Since their addition to the analysis result is limited, it has been decided to exclude these minor scales from the overviews (to keep the graphs clear).

4.4.3. Microbial activity

The results of all biological activity measurements are summarized in the overview of table 4.13. Per location and sample moment, the initial biological activity (<24 hours) and peak growth over time (highest ATP value reached) are shown for production and injection water. Also it shows the effect of corrosion inhibitor (5 times the on-site concentration) on the growth in injection water. The table shows that initial biological activity (measured <24 hours after sampling) in production and injection water is always low (<25.500 ME/mL and often <2.000 ME/mL). Over time, increase in biological activity (microbial growth) is only observed in injection water and only at locations A and C. So the few microbes that are initially present, are able to multiply in injection water over time. An interesting observation, since that does not happen by default when putting any type of water sample in an oven (Appendix A.5). Growth is never measured in production water and at location B. Sometimes, maximum growth value is lower than the initial biological activity. This can imply the death of microbes. Corrosion inhibitor (CI) always increases the achieved peak in biological activity when there is growth.

Table 4.14 shows a summary of other factors that can possibly influence the biological activity at the different locations: which reservoirs they produce from, whether basin water from the well testing phase has been reinjected or not, and to what extent they experience in-

jectivity reduction. Also whether energy carriers/nutrients such as volatile fatty acids (VFA), nitrate and nitrite have been measured and which corrosion inhibitor is used on-site.

Table 4.13: Summary of all biological activity measurements

Location	Sampling moment		Biological activity [pg ATP/mL]					*Comments*
			Prod.		Inj.			
			Initial	Growth	Initial	Growth	+ CI	
A	29-01		1.4	-	8.5	540.1	877.5	*growth measured, CI enhances growth*
	04-02		0.2	-	25.5	566.3	1015.6	
	27-03		0.6	0.7	1.8	0.5	0.8	
		N_2	1.2	0.3	1.9	0.4	0.9	
B	05-03		0.3	1.6	0.4	0.5	0.4	*no growth measured*
		N_2	0.7	1.7	0.6	1.0	0.5	
C	08-04	N_2	0.5*	0.3*	1.0	215.7	1884.7	*growth measured, CI enhances growth*
	15-04		0.5*	0.3*	0.2	117.3	-	
		N_2	0.3*	0.7*	0.2	146.9	1790.2	

**water sampled at point C4 (after heat exchanger)*

Based on tables 4.13 and 4.14, microbial growth is measured at locations (A and C) that also experience injectivity reduction. Location B does not experience injectivity reduction, and microbial growth is not measured here. So biological activity is correlatable to injectivity reduction. Furthermore, basin water (stored during the well testing phase) has been reinjected at these locations. The difference in reservoirs seem not to be correlatable with microbial growth. The same applies to nitrate and nitrite, since these (possible) nutrients are not detected at any of the locations. The presence of volatile fatty acids (VFA) at location C, can be a reason for the peak growth at this location being about twice as high as at location A. VFA's present in the geothermal water can be nutrients for the microbes at location C, and enhance their growth. However, the microbes at location B could obviously not use the VFA's for growing (while VFA's are also present in the water at loation B).

Table 4.14: Summary of important (microbiology related) information per location

Location	Reservoir	Basin water reinjected?	CI	NO_2 /NO_3	VFA	Injectivity reduction?
A	Delft sst (+ Berkel)	CI1	no	no	yes	yes (small)
B	Delft sst	CI2	yes	no	no	no
C	Buntsandstein (Trias)	CI1	yes	no	yes	yes (big)

The effects of chemicals on bacterial activity

- The effect of biocide-shocks on-site is not relatable to initial biological activity nor to microbial growth over time. Injection water samples that were taken after a biocide shock (on 04-02 and 15-04) show similar growth of biological activity as injection water samples taken before those biocide shocks (on 29-01 and 08-04). Only at location C, a small difference after the biocide shock was observed: microbial growth happened a bit slower after the biocide shock (400 ME's/mL at +72h instead of ~35.000 ME's/mL at the same in a samle taken before the biocide shock). However, these differences are too marginal to draw conclusions from them.

- Addition of biocide in aliquots has shown to be very effective in reducing biological activity. At both locations A & C, in any case there was microbial growth it was averted by the biocide (100 ppm). It is difficult to compare these laboratory experiment result to the field. In order to get the same results as in the lab (no growth over the whole

time span), a biocide shock of 120-196 hours should be done in the field because of the continuous water flow, supplying new water.

- Addition of corrosion inhibitor (in aliquots) has shown to enhance microbial growth. At locations A and C, addition of CI1 caused extra growth compared to the growth in the reference sample. In other words: when there is growth, CI1 enhances it. CI2 is used at the location without measured growth. So growth could be correlatable to the type of corrosion inhibitor that is used.

Based on all these observations, possible sources of ingress of microbes into a geothermal system and possible causes of growth/activity in injection water are discussed. Three options for ingress of microbes and three options for microbial growth in injection water are discussed below. Most of these possibilities have already been introduced in the literature review (chapter 2).

Possible sources of ingress of microbes into a geothermal system

- **Microbes originating from reservoir:** Either microbes are introduced from externally into the water in a geothermal system, or they were already initially present in that water. The latter is probable, since microbial presence is common in formation waters (section 2.7.1). Those bacteria are mostly thermophiles (and hyperthermophiles), because they are adapted to the high temperature in the reservoir (and can live and grow there, and most likely not in the colder injection well). Some literature suggests the possibility of 'mesophiles' being present in the deep (and hot) reservoir and are just able to survive there. Qpcr measurements on geothermal water have confirmed the presence of other microbes than just only thermophylic ones (Croese, 2018b). Those bacteria can then be transported in production water towards the surface system. Next, when the temperature of the water is lowered (after passing the heat exchanger), they can become active and start growing.
  Probability: uncertain. This is a microbial ingress option for which no evidence was found in this study, but it should be taken into account as a possibility.
- **Reinjection of produced basin water:** Production water from the well test phase has been temporarily stored in open basins and is later reinjected at locations A & C. Although oxygen scavanger, scale inhibitor and biocides have been used, this water was exposed to the atmosphere and therefore it is likely that it has been contaminated. When reinjected, this water can have contaminated a part of the surface system (from the point where the basin water has been injected) and the injection well with microbes.
  Probability: possible. Locations A and C are the places where growth of biological activity in the injection water has been observed. Basin water was also injected at those locations. It is possible that those systems have been contaminated (most likely with psychrophiles and mesophiles) by the reinjection of this basin water. Growth was only observed in injection water sampled after the injection filters, which matches the fact that these basin water microbes would originate from moderate-cold surface conditions.
- **Replacable elements:** Every time something in a geothermal system has to be replaced, the system is temporarily open to the outside environment. This forms a risk for contamination of the sytem with microbes (human introduction). Examples are: replacing components of the heat exchanger, maintenance in the separator, or changing the filters. The last one forms the biggest risk, since this happens most frequently. Injection filters are present at locations B & C. Since they need to be replaced every now and then, they are a possible source of system contamination.
  Probability: possible. Locations B and C have injection filters. As shown twice (before and after the biocide shock) in the ATP data at location C: water sampled before the injection filters does not show an increase in biological activity over time while water sampled after those filters does show an increase in biological activity over time. Also, at location C the injection filters have shown to contain an orange gunk, which can possibly act as protection for the microbes and enhance growth.

Possible causes of growth/ increasing biological activity

- **Temperature:** mesophiles (figure 2.9) could be naturally present in the produced formation water and as soon as they pass the heat exchanger, they arrive in a more ideal temperature environment where they ”wake up” and start to grow.
  Probability: not plausible. The biological activity measurements at location C show that microbial growth potential is not only dependent on water temperature / sampling before or after the heat exchanger (respectively hot or cold geothermal water).

- **Water composition (nutrients):** Volatile fatty acids (VFA’s) are in theory a good energy source for bacteria and can help efficient growth. Also, nitrate and nitrite can act as nutrients for microbes.
  Probability: not plausible. VFA’s have been proven to be present in the geothermal water at locations B & C, not at location A. This does not relate to the observed growth at those locations. Nitrate & nitrite are not present at any of the locations, so this consequence is unknown.

- **Corrosion inhibitor:** Location B uses a different CI (CI2) than locations A & C (CI1). Different ingredients / solvents can have specific effects (they are nutrients or not).
  Probability: possible. At locations A & C, CI1 has proven to enhance microbial growth. This can be the result of specific nutrients that are present in CI1 which feed the microbes. Also, in the case that the observed growth at location A has been initiated by external contamination during sampling: CI1 still inhibits the growth of those bacteria.

5

Conclusion

Based on the results of this study, it can be concluded that there is a correlation between microbial growth and injectivity reduction. Also, scale is possible in small amounts before (calcite) and after (barite) the heat exchanger. So biological activity and scaling can both be a (partial) cause of injectivity reduction in geothermal wells. Additionally, the quantity of suspended solids is not problematic high. At the same time, it is also not proven to be sufficiently low to exclude TSS as possible cause of injectivity reduction.

5.1. TSS

Geothermal production water from locations A, B and C contains suspended solids concentrations of 35-55 mg/L. Through the systems, these concentrations are reduced by filters below detection limits of 8-16 mg/L at the last point before reinjection. Also, the filters used for TSS measurements in the injection water looked visually clean (hardly any solids were visible). It can be concluded that the filters in the geothermal systems work. The following conclusions can be drawn on TSS:

- TSS concentrations for injection are comfortable based on experiences in the oil & gas industry. On the other hand they are not necessarily low enough to exclude TSS as a cause of injectivity reduction
- Despite the low measured quantities of TSS (~1 mg/L), they could in theory still be problematic, due to the large amount of water that is injected in geothermal wells (up to 400.000 L/h)

Mitigations

- Placement of multiple injection filters with small mesh size (~1 μm or less) in series

5.2. Scaling

Scales can potentially form in the geothermal systems of location A, B and C, although the effects on injectivity reduction have a limited likelyhood to be problematic (most likely, small amounts of precipitation will form). Overall, the following can be concluded about the scaling risk in the geothermal systems:

- Calcite and to a lesser extent siderite have the highest scaling tendency at the hot side of the system (before the heat exchanger). The peak risk is mostly located around (or just after) the separator. Calcite scaling can possibly cause clogging issues in the surface facilities at location B ($\Omega \approx 4.1$). At locations A and C, it is more likely that smaller amounts of precipitation will form, without causing significant problems
- Barite has the highest scaling tendency at the cold side of a geothermal system (after the heat exchanger), with the peak risk always downhole in the injection well. Barite is not likely to cause significant injectivity related problems (because Ω is always <3.1)
- Barite can cause significant problems related to NORM deposition (after the heat exchanger). Exposure to LSA can occur when maintaining or cleaning surface facilities (e.g. replacing filters)

Mitigations

- Preventive usage of scaling inhibitor (continuous injection into the system)

5.3. Microbial activity

Although in initially small concentrations, biological activity is present in all the three geothermal systems and geothermal injection waters (~250-25.000 ME/mL). Over time, biological activity in injection water is able to grow to concentratios of ~500.000-1.000.000 ME/mL. Based on the results of this study, the following conclusions can be drawn on the growth of microbes and mitigation against this:

- Microbial growth potential in the injection water is site-specific and correlatable to injectivity reduction: growth has been measured at locations that have injectivity reduction (A & C) and growth is not measured at the location without injectivity reduction (B)
- Most probable sources of ingress of microbes in a geothermal system are: reinjection of basin water and human introduction by replaceable elements in the system (e.g. injection filters). Another option is natural microbial presence in formation water
- The most probable cause of microbial growth is (the type of) corrosion inhibitor (CI1). Another option is the temperature drop after the heat exchanger (in the case microbes are naturally present in formation water)
- Addition of biocide to samples in the laboratory is always effective in reducing biological activity (or keeping it at initial low value). In injection water samples, a single dosage of 100ppm seems enough. In the geothermal system, this would mean a permanent dosage of 100ppm. Acidification of the water samples to pH=2 has the same effect as biocide in 1 example (location C)
- Biocide shocks do not have a clear effect on measured biological activities at the locations (initially & over time)

Mitigations

- Select a corrosion inhibitor that contains less or no nutrients (in the solvent)
- Addition of biocide to the corrosion inhibitor for mitigation of the 'enhancing growth' effect. This can be done by a permanent in-line biocide dosage. However, look at regulations for this
- Lowering the pH (preferably to pH=2) just before re-injecting the water. However, in practice this may be not feasible because it is very corrosive, unsafe (for the environment) and not economical

6

Recommendations

This chapter contains some recommendations for further research that can be done on injectivity in geothermal wells in the future.

- When measuring amounts of TSS, sample large volumes of water (~10L) in order to significantly lower the detection limit towards values that are of interest for geothermal operations (<1 mg/L)
- Measure TSS at more points in the system (before and after a single filter street). Then, the performance of individual filters in the system can be assessed (production versus injection filters), instead of just the total effect they have together through the whole system
- Analyse complete chemical water compositions also at sample points 5 in te geothermal systems, in order to compare the scaling model with reality (this only holds for the calcite potential)
- Perform qpcr and metagenomics analysis on the microbial content of the geothermal samples
- Scale up this study to more geothermal injection wells, in order to obtain more data

Appendices

A

Appendices

A.1. All samples per location

A list of all the samples that have been acquired during this entire project is given per location in tables A.1, A.2 and A.3.

Table A.1: Sampling summary location A

Sample date	No.	Bottle*	Volume	Purpose	Comment
29-01-2019	A1	T	1L	ATP	
	A1	G	0.5L	TSS	Not taken into account (insufficient flushing of sample point)
	A2	T	1L	ATP	
	A3	T	1L	ATP	
	A4	T	1L	ATP	cultured, aliquots
	A4	G	0.5L	TSS	Not taken into account (insufficient flushing of sample point)
04-02-2019	A1	T	1L	ATP	
	A1	G	1L	ATP, Chem.**	
	A1	G	0.9L	TSS	
	A2	T	1L	ATP	
	A2	G	1L	ATP	
	A3	T	1L	ATP	
	A3	G	1L	ATP	
	A4	T	1L	ATP	cultured, aliquots
	A4 duplo	T	1L	ATP	cultured, aliquots
	A4	G	0.5L	ATP, Chem.**	
	A4	G	0.9L	TSS	
27-03-2019	A2	G	1L	ATP	cultured
	A2 [N_2]	G	1L	ATP	oxygen free, cultured
	A2 @35°C	G	1L	ATP	cultured, stored at 35°C
	A2 [N_2] @35°C	G	1L	ATP	oxygen free, cultured, stored at 35°C
	A3	G	1L	ATP	
	A3 [N_2]	G	1L	ATP	oxygen free
	A4	G	1L	ATP	cultured, aliquots
	A4 [N_2]	G	1L	ATP	oxygen free, cultured, aliquots

**Type of sample bottle: G = coated glass sample bottle, T = thermos can*

***Chem. = chemical composition*

Table A.2: Sampling summary location B

Sample date	No.	Bottle*	Volume	Purpose	Comment
05-03-2019	B1	G	1L	ATP, Chem.**	cultured
	B1 [N_2]	G	1L	ATP	cultured
	B1 @35°C	G	1L	ATP	cultured, stored at 35°C
	B1 [N_2] @35°C	G	1L	ATP	cultured, stored at 35°C
	B1	G	0.75L	TSS	
	B2	G	1L	ATP	
	B2 [N_2]	G	1L	ATP	
	B4	G	1L	ATP	
	B4 [N_2]	G	1L	TSS	
	B5	G	1L	ATP, Chem.**	cultured, aliquots
	B5 [N_2]	G	1L	ATP	cultured, aliquots
	B5	G	0.75L	TSS	

**Type of sample bottle: G = coated glass sample bottle, T = thermos can*
***Chem. = chemical composition*

Table A.3: Sampling summary location B

Sample date	No.	Bottle*	Volume	Purpose	Comment
08-04-2019	C1 [N_2]	G	1L	ATP	cultured
	C1	G	0.6L	TSS, Chem.**	
	C2 [N_2]	G	1L	ATP	cultured
	C4 [N_2]	G	1L	ATP	cultured
	C5 [N_2]	G	1L	ATP	cultured, aliquots
	C5 duplo [N_2]	G	1L	ATP	cultured, aliquots
	C5	G	0.6L	TSS, Chem.**	
15-04-2019	C1 [N_2]	G	1L	ATP	
	C1	G	1L	ATP	
	C2 [N_2]	G	0.5L	ATP	
	C2	G	0.5L	ATP	
	C4 [N_2]	G	1L	ATP	cultured
	C5 [N_2]	G	1L	ATP	cultured, aliquots
	C5	G	1L	ATP	cultured

**Type of sample bottle: G = coated glass sample bottle, T = thermos can*
***Chem. = chemical composition*

The samples in these tables are all ”original”, which means that they are coming right out of the system and they have not been changed afterwards (also kept on original temperature, except for the ”@35°C” samples). These original samples are also called ”reference” samples, when aliquots (sub-samples) have been taken from them and the effects of additives or different environmental conditions are examined in so called ”kill tests” (section 3.3.9).

A.2. Sterile sample bottles test

Whether the sterilising procedure for sample bottles indeed results in sterile sample bottles, has been validated with this experiment. First of all, the biological activity in normal tap-water as well as in demi-water is measured. Also, a beaker with demi-water is warmed up on a cooking plate till 100°C for 10 minutes. This water is cooled down and considered as 'sterile water'. The biological activity is measured and this is considered as the zero measurement (sterile water should have the lowest ATP concentration). Next, a sterilised sample bottle is filled with this sterile water and left for 30 minutes. The bottle is shaken a couple of times. After that, the biological activity of the water from the bottle is measured as well. For comparison, the same thing is done for an untreated (not sterilised) sample bottle. For the sterilisation method to be successful, the ATP concentration in the water from the sterilised sample bottle should not be higher than the biological activity of the 'sterile water' (otherwise, the water is contaminated by a non-clean bottle). The microbial activity of the water from the untreated bottle can be used to check whether the sterilisation procedure is profitable at all (or are the bottles already clean enough after the standard cleaning in the dishwasher in the laboratory?). An illustration and the results of this experiment are visible in figure A.1.

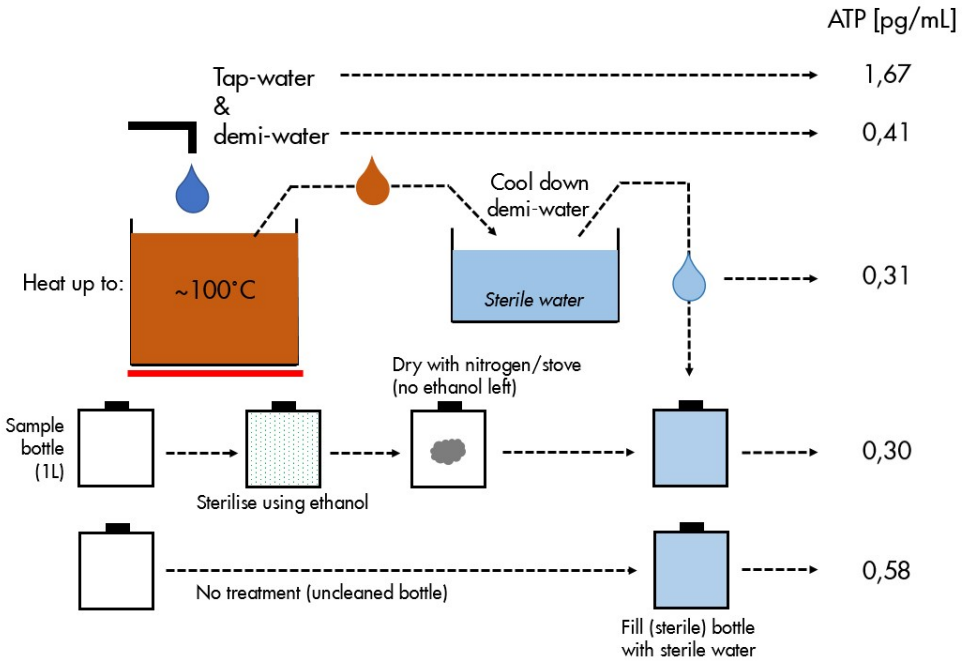

Figure A.1: Sterile sample bottle test illustration & results

Tap-water in the laboratory contains 1.67 pg/mL ATP (1670 ME/mL), which is relatively low (maximum by law is 12 pg/mL). Demi-water is more sterile and boiled demi-water is even lower in biological activity. After being in a sterilised sample bottle, the 'sterile water' has an almost unchanged microbial content. This indicates that the bottle does not add biological activity to the water, in other words: the bottle has been made sterile. After being in an untreated sample bottle, the ATP concentration increases almost by a factor two (0.58 pg/mL instead of 0.31 pg/mL).

Although all these biological activity results are very low (<2 pg/mL) and the microbes in the water have not been able to grow yet and create larger differences between the bottles, the numbers indicate that the sterilised sample bottles are sterile and the sterilisation procedure is successful. Also it is worth it to sterilise sample bottles like this (since a bottle which is cleaned by the dishwasher does increase the biological activity of the sterile water).

A.3. Temperature decline test

An experiment has been performed to check the temperature declines of hot water in both thermos cans and coated glass bottles. Both types of bottles are filled with hot water (60°C and 90°C) and stored inside an isolated sample box (exactly how they will be transported from the field to the laboratory). After that time, the temperature decline has been measured. See figure A.2.

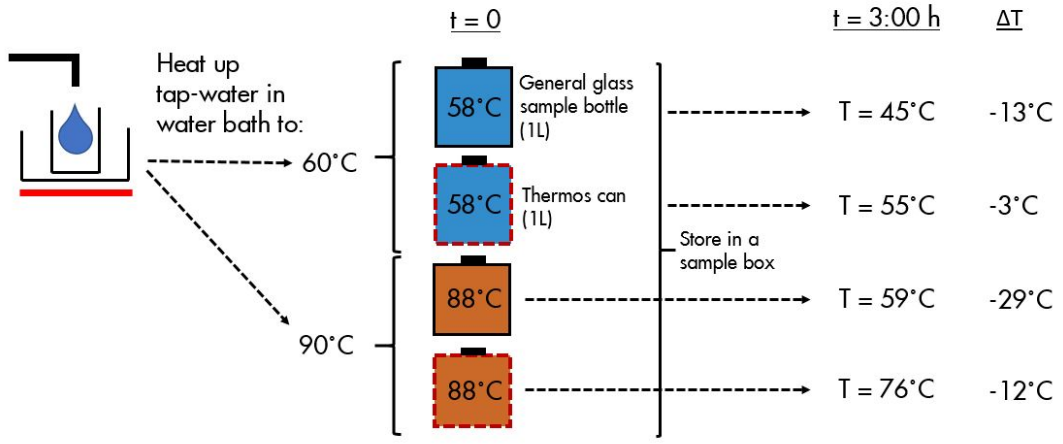

Figure A.2: Temperature decline experiment in sample bottles, illustration & results. Temperature drop in glass bottles is more than in thermos cans

From the test results it can be concluded that thermos cans isolate better. Therefore, it has (initially) been decided to use thermos cans for the microbial samples.

A.4. O2 measurements

The amount of oxygen in a water sample can be measured using an orbisphere (figure A.3). The oxygen detector of the orbisphere is connected to the sample bottle and kept under water. The boundary between the bottle and the orbisphere is made airtight using a very thin parafilm tape. Once that is done, you wait untill the displayed oxygen concentration (in ppm) does not change anymore. This can take up to 15 minutes.

Figure A.3: Orbisphere for measuring oxygen

Figure A.4 shows 4 sample bottles from location B, 24 hours after the moment of sampling. It is clearly visible that in the samples that are treated with nitrogen, less iron has reacted and consequently the water is much clearer.

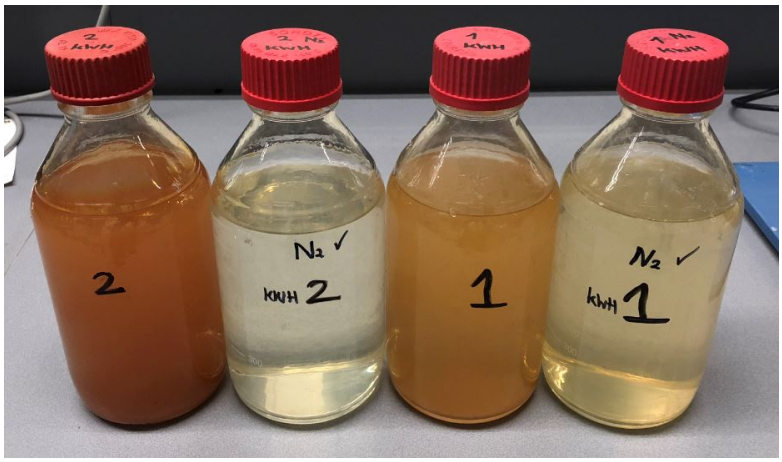

Figure A.4: Samples from location B, 24 hours after sampling

Table A.4 displays the amounts of oxygen that have been measured in those samples.

Table A.4: Oxygen concentration measurements

	+24h		+216h	
Sample	**[O_2]**	**Temp**	**[O_2]**	**Temp**
B5	1290 ppb	25.0°C	3940 ppb	21.7°C
B5 (N_2)	85 ppb	24.5°C	111 ppb	21.3°C

Oxygen concentrations are obviously lower in the samples that have been kept ”oxygen free” (using nitrogen). Normal samples contain 15-35 times more oxygen. It is likely that the oxygen concentrations in the B5 sample will actually be even higher (especially the +216h measurement). Based on the brown colour of the water, it can be said that iron reacted with oxygen and therefore some of the oxygen in the water has been removed.

Air has a density of 1293 kg/m^3 and consists of ~21% oxygen. That means that air has an oxygen concentration of 217.53*10^6ppb. Water (at 35°C) that is in contact with air has a dissolved oxygen saturation of ~6.8 mg/L, which is equal to 6800ppb. The normal sample (B5) is 19% saturated with oxygen after 24 hours and 58% saturated after 216 hours. The ”oxygen free” sample is just 1% saturated after 24 hours and 2% after 216 hours. With the resources that are available (nitrogen), this is a good result (low in oxygen).

Although the ”oxygen free” sample is not completely free of oxygen, the amounts of oxygen are much lower than the normal sample. So based on those results, the oxygen free samples are kept very low in oxygen by this procedure, until sufficient time after sampling (+216 hours). So they will be called oxygen free and they represent to a certain extent anaerobic conditions.

A.5. Demi water microbial growth experiment

The initial amount of biological activity and the possible microbial growth in demi-water has been investigated. This is done to assess what growth is possible in an environment without any nutrients (demi-water). See figure A.2.

Table A.5: ATP data Demi-water test

	ATP content [pg/mL]					
(Sub-)sample	**< 24h**	**+48h**	**+96h**	**+168h**	**+240h**	**+384h**
DW	2.1	5.7	-	13.6	-	7.4
DW + CI1 [10ppm]	1.3	1.1	2.5	19.5	61.6	-
DW + CI1 [20ppm]	1.3	3.3	3.0	71.4	107.06	-

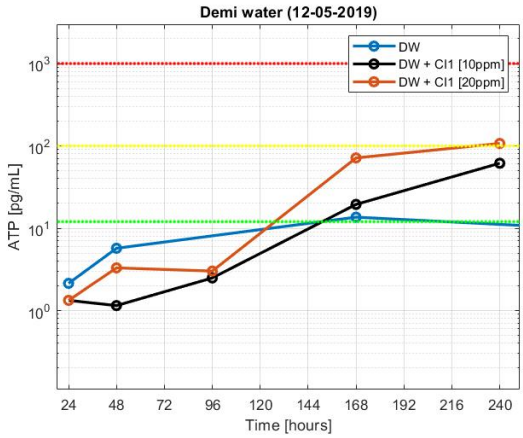

Figure A.5: Microbial growth in demi-water over time. The ATP concentration in demi-water (DW) is initially low and increases to a value or around 100 pg/mL. Addition of corrosion inhibitor (DW + CI1) enhances microbial growth slightly.

The results show that there is limited microbial growth possible in demi-water. However, in pure demi-water the growth does not exceed a biological activity of about 15.000 ME's/mL (close to the Dutch tap water norm). When adding corrosion inhibitor to demi-water, more microbial growth is possible. Concentrations of ~100.000 ME's/mL are reached in an aliquot with 20ppm CI1.

A.6. Bulk precipitation analysis with EDXRF

Once the sample bottles were stored in the laboratory, solids arose in the oxygen free samples of location B (~30 hours after moment of sampling). Solids from sample B1 (before separator and production filters) have been analysed under the microscope and using Energy Dispersive X-ray Fluorescence (EDXRF). Table A.6 displays the results of the EDXRF scan. The solids consist mainly of iron, which makes it likely that they are corrosion products or scale (siderite). Microscopic pictures of the samples found at the bottom and at the surface of the sample are shown in respectively figures A.6 and A.7.

Table A.6: Elements found in solids of sample B1 with EDXRF scan

	B1 bottom solids	**B1 surface solids**
Major components	Fe	Fe
Minor components	Si, Ca	Si, Ca
Traces	Cl, Sr	Ti, Sr

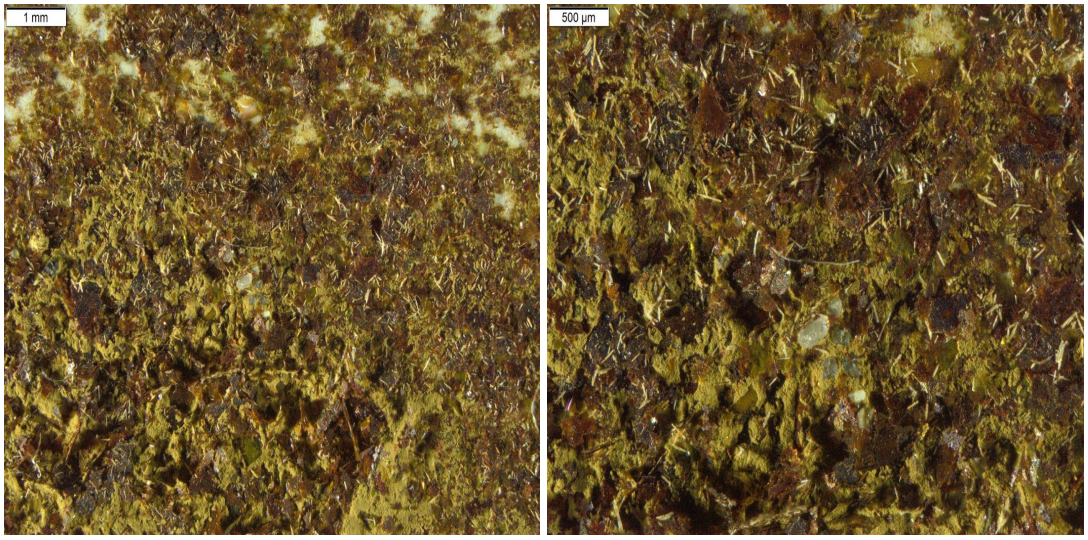

Figure A.6: Two microscopic images of the bottom solids in sample B1

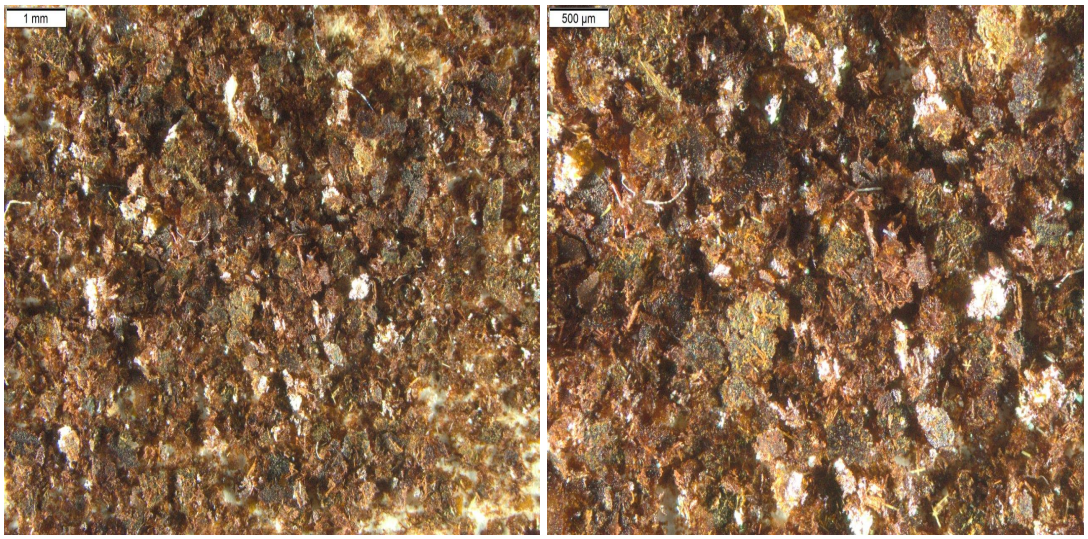

Figure A.7: Two microscopic images of the water surface solids in sample B1

A.7. Thermos cans versus Glass bottles

After the first time sampling at location A (29-01-2019), deposits were formed on the sides of some of the thermos cans over time when they were stored in the laboratory. The content of the deposits was unclear although it seemed to be scales. They were difficult to remove, but it worked after long flushing with acetic acid and then scraping inside the cans with a brush. However, it is very time consuming to have to clean the thermos cans in this way before every new sampling moment. Furthermore, the chance on contamination increases when minor parts of the deposits stay behind in the cans. Therefore, it has been tested whether it is possible to use glass bottles for sampling.

During the second sampling moment at location A (04-02-2019), double samples have been taken; at every sample point one sample has been taken with a thermos can and another one with a glass bottle. Both type of bottles have been sterilized using the same method as described in section 3.3.3. Transport and storage procedures (section 3.3.7) are equal for all the samples. Within 24 hours after sampling, thermos cans and glass bottles give ATP readings which are comparable through the system (table A.7). Both types of sample bottles contain very low concentrations of ATP (<0.25 pg/mL) at all sample points before the heat exchanger, while after the heat exchanger they both contain about 100 times more ATP. So based on these results, it can be concluded that using glass bottles instead of thermos cans does not influence the microbial activity in the samples.

Table A.7: ATP concentrations in geothermal water at location A (04-02-2019, <24h after sampling), thermos cans vs glass bottles

Type	Sample point			
	1	2	3	4
Thermos can	0.2	0.2	0.1	26.7
Glass bottle	0.2	0.2	0.1	19.7

A.8. Scale analysis workflow in *Stream Analyzer*

This section contains screen-shots of the different steps performed during the scaling modeling process in *Stream Analyzer*.

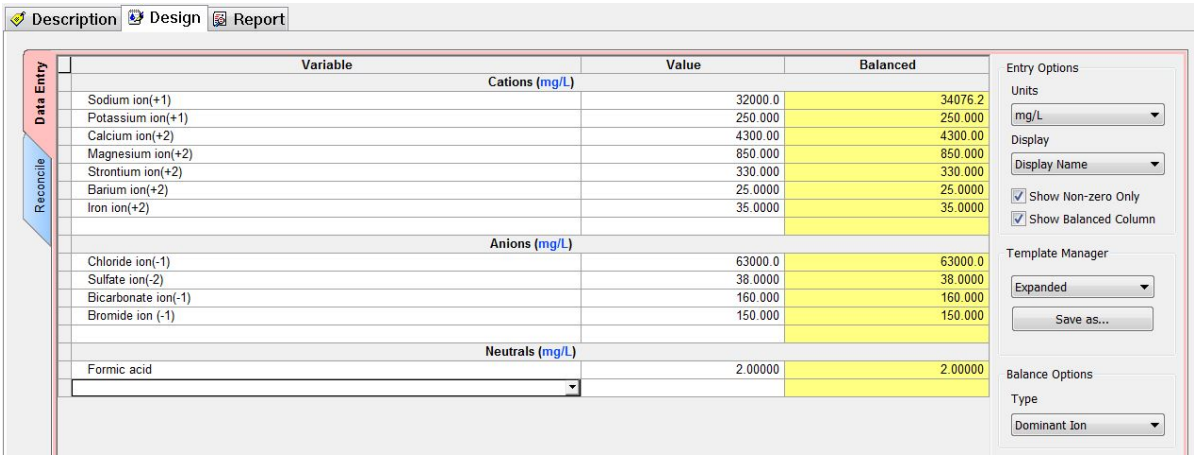

Figure A.8: Chemical composition data entry to create a 'brine' in the model

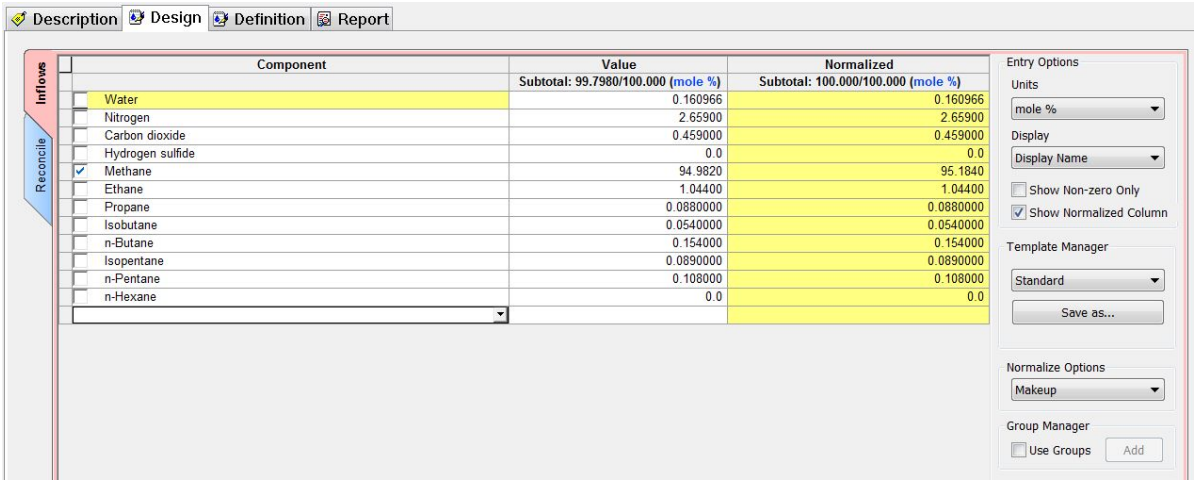

Figure A.9: Gas composition data entry to create a gas phase in the model

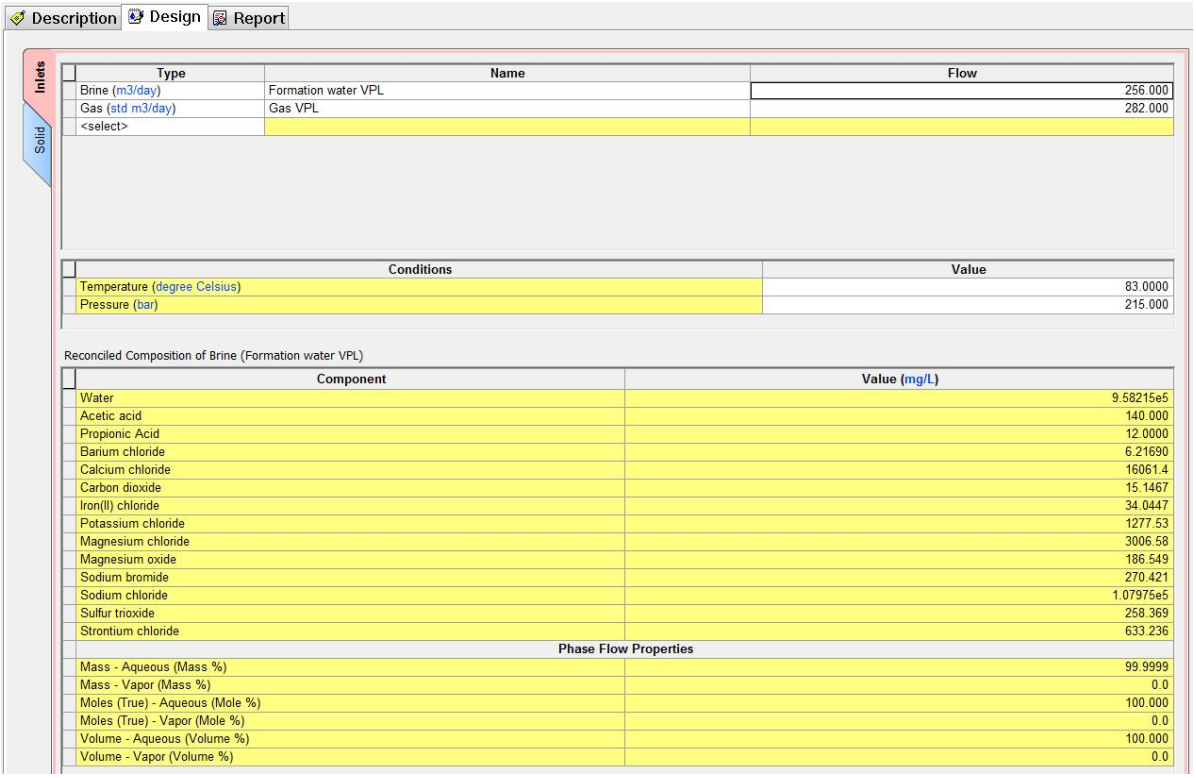

Figure A.10: Combine water & gas data to create a saturate (whole fluid)

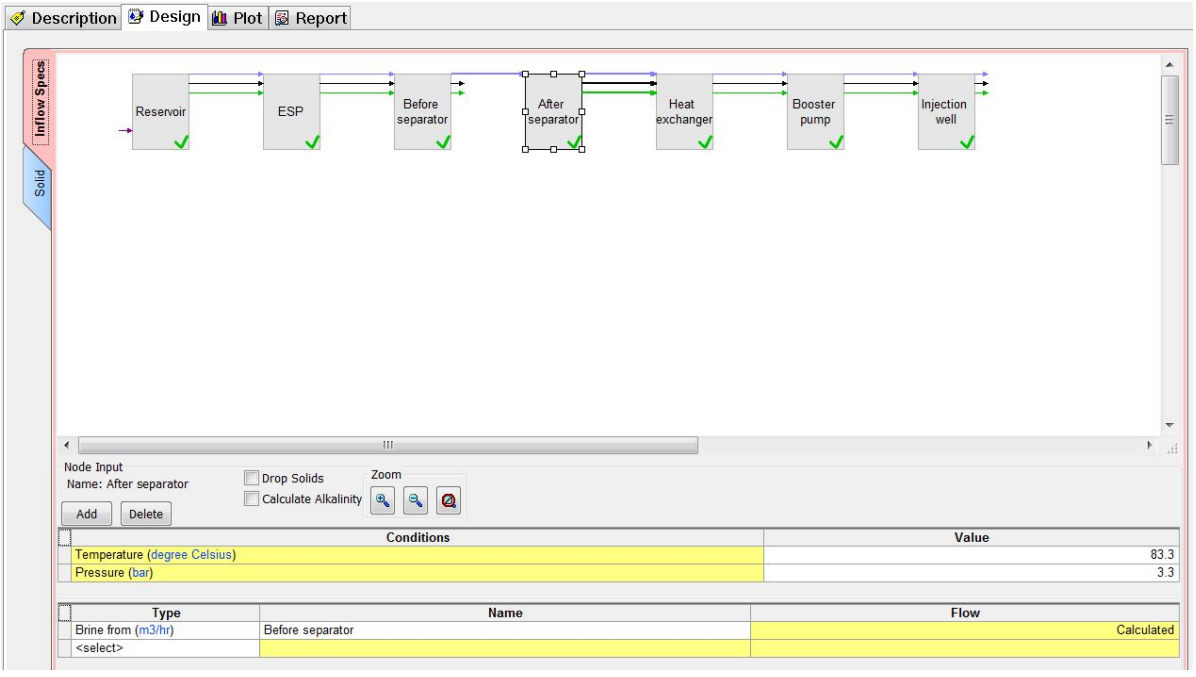

Figure A.11: Add facilities to model the geothermal system

A.9. Major & minor scales

The graph in figure A.12 shows the scale analysis result for location A. All scale types are plotted, also the minor ones. All minor scales have scaling tendencies very close to zero. This is also the case for locations B and C. The only exception is aragonite. However, this scale will never form when calcite has a higher scaling tendency. In order to keep the scaling graphs clear, only barite, siderite and calcite will be included.

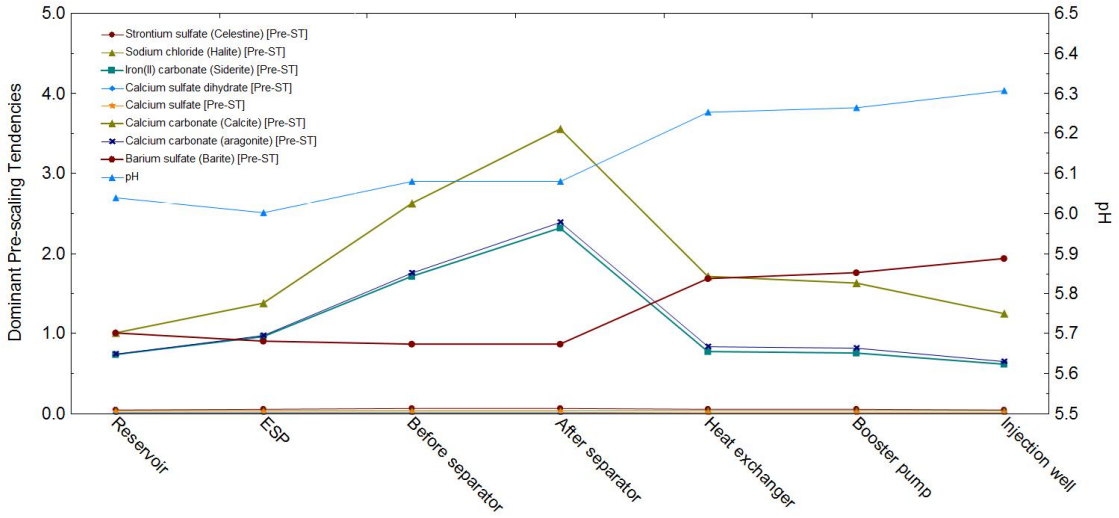

Figure A.12: Result of the scale analysis for location A, including minor scales

A.10. Sampling influence on TSS

To double check the potential influence of sampling and associated degassing and slightly temperature decrease (during transport) on TSS measurements, the process of sampling has been modeled in *Stream Analyser* for location C. The graphs in figures A.13, A.14, A.15 show the evolution of the scaling tendency after the moment of sampling (at three points in the system), till arriving in the laboratory in Assen. First the pressure is dropped (”sampling”), then the gas escapes and only the fluid is left (”sample brine”) and finally the temperature decreases a bit (”sample cools off”). The modeled temperature decrease in the last step is based on the temperature decline test in Appendix A.3.

Figure A.13 shows the evolution of the scaling tendency after sampling at the point before the separator. As can be seen, the scaling tendency for calcite increases rapidly towards $\Omega \approx 10$ just after sampling. One would expect direct calcite precipitation in the sample bottle here, resulting in an increased TSS measurement. Since the sample point before the separator spits out a lot of gas during sampling, some water reaches the ground and also precipitation was visible as whitish salt. However, this does not necessarily mean this also happens in the sample bottle (and influences the TSS measurement). Using the option ’drop solids’ in *Stream Analyzer*, the amount of solid formation can be calculated through the system. After sampling, calcite minerals from at a rate of 100-150 mol/h (based on the system flow rate of 256 m^3/h). Converting this amount to the quantity in a 1L sample bottle gives 20-40 mg/L of calcite. This is a significant amount, although those minerals can be present in the sample bottle as nano crystals. Then they are not bound together and will pass through the 0.45μm filter in suspension (not creating a higher TSS measurement). Another very likely option is that the formed calcite will attach (as a thin film) to the side of the glass. This is typical for calcite (think about chalk, making glasses dull). When this is the case, the mineral stays on the glass and will not be measured as TSS.

So although the scaling tendency graph suggests otherwise, it is likely that the calcite did not form as suspended solids, large enough to influence the TSS measurement. This matches with the visual observation (no mineral formation was seen in the bottle after sampling).

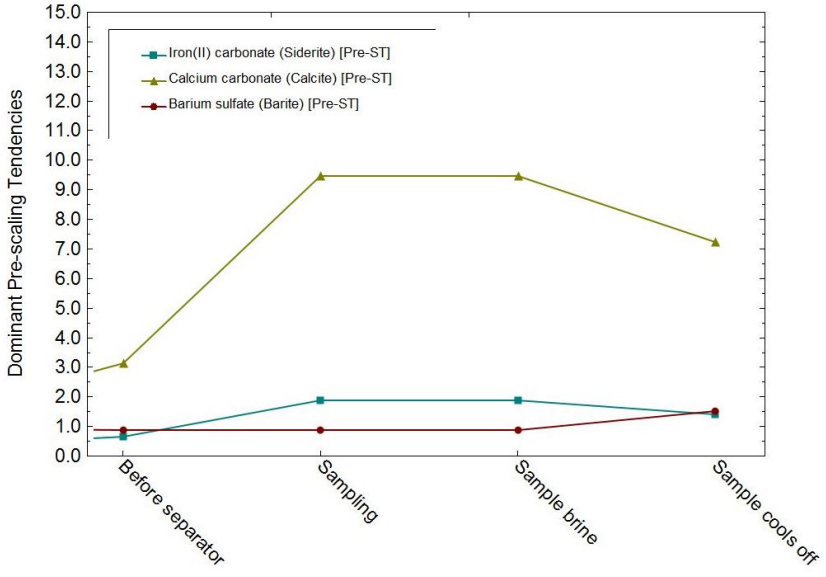

Figure A.13: Scale modeling of sampling before the separator at location C

At the points after the separator (2 & 3) and after the heat exchanger (4 & 5), the scaling tendencies do not increase significantly after sampling (figure A.14 and A.15). This means that no extra precipitation will influence the TSS measurements in the injection water.

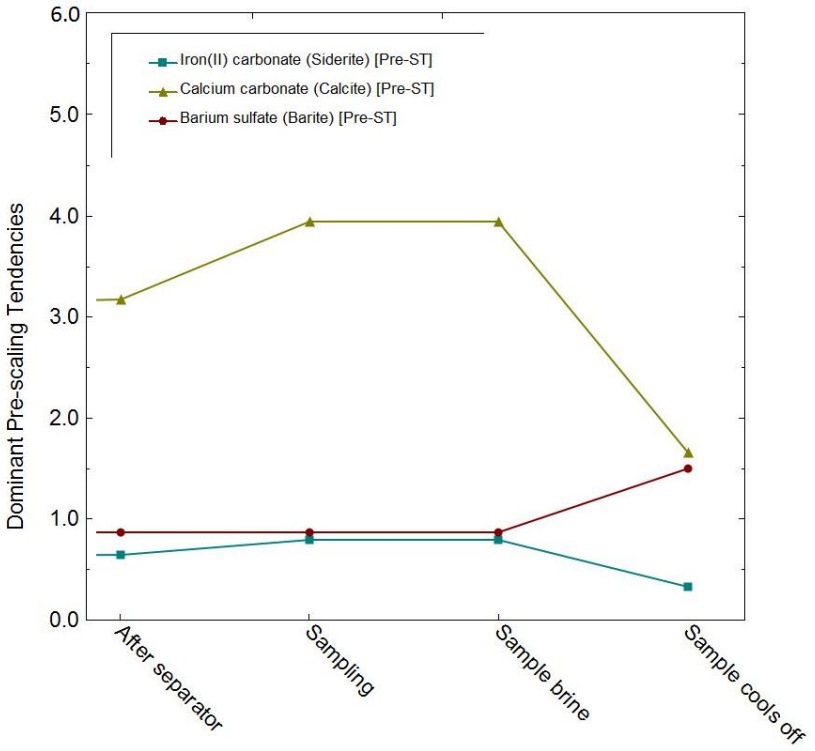

Figure A.14: Scale modeling of sampling after the separator at location C

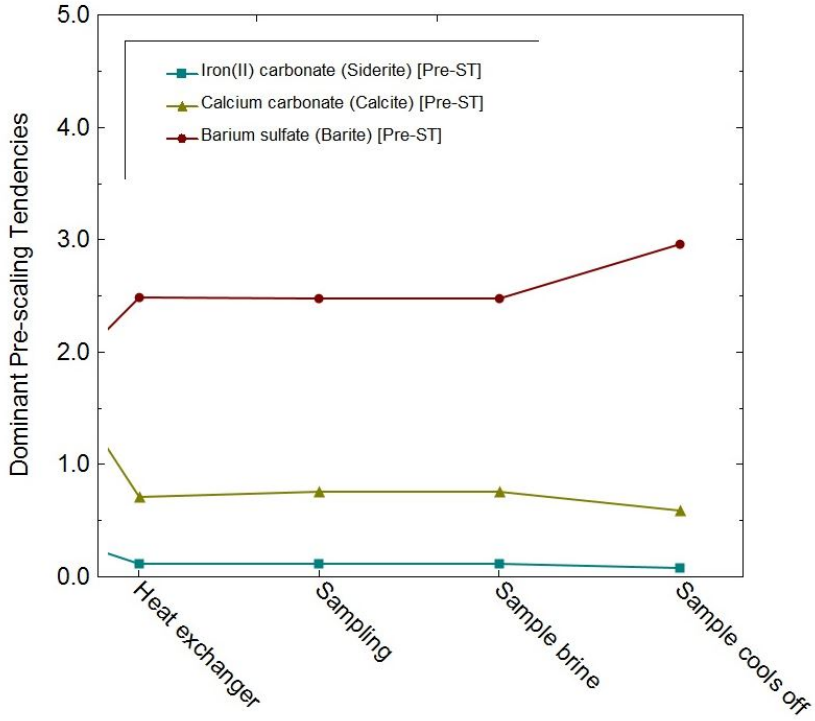

Figure A.15: Scale modeling of sampling after the heat exchanger at location C

Bibliography

International standard: Water quality - determination of ph. Technical report, International Organization for Standardization (ISO), 2008. ISO 10523.2008.

Mic risk assessment tool - propriatory. Technical report, NAM, 2016.

A.M. Badawi, M.A. Hegazy, A.A. El-Sawy, H.M. Ahmed, and W.M. Kamel. Novel quaternary ammonium hydroxide cationic surfactants as corrosion inhibitors for carbon steel and as biocides for sulfate reducing bacteria (srb). *Materials Chemistry and Physics*, 124:458–465, 2010.

A. Bender. Geomec-4p geothermal energy brielle. Technical report, PanTerra, January 2012. Prepared for: GeoMEC-4P.

Bioclear. Private Communication, January 2019. Email contact about microbiological growth associated with the cooling of water.

D. Bonté, J.-D. van Wees, and J.M. Verweij. Subsurface temperature of the onshore netherlands: new temperature dataset and modelling. *Netherlands Journal of Geosciences - Geologie en Mijnbouw*, 91, 2012.

A. Braissant, A. Decho, C. Dupraz, C. Glunk, K. Przekop, and P. Visscher. Exopolymeric substances of sulfate□reducing bacteria: Interactions with calcium at alkaline ph and implication for formation of carbonate minerals. *Geobiology*, pages 401–411, 2007.

CBS Statline. Hernieuwbare energie; verbruik naar energiebron, techniek en toepassing, 2019. URL `https://opendata.cbs.nl/statline/#/CBS/nl/dataset/83109NED/table?ts=1560943563675`. last updated 29-05-2019.

Q. Clevis. Thermal re-equilibration after geothermal, March 2018. Presentation, copyright of Shell International.

B. Cox. Private Communication, December 2018. MSc Thesis introductory meeting with Veegeo & Hydreco.

B. Cox. Private Communication, January 2019. Email contact about the costs of a geothermal doublet shutdown.

E. Croese. Microbiology in geothermal operations. Technical report, Bioclear, Ministry of Agriculture, Nature and Food Quality, December 2018a. Client: Kennisagenda Aardwarmte.

E. Croese. Development of sustainable geothermal operations. Technical report, Bioclear, Ministry of Agriculture, Nature and Food Quality, February 2018b. Client: Kennisagenda Aardwarmte.

DAGO. Wat is geothermie?, 2018. URL `https://geothermie.nl/images/geothermie-aardwarmte/Infographic_Geothermie_PG_DEF_NOV.jpg`.

DAGO, EBN, Platform Geothermie, and Stichting Warmtenetwerk. Hoe werkt aardwarmte, 2018. URL `https://geothermie.nl/images/Hoe_Werkt_Aardwarmte_flyer.pdf`.

J. de Jager. *Geology of the Netherlands, Geological development.* Royal Netherlands Academy of Arts and Sciences, 1st edition, 2007. ISBN 978-90-6984-481-7.

EBN. Energie in nederland 2017, 2019. URL `http://www.energieinnederland.nl/2017`. last visited 01.04.2019.

J. Eilers. Private Communication, July 2019a. Conversation about biofilm formation and SRB's and corrosion inhibitors.

J. Eilers. Private Communication, March 2019b. Weekly meeting: microbiology ATP measurements update and interpretation.

J. Eilers. Private Communication, May 2019c. Weekly meeting: scale analysis update.

J. Eilers. Private Communication, April 2019d. Scale analysis session and conversation about scaling tendency interpretation.

H.-C. Flemming, J. Wingender, T. Griebe, and C. Mayer. Physico-chemical properties of biofilms. *Biofilms: Recent Advances in their Study and Control*, pages 19–34, 2000.

D.T. Gilding. Heterogeneity determination of the delft subsurface for heat flow modelling. Msc thesis, Petroleum Engineering, Delft University of Technology, Delft, the Netherlands, 2010.

J. Goldstein. *Scanning Electron Microscopy and X-Ray Microanalysis*. Springer US, 3rd edition, 2003. ISBN 978-0-306-47292-3.

R. Gras and M.C. Geluk. Late cretaceous-early tertiary sedimentation and tectonic inversion in the southern netherlands. *Geologie en Mijnbouw*, 78:1–19, 1999.

J. Griffioen, H. Verweij, and R. Stuurman. The composition of groundwater in palaeogene and older formations in the netherlands. a synthesis. *Netherlands Journal of Geosciences - Geologie en Mijnbouw*, 95(3):349–372, 2016.

H.K. Gupta. *Geothermal resources: an energy alternative*. Elsevier Scientific Publishing Company, Amsterdam, 1st edition, 1980. ISBN 0-444-41250-6.

M. Hanegraaf. Geothermal engergy: A century of dedication to geothermal energy, 2018. URL `https://www.tno.nl/media/9703/geo_strategy.pdf`.

D.C. Harris. *Quantitative Chemical Analysis*. W.H. Freeman and Company, 6th edition, 2007. Library of Congress Control Number: 2002105823.

C.D Hsi, D.S. Dudzik, R.H. Lane, J.W. Buettner, and R.D. Neira. Formation injectivity damage due to produced water reinjection. 1994. SPE 27395.

Y. Huang and J. Zhang. *Materials Corrosion and Protection*. De Gruyter, Shanghai Jiao Tong University Press, Shanghai, China, 2018. ISBN 978-3-11-030987-4.

Kas als Energiebron. Report assessment of injectivity problems in geothermal greenhouse heating wells. Technical report, IP, KWR, Ministry of Economic Affairs, Productschap Tuinbouw, Kas als Energiebron, February 2015. Financed by: Programma Kas als Energiebron.

J. Kweekel. Private Communication, August 2019a. Explanation of measuring and interpreting alkalinity, pH and TSS.

J. Kweekel. Private Communication, April 2019b. Total Carbonate conservation in sampled water. Explanation of method.

J. Lee and R. Deininger. Rapid quantification of viable bacteria in water using atp assay. *American Laboratory News*, 33:24–26, 10 2001.

A. Lokhorst and T. Wong. *Geology of the Netherlands, Geothermal energy*. Royal Netherlands Academy of Arts and Sciences, 1st edition, 2007. ISBN 978-90-6984-481-7.

Lumen Microbiology. Temperature and microbial growth, 2019. URL `https://courses.lumenlearning.com/microbiology/chapter/temperature-and-microbial-growth/`. last visited 15.07.2019.

LuminUltra. What is atp and how does atp monitoring work?, 2016. URL `https://www.luminultra.com/tech/`. last visited 09-07-2019.

R. Martin. *Clogging issues associated with managed aquifer recharge methods*. IAH Commission on Managing Aquifer Recharge, Australia, 1st edition, 2013. ISBN 978-0-646-90852-6.

Ministry of EZK. Ontwerp van het klimaatakkoord, 2018. URL https://www.rijksoverheid.nl/documenten/rapporten/2018/12/21/ontwerp-klimaatakkoord.

NAM. Feiten en cijfers: Gas- en oliewinning, 2019. URL https://www.nam.nl/feiten-en-cijfers/gaswinning.html#iframe=L2VtYmVkL2NvbXBvbmVudC8_aWQ9Z2Fzd2lubmluZw. last visited 29.04.2019.

NLOG. Injection process water, 2015. URL https://www.nlog.nl/en/injection-process-water. last visited 30-06-2019.

NLOG. Aardwarmte vergunningen per 1 mei 2019, opsporingsvergunningen, nederlands territoir, 2019. URL https://www.nlog.nl/sites/default/files/2019-05/vergunningenaardwarmte_mutaties_20190501.pdf.

OLI systems inc. Scaling tendencies, 2019. URL https://wiki.olisystems.com/wiki/Scaling_Tendencies. last visited 27.07.2019.

C.C. Patton and A. Foster. *Applied Water Technology, Water Formed Scales*. John M. Campbell and Company, 3rd edition, 2007a. ISBN 0-9703449-5.

C.C. Patton and A. Foster. *Applied Water Technology, Water Injection Systems*. John M. Campbell and Company, 3rd edition, 2007b. ISBN 0-9703449-5.

C.C. Patton and A. Foster. *Applied Water Technology, Water Sampling and Analysis*. John M. Campbell and Company, 3rd edition, 2007c. ISBN 0-9703449-5.

C.C. Patton and A. Foster. *Applied Water Technology, Water Treatment Microbiology*. John M. Campbell and Company, 3rd edition, 2007d. ISBN 0-9703449-5.

M.J. Pelczar, E.C.S. Chan, and N.R. Krieg. *Microbiology*. McGraw-Hill, New York, 1986. TU Delft Library call number: 21714031.

PetroSkills LLC. Course, 2016. Section 7 (Microbial Fooling and Corrosion) and section 9 (Production Chemistry).

L. Pirlea. Pvt water and scale analysis report [location c]. Technical report, Panterra Geoconsultants B.V., October 2015.

L. Pirlea. Draft pvt water report [location b]. Technical report, Panterra Geoconsultants B.V., November 2016.

L. Pirlea. Pvt analysis report [location a]. Technical report, Panterra Geoconsultants B.V., December 2017. Project 17039.

Platform Geothermie. Masterplan geothermal energy in the netherlands. Technical report, DAGO, EBN, Platform Geothermie, Stichting Warmtenetwerk, May 2018. Signed by: Schoof, F., Van der Hout, M., Van Zanten, J., Van Hoogstraten, J. W. In collaboration with ministries of EZK and BZK.

M. Provoost, L. Albeda, B. Godschalk, B. van der Werff, and F. Schoof. Geothermal energy use, country update for the netherlands. 2019. European Geothermal Congress 2019.

A. Reerink. Private Communication, December 2018. Email contact about injectivity reduction at geothermal location C.

A. Reerink. Private Communication, May 2019a. Conversation about the use of corrosion inhibitors in geothermal systems.

A. Reerink. Private Communication, June 2019b. Email contact about TSS.

H.E. Rondeel, D.A.J. Batjes, and W.H. Nieuwenhuijs. Geology of gas and oil under the netherlands. *Geologie en Mijnbouw*, 74(4):736–739, 1996.

D. Rousseau, H. Latifa, and L. Nabzar. Injectivity decline from produced-water reinjection: new insights on in-depth-particle-deposition mechanisms. *SPE Production & Operations*, 23, 2008. Document ID: SPE-107666-PA.

P.F. Sanders and P.J. Sturman. *Petroleum Microbiology: Biofouling in the oil industry*. ASM Press, Washington D.C., 2005.

Schlumberger. Oilfield glossary - well testing, 2019. URL `https://www.glossary.oilfield.slb.com/en/Disciplines/Well-Testing.aspx`. last visited 16.06.2019.

M.J. Schofield. *Plant Engineer's Reference Book, Corrosion*. 2nd edition, 2003. ISBN 978-0-7506-4452-5.

Shell & Eneco. Eneco en shell willen samen nederlandse aardwarmte ontwikkelen, May 2019. URL `https://www.shell.nl/media/nieuwsberichten/eneco-en-shell-willen-samen-nederlandse-aardwarmte-ontwikkelen.html`.

SodM & TNO. Protocol bepaling maximale injectiedrukken bij aardwarmtewinning. Technical report, 2013.

H.A. Stiff. The interpretation of chemical water analysis by means of patterns. *SPE Production & Operations*, 3, 1951. Document ID: SPE-951376-G.

D.L. Turcotte and G. Schubert. *Geodynamics*. Cambridge University Press, Cambridge, England, UK, 2nd edition, 2002. ISBN 978-0-521-66624-4.

United Nations. Adoption of the paris agreement, 2015. URL `https://unfccc.int/resource/docs/2015/cop21/eng/l09r01.pdf`. UNTC XXVII 7.d.

H.A. Van Adrichem Boogaert and W.F.P. Kouwe. Berkel sandstone member knnsb. in: Stratigraphic nomenclature of the netherlands, 1993-1997a. URL `https://www.dinoloket.nl/en/berkel-sandstone-member-knnsb`. Retrieved on 08-05-2019.

H.A. Van Adrichem Boogaert and W.F.P. Kouwe. Nederweert sandstone member rbshn. in: Stratigraphic nomenclature of the netherlands, 1993-1997b. URL `https://www.dinoloket.nl/en/nederweert-sandstone-member-rbshn`. Retrieved on 27-07-2019.

R.T. van Balen, F. van Bergen, C. de Leeuw, H. Pagnier, H. Simmelink, J.D. van Wees, and J.M. Verweij. Modelling the hydrocarbon generation and migration in the west netherlands basin, the netherlands. *Geologie en Mijnbouw / Netherlands Journal of Geosciences*, 79: 29–44, 2000.

M.J.J. van der Weiden. Een hydrochemisch onderzoek in berband met de winning van aardwarmte uit het west-nederland bekken, toegespitst op het demonstratieproject delfland. Msc thesis, Geochemie, faculteit Aardwetenschappen, Universiteit Utrecht, Utrecht, the Netherlands, 1983.

P. van der Wielen and D. van der Kooij. Atp-metingen geven informatie over kans op nagroeiproblemen bij drinkwaterdistributie. *H2O*, 21:38–40, 2010.

I. Vance and D.R. Thrasher. Reservoir souring: mechanisms and prevention in: Ollivier, b., magot, m. (eds) petroleum microbiology, 2005. URL `http://www.osha.gov/OshDoc/data_Hurricane_Facts/hydrogen_sulfide_fact.pdf`. last visited 25-06-2019.

J.G. Veldkamp, T.V. Goldberg, P.M.M.C. Bressers, and F. Wilschut. Corrosion in dutch geothermal systems. Technical report, TNO, March 2016. URL `https://www.nlog.nl/sites/default/files/2016.03.15_tno%202015%20r10160_corrosion%20in%20dutch%20geothermal%20systems_public.pdf`. Sponsored by several geothermal companies.

L. Watkins and J. W. Costerton. Growth and biocide resistance of bacterial biofilms in industrial systems. *Chemical Times & Trends*, pages 35–40, October 1984.

C. Whitby and T.L. Skovhus. *Applied Microbiology and Molecular Biology in Oilfield Systems: Introduction*. Springer, Dordrecht Heidelberg London New York, 2009. ISBN 978-90-481-9251-9.

C.J.I. Wiggers. The delft sandstone in the west netherlands basin. Bsc thesis, Applied Earth Sciences, Delft University of Technology, Delft, the Netherlands, 2009.

N. Williamson. *Applied Microbiology and Molecular Biology in Oilfield Systems: Problems Caused by Microbes and Treatment Strategies: Health and Safety Issues from the Production of Hydrogen Sulphide*. Springer, Dordrecht Heidelberg London New York, 2009. ISBN 978-90-481-9251-9.

S. Yoo, T. Myojo, T. Matsuoka, and A. Ueda. Experimental studies of injectivity reduction due to carbonate mineralization. *Procedia Earth and Planetary Science*, 7:920–923, 2013.

P.A. Ziegler. North-western europe: Tectonics and basin development. *Geologie en Mijnbouw*, 57:589 – 626, 1978.

P.A. Ziegler. *Geological Atlas of Western and Central Europe*. Geological Society Publishing House (Bath distributors), 2nd edition, 1990. ISBN 978-9066441255.